Role of calcium during plant infection by *Xylella fastidiosa*

by

Laura Melissa Gomez Arias

A dissertation submitted to the Graduate Faculty of
Auburn University
in partial fulfillment of the
requirements for the Degree of
Doctor of Philosophy

Auburn, Alabama
May 1, 2021

Keywords: *Xylella fastidiosa*, Calcium, twitching motility, disease development, virulence assays, adhesion force

Approved by

Leonardo De La Fuente, Chair, Professor of Plant Pathology
Paul A. Cobine, Professor of Biological Sciences
Sang Wook Park, Associate Professor of Plant Pathology
Aaron Rashotte, Professor of Biological Sciences

Abstract

Xylella fastidiosa (Xf) is a Gram-negative plant pathogenic bacterium that lives in the xylem vessels of infected plants and the foregut of sharpshooter insect vectors. *X. fastidiosa causes* diseases in many economically important crops worldwide. Virulence mechanisms of *X. fastidiosa* involve colonization of host plants through twitching movement, and development of biofilm leading to vessel occlusion and water stress. Essential micro- and macronutrients including calcium (Ca) are required for a myriad of functions within cells and are under tight homeostatic control. Previous results from our group show that: 1) *X. fastidiosa* uses Ca to enhance virulence traits, and 2) *X. fastidiosa* infection triggers a host response that leads to accumulation of Ca in plant tissue.

In *X. fastidiosa*, Ca has been demonstrated to increase biofilm formation, surface attachment, cell-to-cell aggregation, and twitching motility. In tobacco plants a significant component of the defense response includes numerous genes involved in Ca signaling. These observations suggest that interactions between plant hosts and the bacterium are affected by Ca. This led us to hypothesize that *X. fastidiosa* is hijacking the Ca-defense response of the plant host to increase its virulence. Previous studies showed that Xf uses Ca to enhance virulence traits, such as twitching motility, while Xf infection triggers a host response that leads to accumulation of Ca in the plant tissue. Among genes transcriptionally regulated by Ca, *PD0913* was selected for functional analysis because it has putative Ca-binding motifs in its sequence and is part of a putative genomic island absent in a non-virulent strain, as revealed by comparative genomics. For my first objective, PD0913-*X. fastidiosa* mutant was generated by site-directed mutagenesis. Analysis in vitro and in planta were performed to determine the role of this gene in bacterial virulence under different Ca concentrations. Our results showed that the absence of PD0913

increased twitching motility, surface attachment at 2mM Ca concentration, and virulence at 8mM Ca concentration, compared to the WT. This suggests that the PD0913 gene negatively regulates twitching motility and virulence of *X. fastidiosa* under different levels of Ca concentrations.

For my second objective, tobacco plant inoculation in greenhouse and virulence assessments over time were performed in 41 selected *X. fastidiosa* isolates obtained from vineyards in California. For virulence assessments, area under disease progression curve (AUDPC), percentage of leaf scorch, and severity were determined. Isolates Je32, Je86, Je96 and Je121 showed the highest numbers in virulence assays when compared to TemeculaL and WM1-1 (reference controls). Contrastingly, Je98, Je111 and Je118 showed the lowest values on AUDPC, incidence and severity. No correlation was found between virulence and host cultivar or geographical location of the isolates. These results indicate that virulence differences between isolates were apparent, and have potential implications for understanding the context of genomic variability, host adaptation and geographic location on the identification and selection of resistant cultivars for the development and improvement of disease management on this bacterium.

For my third objective, to define the role of CAX3 in the interaction with Xf and prove that more Ca flowing through the xylem will cause higher disease severity, an overexpression of CAX3 was made using the Gateway system. Two different markers were used: GUS and GFP, and tobacco plants were transformed by Agrobacterium. Plants could not develop from the calli generated by Agrobacterium- mediated transformation. We hypothesized that CAX3 can alter the phenotype and development of the plants and that is why no plant was grown, and we propose that Ca application in the medium can restore the phenotype.

In summary, during my research I contributed to the understanding of the molecular basis of the role of Ca in the *X. fastidiosa* infection process, using the knowledge acquired by the interaction

of the bacterium with different concentrations of Ca *in vitro* and *in planta* along with the analysis of a group of proteins that export cations of the cytosol to maintain optimal ionic concentrations in the cell and how different isolates can influence the virulence in tobacco plants.

Acknowledgments

I really want to thank my committee; as professors from different areas, they give me the opportunities, point of view and tools to learn to see the different angles that my research could take and to don't give up through this journey.

Special thanks to my advisor Dr. Leonardo De La Fuente and Dr Paul Cobine who both took time to make some extra appointment to help me improve my research skills and knowledge. Without their patience and endless support, my dissertation would not have been possible.

I would like to sincerely thank, Dr Sang Wook Park and Dr. Aaron Rashotte for serving on my graduate committee offering their suggestions for my research.

In addition, I want to thank my outside university reader Dr. Soledad Peresin for her constructive suggestions.

Quiero agradecer especialmente a mi familia, que a pesar de la distancia siempre estuvo presente sobretodo en los momentos mas dificiles de esta jornada. Su apoyo y estimulo me permitieron superar todas las dudas que surgieron durante este proyecto.

Quero agradecer tambem minha familia de coracao, os amigos que ficaram tao proximos que se converteram na minha familia aqui em Auburn, Marquitos que sempre revisou as minhas contas e conversoes, os meus abstracts e meus papers. Ma e Iza que me acompanharam em aulas, almocos, estudos na biblioteca e algumas outras aventuras. Le e Mariane pelos almocos, jogos e inspiracao. Um agradecimento muito especial para Andresa quem estuvo presente nos momentos mais fodas dessa jornada, quem realmente lidou com este lindo demonio quando estava na epoca de maior duvida e desespero. Obrigada pelas caronas e os paseios de carro para me acalmar e ver as coisas de outro jeito e assim poder voltar pro lab e tentar mais uma vez.

Cele es otra persona que me gustaria agradecerle, por todos los momentos compartidos, las risas y lagrimas, almuerzos y cervezas, y por todas las buenas conversaciones que me ayudaron durante el doctorado.

And finally, my office mates two amazing ladies that shared one on one this amazing and excruciating journey together. Qing and Ambika we spent 4 years and a half growing together and I could not be here if is not for you ladies, thank you!

I have learned a lot and none of this could be happening if not for all the people named above! Thank you so much!

Table of Contents

List of Tables

List of Figures

List of Abbreviations

PD	Pierce's Disease
CVC	Citrus Variegated Chlorosis
OQDS	Olive Quick Decline Syndrome
MLST	Multi-Locus Sequence Typing
BLS	Bacterial Leaf Scorch
EPS	Exopolysaccharides
LPS	Lipopolysaccharide
OMVs	Outer membrane vesicles
DSF	Diffusible signal factor
CAX1	*CALCIUM EXCHANGER 1*
PG	Polygalacturonase
EGase	Endo-1,4-βglucanase

Chapter 1

Literature Review

1. *Xylella fastidiosa*

Xylella fastidiosa is a xylem-limited, fastidious bacterial plant pathogen (Hopkins & Purcell, 2002). The bacterial cells are rod-shaped with dimensions of 0.25 to 0.35 µm in radius and 0.9 to 3.5 µm in length (Wells et al., 1987). Gram-negative, is a slow-growing bacterium, strictly-aerobic, and optimum growth occurs between 26-28°C (Wells et al., 1987). This non-flagellated bacterium possesses two type of pili positioned at one of the cell poles. Type I pili (0.4 to 1.0 µm) associated with bacterial adhesion and auto-aggregation, and type IV pili (1.0 to 5.8 µm) involved with twitching motility (Meng et al., 2005).

X. fastidiosa is transmitted mainly by sharpshooters and spittlebugs insects from the Cicadellidae family, specifically the glassy-winged sharpshooter (*Homalodisca vitripennis*) and the blue-green sharpshooter (*Graphocephala atropunctata*) (Janse & Obradovic, 2010), among others. The bacterium shows ability to multiply in the foregut of the insect and vector colonization occurs in a persistent and non-circulative manner (Janse & Obradovic, 2010, Chatterjee et al., 2008a). This means that the bacteria is able to survive in two habitats: the foregut of the vector and the plant xylem vessels (Chatterjee et al., 2008a). Vectors are distributed world-wide and can feed on the xylem of a diverse group of plants, which confers two important aspects of the transmission by this vector: i) no specificity between vector species and *X. fastidiosa* isolates, and ii) no latent period for transmission (Almeida & Nunney, 2015).

Diseases caused by this bacterium were described for the first time in 1884 in the USA as the cause of Pierce's disease (PD) of grapevine, *Vitis vinifera* (Davis et al., 1978). In 1993 it was reported in Brazil as the cause of citrus variegated chlorosis (CVC) (Chang et al., 1993). More

recently it was described in olives as olive quick decline syndrome (OQDS) (Martelli et al., 2015). This bacterium also affects economically important plants as blueberry, peach, plum, almond, coffee, elm, oak, sycamore, maple, and others. Host plant species of *X. fastidiosa* has been constantly expanding with positives plant species reported in 595 plant species, 275 genera and 85 families (European Food Safety, 2020). Initially, three subspecies were described within the species of *X. fastidiosa* by DNA-DNA hybridization: subsp. *fastidiosa*, subsp. *multiplex*, and subsp. *pauca* (Schaad et al., 2004). This subspecific designation was later confirmed by Multi Locus Sequence Typing (MLST) of seven housekeeping genes with two more subspecies described from isolates not included in the previous studies: subsp. *sandyi*, and subsp. *morus* (Scally et al., 2005, Yuan et al., 2010, Nunney et al., 2014b). Currently, there is no cure for any of these diseases leading to devastating economic losses.

2. Virulence mechanisms of *X. fastidiosa*

Disease symptoms caused by *X. fastidiosa* differ depending on plant host and severity of infection. Typically those symptoms involve leaf scorch, cupping and curling of the leaves, uneven maturation of the periderm, twig dieback and mummification of the berries for PD and bacterial leaf scorch (BLS) in almond and blueberry (Stevenson et al., 2005). In citrus, symptoms involved interveinal chlorotic areas on the upper surface of the leaf, with gummy lesions in mature leaves, reduced size of the fruit and vigor. Such symptoms as leaf scorch are associated with the extensive colonization of the xylem vessels. Although the virulence mechanisms of *X. fastidiosa* remain uncertain, they involve attachment of the cells and biofilm formation causing the blockage of xylem vessels affecting the supply of water and nutrients on the plant (Chatterjee et al., 2008a). Furthermore, occlusion of the xylem vessel can be the response of the host plant to *X. fastidiosa*

infection causing the production of tyloses, pectin-rich gels and crystals inside the xylem vessels (Sun et al., 2013).

Biofilm are complex bacterial assemblages attached to a surface and encapsulated in a matrix that generally consists of exopolysaccharides (EPS) (Castiblanco & Sundin, 2016). EPS is critical for the structural integrity of biofilms, which also contributes to *X. fastidiosa* virulence. Biofilms are also established in the mouthparts of vectors. In both environments, mutants deficient in EPS production are generally avirulent. *X. fastidiosa* produces an EPS, termed fastidian gum. Fastidian gum is predicted to be similar in structure to the xanthan gum (Da Silva et al., 2001). The xanthan gum operon of *Xanthomonas campestris* consists of a tandem array of 12 genes, *gumB, C, D, E, F, G, H, I, J, K, L* and *M*, which encode the enzymes responsible for EPS synthesis (Katzen et al., 1998). *X. fastidiosa* contain a gum operon that had nine ORFs homologous to genes *gumB, C, D, E, F, H, J, K* and *M*. Three genes are missing in the *X. fastidiosa* gum operon, *gumG, I* and *L (Da Silva et al., 2001)*. Mutants in *gumD* and *gumH* were deficient in movement within plants due to significantly less EPS production than wild type, generating an avirulent type in grapevine (Killiny et al., 2013). Another non-proteinaceous, cell surface, carbohydrate molecule important for adhesion in the *X. fastidiosa* association with the host is the lipopolysaccharide (LPS). LPS has a conserved lipid A-core oligosaccharide and a variable O-antigen. Truncation of the long chain in the O-antigen has a significant impact in cell surface attachment and cell-to-cell aggregation in *X. fastidiosa* in both the plant and the insect (Clifford et al., 2013). Type I pili has been associated with bacterial adhesion (De La Fuente et al., 2008). Afimbrial adhesins are surface proteins that are in the outer membrane and facilitate cell–cell attachment. *X. fastidiosa* hemagglutinin-like proteins (Hxf afimbrial adhesins) are typical proteins in this group of adhesins. Mutants of *hxfA* or *hxfB* genes encoding hemagglutinins resulted in hypervirulence in *X. fastidiosa*

(Guilhabert & Kirkpatrick, 2005). Interestingly, *X. fastidiosa* produces outer membrane vesicles (OMVs). *X. fastidiosa*, OMVs modulate plant colonization by blocking attachment to xylem surfaces (Ionescu et al., 2014). Cell adhesion, twitching motility and biofilm formation are regulated in a dependent cell-density manner in *X. fastidiosa*. The cell-to-cell signaling system in *X. fastidiosa* is mediated by diffusible signal factor (DSF), encoded by the *rfp* cluster that interacts with the cyclic-di-GMP to regulate bacterial aggregation, attachment, insect transmission, biofilm formation and virulence (Chatterjee et al., 2008a, Chatterjee et al., 2008b).

X. fastidiosa is directly injected into xylem vessels by sap-feeding insects (sharpshooters and spittlebugs) during the feeding process (Janse & Obradovic, 2010). To systematically colonize xylem vessels, *X. fastidiosa* needs to digest pectin in pit membranes to enable its spread through the plant (Roper et al., 2007). Previous studies have shown that cell wall-degrading enzymes (polygalactuoronase and endo-1,4-β-glucanase) produced by virulent *X. fastidiosa* leads to damage and an increase in pit membrane pore size (Perez-Donoso et al., 2010). Once inside the plant, the bacteria need to be able to spread against the direction of the transpiration stream. Fimbrial and afimbrial adhesins are important for cell adhesion, migration within the plant, and biofilm formation in *X. fastidiosa*. Since *X. fastidiosa* lacks flagella, Type IV pili it is currently the only known means of motility in the xylem. Twitching motility in *X. fastidiosa* is characterized by the extension, tethering and retraction of the type IV pili facilitating the dragging of the cells on surfaces (Meng et al., 2005). More than 40 genes are annotated encoding pili related proteins in the *X. fastidiosa* Temecula1 genome. Reduction in virulence can be observed when some pili genes are mutated (Cursino et al., 2011). Calcium enhances the twitching motility via PilY1, a Type IV pilus structural protein. It has been demonstrated that calcium concentrations regulate the twitching

motility in the xylem as ionic concentrations of calcium fluctuate in the xylem sap (Cruz et al., 2012, Cruz et al., 2014).

3. Influence of mineral elements on the virulence of *X. fastidiosa*

X. fastidiosa is restricted to the xylem vessels of the plant. Xylem sap is known to contain various amino acids, sugars, organic acids, inorganic ions, proteins, and low concentration of organic compounds essential to support bacterial growth (Biles & Abeles, 1991). Xylem fluid is extremely dilute (typically 5–20 mM) and consists mainly of amino acids, organic acids and inorganic ions (Andersen & Brodbeck, 1989). Xylem fluid chemistry is dynamic and may vary with plant genotype, time of year, time of day, soil fertilization status and temperature (Andersen & Brodbeck, 1989).Thus, it can be hypothesized that xylem sap chemistry has an important effect on bacterial growth and virulence. A functional relationship has been reported between xylem chemistry and *X. fastidiosa* planktonic growth, aggregation and biofilm formation within *Vitis* germplasms (Andersen et al., 2007). It has been shown that both *X. fastidiosa* proliferation and biofilm formation may be impacted by a variety of constituents including inorganic ions, O_2, antioxidants, amino and organic acids and sulfhydryl groups (Leite et al., 2004).

The concept of ionome was defined as “the mineral nutrient and trace elements found in an organism” (Lahner et al., 2003). Elemental profiling can be used as a practical functional genomics tool for the identification of genes involved in the accumulation of mineral nutrients and trace elements in plants (Lahner et al., 2003). Characterization of plant ionome has been used to understand plant adaptation to environmental biotic and abiotic stress (De La Fuente et al., 2013, Nicolas et al., 2019, Sánchez-Rodríguez et al., 2010) and to identify plant gene networks that control element homeostasis (Salt et al., 2008). Ionome analysis of xylem sap has shown that

planktonic growth correlates with the levels of certain amino acids as well as copper (Cu), magnesium (Mg), phosphorus (P), and zinc (Zn). Also, cell aggregation was promoted when calcium (Ca) and Mg are added together to extracted xylem sap used as an *in vitro* culture medium (Andersen et al., 2007). In fact Ca, added to synthetic media, was shown to promote several virulence traits as twitching motility, attachment to surfaces, and biofilm formation in *X. fastidiosa* (Cruz et al., 2012). Ca, together with Mg, has been proposed to act as bridge between the negatively charged surfaces of the xylem vessels and the bacterial cells to promote cell attachment and aggregation (Leite et al., 2002). Iron is essential for the activity of several enzymes acting in electron transport processes (Hood & Skaar, 2012). Production of siderophores (low molecular weight molecules that possess an affinity for Fe) has received special attention for its role in plant pathogen interactions. The presence of genes encoding receptors for siderophores and proteins involved in iron uptake suggests the importance of iron for the growth of the bacteria in the xylem (Silva-Stenico et al., 2005). In *X. fastidiosa* iron has been implicated in the regulation of virulence. This metal promotes the expression of genes involved the synthesis of type IV and type I pili, as well as the synthesis of bacteriocins, which act in the competition against other bacteria inside the xylem (Zaini et al., 2008). Chemical analysis of biofilm-forming versus planktonic *X. fastidiosa* cells has shown a markedly different metal composition. Biofilm cells accumulate high levels of Cu, Manganese (Mn) and Zn compared to planktonic ones. Cu is an essential micronutrient metal for both plants and plant pathogens (Evans et al., 2007). It is recognized for its effects as a biocide and has been associated with denaturation of nucleic acids, inhibition of protein activity, and changes in plasma membrane permeabilization (Borkow & Gabbay, 2005). *In vitro*, Cu promotes attachment and aggregation at low levels, whereas at higher concentrations it prevents growth. Mn promotes cell-cell aggregation and biofilm production, whereas Zn reduces planktonic and biofilm

growth (Cobine et al., 2013). A Zn-protease is induced in *X. fastidiosa* in planta which utilizes free amino acids in the xylem as nitrogen and carbon (Purcino et al., 2007). Zn metalloproteases are also upregulated during biofilm formation (Silva et al., 2011).

4. Ionome modification of plant host by *X. fastidiosa* infection

Excessive bacterial colonization of the xylem has long been hypothesized to occlude vessels, resulting in reduced water conductance that predisposes plants to drought-stress conditions and symptom development (Choi et al., 2013). Uptake and translocation of mineral ions is essential for plant growth (Guerinot & Salt, 2001). Plants uptake mineral nutrients from soils and move them inside the xylem from roots to leaves; thus, infection of *X. fastidiosa*, that disrupt this function of plant xylem, could trigger a modification of mineral elements accumulation in leaves. This has been demonstrated by studies in our group by comparing leaf ionome between *X. fastidiosa* infected and non-infected host plants, including tobacco (*Nicotiana tabacum*), grapevine (*Vitis* sp.), blueberry (*Vaccinium* sp.) and pecan (*Carya illinoinensis*) (De La Fuente et al., 2013). Changes in leaf ionome of infected *Nicotiana tabacum* correlated with virulence of various *X. fastidiosa* isolates (Oliver et al., 2014). Among those assessed mineral elements, the concentration changes of Ca were most significant. Ca concentration was increased in infected host leaves, and this result was reproduced in other two independent studies (Oliver et al., 2014, Navarrete & De La Fuente, 2015). Mechanisms responsible for the Ca increase in host leaves is unknown, however, we hypothesize that is associated with higher Ca concentration in the host plant due to response to *X. fastidiosa* infection. Ca have been demonstrated to be involved in plant defense responses (Lecourieux et al., 2006, Ma et al., 2009), and transcriptome analysis of *X. fastidiosa* infected plants (citrus and grapevine) indicate that host genes related to Ca signaling are induced upon

infection (Rodrigues et al., 2013, Choi et al., 2013). In addition, this bacterium can also establish asymptomatic colonization in many plants as a commensal endophyte, but the leaf ionome in these asymptomatic host plants have not been characterized. Study of the leaf ionome in *X. fastidiosa* systematically colonized asymptomatic host plants is of interest and could be helpful to complement our understanding in the host plants response to *X. fastidiosa* infection.

5. The regulatory role of Ca in the host-*X. fastidiosa* interaction

5.1. Ca regulatory function and structure

Calcium (Ca^{2+}) likely represents the most versatile ion in eukaryotic organisms. This divalent alkaline cation is one of the most abundant components of plant and animal fluids and tissues, it is involved in nearly all aspects of plant development and participates in many regulatory processes (Kudla et al., 2010, Hepler, 2005). Ca can easily form complexes with proteins, membranes, and organic acids due its flexibility in exhibiting different coordination numbers and complex geometries, making it an important structural component of macromolecules (Kudla et al., 2010). Ca^{2+} plays a crucial role in determining the structural rigidity of the cell wall. It has also been known for many years that Ca^{2+} plays an important role in controlling membrane structure and function (Hepler, 2005). Similar to eukaryotic cells, mechanisms of Ca^{2+} signaling in bacterial cells are based on local changes of free Ca concentration [Ca^{2+}] in the cytoplasm. In viable bacteria, [Ca^{2+}] has been shown to be maintained at a low level, approximately 1000 times lower than in the extracellular medium (Norris et al., 1996). Ca gradients are the base of mechanisms that transmit information into cells, transducing signals to target different Ca-binding proteins. Its low cytosolic concentration and the cellular capacity to increase its concentration in response to

environmental signals has been associated with the function of Ca as a regulatory molecule (Shemarova & Nesterov, 2005).

In xylem sap Ca is an important inorganic compound, which has multiple functions for both the plant host and bacterial pathogen (De La Fuente et al., 2014). The role of Ca in plants has been extensively studied, which not only involves the stabilization of cell wall structures, but also as a secondary messenger that mediates a sophisticated signaling network (Demarty et al., 1984, Dodd et al., 2010). The role of Ca in bacteria remains elusive, however, recent indirect evidence suggest multiple regulatory functions of Ca in bacteria (Dominguez, 2004, Dominguez et al., 2015). Ca regulates a variety of bacterial behaviors including spore germination (Wang et al., 2008), secretion activity (DeBord et al., 2003, Dasgupta et al., 2006), biofilm formation (Sarkisova et al., 2005, Rinaudi et al., 2006), motility (Gode-Potratz et al., 2010, Guragain et al., 2013), and quorum sensing (Werthen & Lundgren, 2001). A series of studies conducted by our group has shown that Ca influences key virulence-related traits of *X. fastidiosa*. An increase of external Ca concentration has led to higher surface adhesion force, twitching speed and more biofilm formation by *X. fastidiosa* (Cruz et al., 2012), and these Ca effects were indicated to be related with de novo protein synthesis, however most of the molecular targets remain unknown (Cruz et al., 2012).

5.2. Ca in plants: acquisition and distribution

The essential nature of Ca as a plant nutrient has been recognized now for well over a hundred years. The regular application of Ca to soils either directly by liming in order to prevent soil acidity, or indirectly in the form of inorganic fertilizers such as superphosphate or basic slag has meant that agricultural soils are often relatively well supplied with Ca (Kirkby & Pilbeam, 1984). Plants absorb Ca from the soil solution as divalent cations. The total amount of

exchangeable Ca in a soil is usually not so important in plant supply as the soil mineral composition, the presence of other elements as Mg, K and ammonium, and soil pH (optimal range is 4.5-6.0) (Kirkby, 2008). Ca is moved largely in the xylem vessels by the transpiration stream and only to a very limited extent in the phloem (Kirkby & Pilbeam, 1984). Accumulation of Ca occurs in leaves and in older parts of the plant. The highest content of Ca is found in the leaves of the plant. At the cellular level, Ca is mainly located in the cell wall bound as pectates in the middle lamella; this characteristic is important for cell wall stabilization and cation exchange (Marschner, 1995a). The intracellular free Ca concentration in bacterial cells ranges from 100 to 200 nM, similar to the levels found in eukaryotic cells, and homeostasis is tightly regulated by a complex gene network (Jones et al., 1999, Dominguez et al., 2015). Transient elevations in cytosolic Ca^{2+} concentration have been documented to be involved in a multitude of physiological processes, including responses to abiotic stresses, hormones, and pathogens (Kudla et al., 2010).

Eukaryotic Ca export systems have been subdivided into two classes: primary exchangers, which are driven by the energy derived from ATP hydrolysis, and secondary exchangers, which use electrochemical gradients of sodium ions or protons (Norris et al., 1996). The plant cation/H^+ exchangers (CAXs) are part of the ensemble of transporters that may coordinate the redistribution of various cations, including Ca^{2+}, in exchange for the protons generated by H^+ pumps (Punshon et al., 2012). Regulation of plant Ca^{2+} gradients, millimolar levels in the vacuole and micromolar levels in the cytoplasm is made by this CAXs to establish Ca^{2+} homeostasis during and after signal transduction events and stress responses (Hirschi, 1999). Arabidopsis gene, *CAX1* (for *CALCIUM EXCHANGER 1*), was identified by its ability to suppress mutants of yeast defective in vacuolar Ca^{2+} transport (Hirschi et al., 1996). Arabidopsis (*Arabidopsis thaliana*) appears to have many putative CAX transporters that may possess different

biochemical properties (Maser et al., 2001). Increased expression of CAX3 in response to infection of *X. fastidiosa* in tobacco plants was observed in an experiment conducted by our group (data not published). This suggest that the increased expression of CAX3 could affect the cytosolic Ca concentrations and in turn initiate a cascade of response leading to leaf scorch.

The lack of a good experimental host created some difficulties to those studying potential pathogenicity genes in *X. fastidiosa* due to extended periods to express symptoms after inoculation. Model host *Nicotiana tabacum* is capable of showing differences in host colonization and symptomatology caused by the infection with *X. fastidiosa* (Lopes et al., 2000, Francis et al., 2008). Tobacco has been used as a model system to evaluate different aspects on the interaction with *X. fastidiosa*, for example ionomic changes (De La Fuente et al., 2013), gene bacterial function (Chen et al., 2017, Navarrete & De La Fuente, 2015), and natural competence and recombination (Kandel et al., 2016). Since studies to predict isolate virulence are lacking, tobacco assays could be a useful tool to evaluate multiple strains in greenhouse conditions, saving considerable time and space. Virulence variation among isolates have only been looked in a small number of studies (Cruz et al., 2012, Oliver et al., 2014, Oliver et al., 2015, Lopes et al., 2000, Francis et al., 2008), even though many *X. fastidiosa* isolates already have their full genome sequenced (Simpson et al., 2000, Vanhove et al., 2019, Vanhove et al., 2020). Severity of disease differs greatly among hosts and virulence comparisons among *X. fastidiosa* strains can be useful to understand the biology of this pathogen. Differences in the virulence of a pathogen among host species can occur because i) hosts differ in their resistance or tolerance to infection, or ii) due to underlying genetic variation in the pathogen. Understanding the complex interactions between plant, pathogen and vector can lead to effective disease control.

5.3. Role of Ca in *X. fastidiosa*

Ca have been linked to diverse prokaryotic cellular processes that varied between regulatory functions including cell cycle, cell division, phospholipid synthesis and configuration, nucleoid structure, protein phosphorylation, and alteration in the distribution of membrane lipids ((Norris et al., 1996, Dominguez, 2004). In addition, as discussed before Ca plays structural roles by preserving the integrity and stability of the LPS layer and the cell wall (Smith, 1995). Specifically in *X. fastidiosa* Ca regulates cell-to-cell attachment, adhesion force, biofilm formation and twitching motility (Cruz et al., 2012).

Multiple Ca-binding proteins implicated in Ca homeostasis have also been described as having different functions. Calmodulins (calcium modulated proteins) initially described in eukaryotic organisms are the most studied type of Ca-binding proteins (Gifford et al., 2007). Calmodulins are acidic proteins of small size (15-22KDa) that contain a typical helix-loop-helix motif called EF-hand, which is in charge of Ca binding. In bacteria, calmodulin-like proteins have been identified, and they are believed to play a significant role in cellular regulation as in their eukaryotic counterparts (Michiels et al., 2002). Some of the bacterial calmodulin-like proteins exhibit a similar structure to the eukaryotic ones, though some variation in the number of EF-hand motifs and their organization has also been observed (Michiels et al., 2002, Zhou et al., 2006). The functions of the proteins holding the EF-hand binding motives are diverse and include proteins related to buffering and transport of Ca, extracellular degrading enzymes, galactose, glucose and ion transport, chemotaxis, protein metabolism, DNA modification, and stress response (Michiels et al., 2002). Four conserved sequence patterns representing EF-hand motifs in bacteria have been reported: DxDxDG (Rigden & Galperin, 2004), Dx[DN]xDGxxD (Orans et al., 2010), DxDxNxxxD (Johnson et al., 2011), and Dx[DN]xDxxxxxx[DE] (Porsch et al., 2013). In *X.*

fastidiosa, 42 genes were identified encoding potential Ca-binding proteins by searching these sequence patterns in the Temecula1 genome (Parker et al., 2016). One of the 42 genes, pilY1 encoding a TFP protein, had been studied by mutagenesis analysis indicating it is linked to Ca enhanced twitching motility, and Ca binding ability of PilY1 was inferred by homology and indirect evidence from biochemical studies (Cruz et al., 2014). From the 42 sequences, *PD0913* a "phage-related protein" that has a Ca-binding motif, showed here to be related with movement, since the absence of the gene has a negative influence in the twitching motility of *X. fastidiosa* suggesting that this trait might affect the virulence in the plant (Chapter 2). Another known Ca binding motif in bacteria is the haemolysin-type, also called the repeats in toxin (RTX) motif. This motif is common to proteins secreted by the type I secretion system of Gram-negative bacteria (Linhartova et al., 2010). RTX-containing proteins are characterized by the presence of tandem repeats of nine conserved residues rich in glycine and aspartame, located in the C terminal of the protein. Ca ions bind to the C-terminal once the protein is secreted, changing the conformation of the protein to secondary structure and then to tertiary structure to make it functional. RTX proteins have a broad spectrum of functions including toxins, proteases, lipases, bacteriocins, and nodulation proteins (Linhartova et al., 2010). The binding of Ca to specific Ca-binding motifs in enzymes prevents polypeptide unfolding, resulting in greater resistance to denaturation and proteolysis (Nardini et al., 2000). *X. fastidiosa* has four loci encoding homologues to hemolysin RTX proteins (RTX1, RTX2, RTX3 and RTX4). A study provides the first direct evidence of their expression during pathogenesis in grapevine during Pierce's disease (Gambetta et al., 2018).

During the infection process, bacterial pathogens require the use of a collection of genetically encoded virulence determinants, which are independently regulated in response to environmental signals (Wilson et al., 2002). Ca works as a signal and regulator of different

pathogenicity determinants in bacterial pathogenesis (Dominguez, 2004). *Xanthomonas* protein secretion (*Xps*) is a type II secretion system in *Xanthomonas* species. This system is largely involved in the secretion of extracellular enzymes required for the hydrolysis of different components of the cell wall (Chatterjee et al., 2008b). *X. fastidiosa* genome has a complete set of *Xps* homologs and contains several genes similar to those encoding cell wall degrading polygalacturonase (PG) and endo-1,4-βglucanase (EGase) (Perez-Donoso et al., 2010). To systemically infect plant host *X. fastidiosa* utilizes cell wall degrading enzymes to break down pit membranes (Roper et al., 2007). These putative Type II-secreted effectors are likely involved in degradation of different components of pit membranes (Chatterjee et al., 2008a). Effects on virulence and fitness has to be determined for the mutation in the *Xps* homologs in *X. fastidiosa*. On the other hand, *pglA* (one ortholog of PG) mutant in *X. fastidiosa* was impeded in long distance movement along the grapevine xylem, suggesting the inability to degrade pit membranes (Roper et al., 2007).

Host invasion and colonization depends on the initial bacterial attachment to surfaces and biofilm formation (Reed & Williams, 1978, Rodriguez-Navarro et al., 2007). There is evidence that Ca is required in the function of extracellular proteins essential for the attachment of bacteria to surfaces. Ca acts as cross-bridging between cells and substrate and stabilizer of the biofilm matrix (Fletcher, 1988, Rose, 2000, Leite et al., 2002). Leite et al. (2002) examined the *X. fastidiosa* biofilm in planta and proposed a model where Ca and Mg work as a bridge between the negatively charged xylem vessels and the negatively-charged bacterial EPS (Leite et al., 2002). In addition to its electrostatic effect in the accumulation of *X. fastidiosa* biofilms, evidence indicated that Type I pili is implicated in the response to Ca increasing cell attachment (Cruz et al., 2012). A functional study of Type I afrimbial adhesins *fimA* and *fimF*, revealed that less efficient

adherence to glass surfaces occurred on mutant cells compared to wild-type strain, suggesting that type I pili have a particularly important role in cell-to-cell aggregation (Feil et al., 2007). In assessment of biofilm formation at different concentrations of Ca, *fimA* mutant increased by 600% at 2mM Ca, leading to believe that Ca significantly increases the strength of the attachment of cells to surface (Cruz et al., 2012). Bacterial biofilms have been thought to improve nutrient acquisition through the formation of EPS, which have a high capacity for ion retention, a strategy particularly important under nutrient-dilute conditions, such as those of xylem sap (Costerton et al., 1995). No evidence for an effect of Ca on EPS production was found in *X. fastidiosa* (Cruz et al., 2012).

Bacteria use a variety of mechanisms to move in response to environmental stimuli, escape from unfavorable conditions, and access optimal colonization sites and nutrient sources (Ottemann & Miller, 1997). Among other functions, flagella assist bacterial locomotion and also have a role in bacterial adhesion in several species (Moens & Vanderleyden, 1996). Ca has been associated with the structure of the flagella of the nitrogen-fixing bacterium *Rhizobium meliloti* (Robinson et al., 1992). Flagellar-driven chemotaxis and motility have been implicated in the colonization in *Xanthomonas oryza*e pv. *oryzae* (Shen et al., 2001). Although *X. fastidiosa* is a non-flagellated bacterium, it is efficient in the colonization of plants and even upstream movement in the xylem of grape. Genome analysis of *X. fastidiosa* revealed the presence of several gene orthologs that may encode proteins involved in biogenesis and function of Type IV pili (Simpson et al., 2000, Van Sluys et al., 2003). Type IV pili is involved in bacterial movement. Functions of type IV pili include cell adhesion, cell signaling, biofilm formation, virulence, and twitching motility (Burdman et al., 2011). Mutation in the Type IV pili genes *pilB* and *pilQ* of *X. fastidiosa* causes loss of twitching motility and inhibition of basipetal movement in planta (Chatterjee et al., 2008a). The role of Ca in type IV pili could be related to the primary function of these fimbriae that assist

in cell twitching motility. Ca binding ability of PilY1 was inferred by homology and indirect evidence from biochemical studies (Cruz et al., 2014). Increase in Ca concentration was correlated with the increase in cells twitching motility speed of *X. fastidiosa* (Cruz et al., 2012).

Overall hypothesis:

Xylella fastidiosa is hijacking the plant defense response based on calcium accumulation to enhance its virulence.

Research goals:

- Determine the functional role of *PD0913* in bacterial growth and virulence
- Determine the role of *CAX3* in the transport and homeostasis of Calcium in plants during *X. fastidiosa* infection

Specific objectives:

- Site-directed mutagenesis of PD0913 in virulent strains of *X. fastidiosa*
- Functional analysis *in vitro* of PD0913
- Functional analysis *in planta* of PD0913 infection
- Construction of expression cassettes for overexpression of CAX3
- Tobacco transformation mediated by *Agrobacterium tumefaciens*
- Confirmation of transformed plants
- Infection of transformed plants at different concentrations of Calcium

Hypothesis 2

Infection of tobacco plants with *X. fastidiosa* isolates from the same host and location differ in virulence

Research goals:

- Characterize the virulence of *X. fastidiosa* isolates from California's grapevines in tobacco plants

Specific objectives:

- Select isolates from 122 *X. fastidiosa* subsp. *fastidiosa* to infect Tobacco
- Infection of tobacco plants
- Perform virulence assays: evaluate incidence and severity: leaf scorch and AUDPC on infected plants

REFERENCES

Almeida RPP, Nunney L, 2015. How Do Plant Diseases Caused by *Xylella fastidiosa* Emerge? *Plant Dis* **99**, 1457-67.

Andersen PC, Brodbeck BV, 1989. Diurnal and Temporal Changes in the Chemical Profile of Xylem Exudate from Vitis-Rotundifolia. *Physiologia Plantarum* **75**, 63-70.

Andersen PC, Brodbeck BV, Oden S, Shriner A, Leite B, 2007. Influence of xylem fluid chemistry on planktonic growth, biofilm formation and aggregation of *Xylella fastidiosa*. *FEMS Microbiol Lett* **274**, 210-7.

Biles CL, Abeles FB, 1991. Xylem sap proteins. *Plant Physiol* **96**, 597-601.

Borkow G, Gabbay J, 2005. Copper as a Biocidal Tool. *Current Medicinal Chemistry* **12**, 2163.

Burdman S, Bahar O, Parker JK, De La Fuente L, 2011. Involvement of Type IV Pili in Pathogenicity of Plant Pathogenic Bacteria. *Genes (Basel)* **2**, 706-35.

Castiblanco LF, Sundin GW, 2016. New insights on molecular regulation of biofilm formation in plant-associated bacteria. *J Integr Plant Biol* **58**, 362-72.

Chang CJ, Garnier M, Zreik L, Rossetti V, Bove JM, 1993. Culture and Serological Detection of the Xylem-limited Bacterium Causing Citrus Variegated Chlorosis and Its Iden.

Chatterjee S, Almeida RP, Lindow S, 2008a. Living in two worlds: the plant and insect lifestyles of *Xylella fastidiosa*. *Annu Rev Phytopathol* **46**, 243-71.

Chatterjee S, Newman KL, Lindow SE, 2008b. Cell-to-cell signaling in *Xylella fastidiosa* suppresses movement and xylem vessel colonization in grape. *Mol Plant Microbe Interact* **21**, 1309-15.

Choi HK, Iandolino A, Da Silva FG, Cook DR, 2013. Water deficit modulates the response of Vitis vinifera to the Pierce's disease pathogen *Xylella fastidiosa*. *Mol Plant Microbe Interact* **26**, 643-57.

Clifford JC, Rapicavoli JN, Roper MC, 2013. A rhamnose-rich O-antigen mediates adhesion, virulence, and host colonization for the xylem-limited phytopathogen *Xylella fastidiosa*. *Mol Plant Microbe Interact* **26**, 676-85.

Cobine PA, Cruz LF, Navarrete F, Duncan D, Tygart M, De La Fuente L, 2013. *Xylella fastidiosa* differentially accumulates mineral elements in biofilm and planktonic cells. *PLoS One* **8**, e54936.

Costerton JW, Lewandowski Z, Caldwell DE, Korber DR, Lappin-Scott HM, 1995. Microbial biofilms. *Annu Rev Microbiol* **49**, 711-45.

Cruz LF, Cobine PA, De La Fuente L, 2012. Calcium increases *Xylella fastidiosa* surface attachment, biofilm formation, and twitching motility. *Appl Environ Microbiol* **78**, 1321-31.

Cruz LF, Parker JK, Cobine PA, De La Fuente L, 2014. Calcium-Enhanced Twitching Motility in *Xylella fastidiosa* Is Linked to a Single PilY1 Homolog. *Appl Environ Microbiol* **80**, 7176-85.

Cursino L, Galvani CD, Athinuwat D, *et al.*, 2011. Identification of an Operon, Pil-Chp, That Controls Twitching Motility and Virulence in *Xylella fastidiosa*. *Molecular Plant-Microbe Interactions* **24**, 1198-206.

Da Silva FR, Vettore AL, Kemper EL, Leite A, Arruda P, 2001. Fastidian gum: the *Xylella fastidiosa* exopolysaccharide possibly involved in bacterial pathogenicity. *FEMS Microbiol Lett* **203**, 165-71.

Dasgupta N, Ashare A, Hunninghake GW, Yahr TL, 2006. Transcriptional induction of the Pseudomonas aeruginosa type III secretion system by low Ca2+ and host cell contact proceeds through two distinct signaling pathways. *Infect Immun* **74**, 3334-41.

Davis MJ, Purcell AH, Thomson SV, 1978. Pierce's disease of grapevines: isolation of the causal bacterium. *Science* **199**, 75-7.

De La Fuente L, Burr TJ, Hoch HC, 2008. Autoaggregation of *Xylella fastidiosa* cells is influenced by type I and type IV pili. *Appl Environ Microbiol* **74**, 5579-82.

De La Fuente L, Navazio L, Oliver JE, Cruz LF, Cobine PA, 2014. The Influence of Metal Elements on Virulence in Plant-Pathogenic Bacteria. In. *Virulence Mechanisms of Plant-Pathogenic Bacteria.* 231-62.

De La Fuente L, Parker JK, Oliver JE, *et al.*, 2013. The bacterial pathogen *Xylella fastidiosa* affects the leaf ionome of plant hosts during infection. *PLoS One* **8**, e62945.

Debord KL, Galanopoulos NS, Schneewind O, 2003. The ttsA gene is required for low-calcium-induced type III secretion of Yop proteins and virulence of Yersinia enterocolitica W22703. *J Bacteriol* **185**, 3499-507.

Demarty M, Morvan C, Thellier M, 1984. Calcium and the Cell-Wall. *Plant Cell and Environment* **7**, 441-8.

Dodd AN, Kudla J, Sanders D, 2010. The language of calcium signaling. *Annu Rev Plant Biol* **61**, 593-620.

Dominguez DC, 2004. Calcium signalling in bacteria. *Mol Microbiol* **54**, 291-7.

Dominguez DC, Guragain M, Patrauchan M, 2015. Calcium binding proteins and calcium signaling in prokaryotes. *Cell Calcium* **57**, 151-65.

European Food Safety A, 2020. Update of the Xylella spp. host plant database - systematic literature search up to 30 June 2019. *EFSA J* **18**, e06114.

Evans I, Solberg E, Huber DM, 2007. Copper and plant disease. *Mineral Nutrition and Plant Disease*, 177-88.

Feil H, Feil WS, Lindow SE, 2007. Contribution of Fimbrial and Afimbrial Adhesins of *Xylella fastidiosa* to Attachment to Surfaces and Virulence to Grape. *Phytopathology* **97**, 318-24.

Fletcher M, 1988. Attachment of Pseudomonas fluorescens to glass and influence of electrolytes on bacterium-substratum separation distance. *J Bacteriol* **170**, 2027-30.

Gambetta GA, Matthews MA, Syvanen M, 2018. The Xylella fastidosa RTX operons: evidence for the evolution of protein mosaics through novel genetic exchanges. *Bmc Genomics* **19**, 329.

Gifford JL, Walsh MP, Vogel HJ, 2007. Structures and metal-ion-binding properties of the Ca2+-binding helix-loop-helix EF-hand motifs. *Biochem J* **405**, 199-221.

Gode-Potratz CJ, Chodur DM, Mccarter LL, 2010. Calcium and iron regulate swarming and type III secretion in Vibrio parahaemolyticus. *J Bacteriol* **192**, 6025-38.

Guerinot ML, Salt DE, 2001. Fortified foods and phytoremediation. Two sides of the same coin. *Plant Physiol* **125**, 164-7.

Guilhabert MR, Kirkpatrick BC, 2005. Identification of *Xylella fastidiosa* antivirulence genes: hemagglutinin adhesins contribute a biofilm maturation to X. fastidios and colonization and attenuate virulence. *Mol Plant Microbe Interact* **18**, 856-68.

Guragain M, Lenaburg DL, Moore FS, Reutlinger I, Patrauchan MA, 2013. Calcium homeostasis in Pseudomonas aeruginosa requires multiple transporters and modulates swarming motility. *Cell Calcium* **54**, 350-61.

Hepler PK, 2005. Calcium: a central regulator of plant growth and development. *Plant Cell* **17**, 2142-55.

Hirschi KD, 1999. Expression of Arabidopsis CAX1 in tobacco: altered calcium homeostasis and increased stress sensitivity. *Plant Cell* **11**, 2113-22.

Hirschi KD, Zhen RG, Cunningham KW, Rea PA, Fink GR, 1996. CAX1, an H+/Ca2+ antiporter from Arabidopsis. *Proc Natl Acad Sci U S A* **93**, 8782-6.

Hood MI, Skaar EP, 2012. Nutritional immunity: transition metals at the pathogen-host interface. *Nat Rev Microbiol* **10**, 525-37.

Hopkins DL, Purcell AH, 2002. *Xylella fastidiosa*: Cause of Pierce's Disease of Grapevine and Other Emergent Diseases. *Plant Dis* **86**, 1056-66.

Ionescu M, Zaini PA, Baccari C, Tran S, Da Silva AM, Lindow SE, 2014. *Xylella fastidiosa* outer membrane vesicles modulate plant colonization by blocking attachment to surfaces. *Proc Natl Acad Sci U S A* **111**, E3910-8.

Janse JD, Obradovic A, 2010. *Xylella fastidiosa*: Its Biology, Diagnosis, Control and Risks. *Journal of Plant Pathology* **92**, S35-S48.

Johnson MDL, Garrett CK, Bond JE, Coggan KA, Wolfgang MC, Redinbo MR, 2011. Pseudomonas aeruginosa PilY1 Binds Integrin in an RGD- and Calcium-Dependent Manner. *PLoS One*.

Jones HE, Holland IB, Baker HL, Campbell AK, 1999. Slow changes in cytosolic free Ca2+ in Escherichia coli highlight two putative influx mechanisms in response to changes in extracellular calcium. *Cell Calcium* **25**, 265-74.

Katzen F, Ferreiro DU, Oddo CG, *et al.*, 1998. Xanthomonas campestris pv. campestris gum mutants: e¡ects on xanthan biosynthesis and plant virulence. *J. Bacteriol* **180**, 1607-17.

Killiny N, Martinez RH, Dumenyo CK, Cooksey DA, Almeida RP, 2013. The exopolysaccharide of *Xylella fastidiosa* is essential for biofilm formation, plant virulence, and vector transmission. *Mol Plant Microbe Interact* **26**, 1044-53.

Kirkby EA, 2008. Maximizing calcium uptake by plants. *Communications in Soil Science and Plant Analysis* **10**, 89-113.

Kirkby EA, Pilbeam DJ, 1984. Calcium as a Plant Nutrient. *Plant Cell and Environment* **7**, 397-405.

Kudla J, Batistic O, Hashimoto K, 2010. Calcium signals: the lead currency of plant information processing. *Plant Cell* **22**, 541-63.

Lahner B, Gong J, Mahmoudian M, *et al.*, 2003. Genomic scale profiling of nutrient and trace elements in Arabidopsis thaliana. *Nat Biotechnol* **21**, 1215-21.

Lecourieux D, Ranjeva R, Pugin A, 2006. Calcium in plant defence-signalling pathways. *New Phytol* **171**, 249-69.

Leite B, Ishida ML, Alves E, Carrer H, Pascholati SF, Kitajima EW, 2002. Genomics and X-ray microanalysis indicate that Ca2+ and thiols mediate the aggregation and adhesion of *Xylella fastidiosa*. *Brazilian Journal of Medical and Biological Research* **35**, 645-50.

Linhartova I, Bumba L, Masin J, *et al.*, 2010. RTX proteins: a highly diverse family secreted by a common mechanism. *FEMS Microbiol Rev* **34**, 1076-112.

Ma W, Qi Z, Smigel A, Walker RK, Verma R, Berkowitz GA, 2009. Ca2+, cAMP, and transduction of non-self perception during plant immune responses. *Proc Natl Acad Sci U S A* **106**, 20995-1000.

Marschner H, 1995. *Mineral Nutrition of Higher Plants*. San Diego, California: Academic Press.

Martelli GP, Boscia D, Porcelli F, Saponari M, 2015. The olive quick decline syndrome in south-east Italy: a threatening phytosanitary emergency. *European Journal of Plant Pathology* **144**, 235-43.

Maser P, Thomine S, Schroeder JI, *et al.*, 2001. Phylogenetic relationships within cation transporter families of Arabidopsis. *Plant Physiol* **126**, 1646-67.

Meng Y, Li Y, Galvani CD, *et al.*, 2005. Upstream migration of *Xylella fastidiosa* via pilus-driven twitching motility. *J Bacteriol* **187**, 5560-7.

Michiels J, Xi C, Verhaert J, Vanderleyden J, 2002. The functions of Ca2++in bacteria: a role for EF-hand proteins? *Trends in Microbiology* **10**, 87-93.

Moens S, Vanderleyden J, 1996. Functions of bacterial flagella. *Crit Rev Microbiol* **22**, 67-100.

Nardini M, Lang DA, Liebeton K, Jaeger KE, Dijkstra BW, 2000. Crystal structure of pseudomonas aeruginosa lipase in the open conformation. The prototype for family I.1 of bacterial lipases. *J Biol Chem* **275**, 31219-25.

Navarrete F, De La Fuente L, 2015. Zinc Detoxification Is Required for Full Virulence and Modification of the Host Leaf Ionome by *Xylella fastidiosa*. *Mol Plant Microbe Interact* **28**, 497-507.

Nicolas O, Charles MT, Jenni S, Toussaint V, Parent SE, Beaulieu C, 2019. The Ionomics of Lettuce Infected by Xanthomonas campestris pv. vitians. *Front Plant Sci* **10**, 351.

Norris V, Grant S, Freestone P, *et al.*, 1996. Calcium signalling in bacteria. *Journal of Bacteriology* **178**, 3677-82.

Nunney L, Schuenzel EL, Scally M, Bromley RE, Stouthamer R, 2014. Large-scale intersubspecific recombination in the plant-pathogenic bacterium *Xylella fastidiosa* is associated with the host shift to mulberry. *Appl Environ Microbiol* **80**, 3025-33.

Oliver JE, Sefick SA, Parker JK, Arnold T, Cobine PA, De La Fuente L, 2014. Ionome changes in *Xylella fastidiosa*-infected Nicotiana tabacum correlate with virulence and discriminate between subspecies of bacterial isolates. *Mol Plant Microbe Interact* **27**, 1048-58.

Orans J, Johnson MD, Coggan KA, *et al.*, 2010. Crystal structure analysis reveals Pseudomonas PilY1 as an essential calcium-dependent regulator of bacterial surface motility. *PNAS* **107**, 5261.

Ottemann KM, Miller JF, 1997. Roles for motility in bacterial-host interactions. *Mol Microbiol* **24**, 1109-17.

Parker JK, Chen H, Mccarty SE, Liu LY, De La Fuente L, 2016. Calcium transcriptionally regulates the biofilm machinery of *Xylella fastidiosa* to promote continued biofilm development in batch cultures. *Environ Microbiol* **18**, 1620-34.

Perez-Donoso AG, Sun Q, Roper MC, Greve LC, Kirkpatrick B, Labavitch JM, 2010. Cell wall-degrading enzymes enlarge the pore size of intervessel pit membranes in healthy and *Xylella fastidiosa*-infected grapevines. *Plant Physiol* **152**, 1748-59.

Porsch EA, Johnson MD, Broadnax AD, Garrett CK, Redinbo MR, St Geme JW, 3rd, 2013. Calcium binding properties of the Kingella kingae PilC1 and PilC2 proteins have differential effects on type IV pilus-mediated adherence and twitching motility. *J Bacteriol* **195**, 886-95.

Punshon T, Hirschi K, Yang J, Lanzirotti A, Lai B, Guerinot ML, 2012. The role of CAX1 and CAX3 in elemental distribution and abundance in Arabidopsis seed. *Plant Physiol* **158**, 352-62.

Purcino RP, Medina CL, Martins De Souza D, *et al.*, 2007. *Xylella fastidiosa* disturbs nitrogen metabolism and causes a stress response in sweet orange Citrus sinensis cv. Pera. *J Exp Bot* **58**, 2733-44.

Reed WP, Williams RC, Jr., 1978. Bacterial adherence: first step in pathogenesis of certain infections. *J Chronic Dis* **31**, 67-72.

Rigden DJ, Galperin MY, 2004. The DxDxDG motif for calcium binding: multiple structural contexts and implications for evolution. *J Mol Biol* **343**, 971-84.

Rinaudi L, Fujishige NA, Hirsch AM, Banchio E, Zorreguieta A, Giordano W, 2006. Effects of nutritional and environmental conditions on Sinorhizobium meliloti biofilm formation. *Res Microbiol* **157**, 867-75.

Robinson JB, Tuovinen OH, Bauer WD, 1992. Role of divalent cations in the subunit associations of complex flagella from Rhizobium meliloti. *J Bacteriol* **174**, 3896-902.

Rodrigues CM, De Souza AA, Takita MA, Kishi LT, Machado MA, 2013. RNA-Seq analysis of Citrus reticulata in the early stages of *Xylella fastidiosa* infection reveals auxin-related genes as a defense response. *Bmc Genomics* **14**.

Rodriguez-Navarro DN, Dardanelli MS, Ruiz-Sainz JE, 2007. Attachment of bacteria to the roots of higher plants. *FEMS Microbiol Lett* **272**, 127-36.

Roper MC, Greve LC, Warren JG, Labavitch JM, Kirkpatrick BC, 2007. *Xylella fastidiosa* requires polygalacturonase for colonization and pathogenicity in Vitis vinifera grapevines. *Mol Plant Microbe Interact* **20**, 411-9.

Rose RK, 2000. The role of calcium in oral streptococcal aggregation and the implications for biofilm formation and retention. *Biochim Biophys Acta* **1475**, 76-82.

Salt DE, Baxter I, Lahner B, 2008. Ionomics and the study of the plant ionome. *Annu Rev Plant Biol* **59**, 709-33.

Sánchez-Rodríguez E, Del Mar Rubio-Wilhelmi M, Cervilla LM, *et al.*, 2010. Study of the ionome and uptake fluxes in cherry tomato plants under moderate water stress conditions. *Plant and Soil* **335**, 339-47.

Sarkisova S, Patrauchan MA, Berglund D, Nivens DE, Franklin MJ, 2005. Calcium-induced virulence factors associated with the extracellular matrix of mucoid Pseudomonas aeruginosa biofilms. *J Bacteriol* **187**, 4327-37.

Scally M, Schuenzel EL, Stouthamer R, Nunney L, 2005. Multilocus sequence type system for the plant pathogen *Xylella fastidiosa* and relative contributions of recombination and point mutation to clonal diversity. *Appl Environ Microbiol* **71**, 8491-9.

Schaad NW, Postnikova E, Lacy G, Fatmi MB, Chang C-J, 2004. *Xylella fastidiosa* subspecies: X. fastidiosa subsp piercei, subsp. nov., X. fastidiosa subsp. multiplex subsp. nov., and X. fastidiosa subsp. pauca subsp. nov. *Systematic and Applied Microbiology* **27**, 763.

Shemarova IV, Nesterov VP, 2005. Evolution of mechanisms of Ca2+-signaling: Role of calcium ions in signal transduction in prokaryotes. *Journal of Evolutionary Biochemistry and Physiology* **41**, 12-9.

Shen Y, Chern M, Silva FG, Ronald P, 2001. Isolation of a Xanthomonas oryzae pv. oryzae flagellar operon region and molecular characterization of flhF. *Mol Plant Microbe Interact* **14**, 204-13.

Silva-Stenico ME, Pacheco FT, Rodrigues JL, Carrilho E, Tsai SM, 2005. Growth and siderophore production of *Xylella fastidiosa* under iron-limited conditions. *Microbiol Res* **160**, 429-36.

Silva MS, De Souza AA, Takita MA, Labate CA, Machado MA, 2011. Analysis of the biofilm proteome of *Xylella fastidiosa*. *Proteome Sci* **9**, 58.

Simpson AJ, Reinach FC, Arruda P, *et al.*, 2000. The genome sequence of the plant pathogen *Xylella fastidiosa*. The *Xylella fastidiosa* Consortium of the Organization for Nucleotide Sequencing and Analysis. *Nature* **406**, 151-9.

Smith RJ, 1995. Calcium and bacteria. *Advances in Microbial Physiology* **37**, 83-133.

Stevenson JF, Matthews MA, Rost TL, 2005. The Developmental Anatomy of Pierce's Disease Symptoms in Grapevines: Green Islands and Matchsticks. *Plant Dis* **89**, 543-8.

Sun Q, Sun Y, Walker MA, Labavitch JM, 2013. Vascular occlusions in grapevines with Pierce's disease make disease symptom development worse. *Plant Physiol* **161**, 1529-41.

Van Sluys MA, De Oliveira MC, Monteiro-Vitorello CB, *et al.*, 2003. Comparative analyses of the complete genome sequences of Pierce's disease and citrus variegated chlorosis strains of *Xylella fastidiosa*. *J Bacteriol* **185**, 1018-26.

Wang SL, Fan KQ, Yang X, Lin ZX, Xu XP, Yang KQ, 2008. CabC, an EF-hand calcium-binding protein, is involved in Ca2+-mediated regulation of spore germination and aerial hypha formation in Streptomyces coelicolor. *J Bacteriol* **190**, 4061-8.

Wells JM, Raju BC, Hung HY, Weisburg WG, Mandelcopaul L, Brenner DJ, 1987. Xylella-Fastidiosa Gen-Nov, Sp-Nov - Gram-Negative, Xylem-Limited, Fastidious Plant Bacteria Related to Xanthomonas-Spp. *International Journal of Systematic Bacteriology* **37**, 136-43.

Werthen M, Lundgren T, 2001. Intracellular Ca(2+) mobilization and kinase activity during acylated homoserine lactone-dependent quorum sensing in Serratia liquefaciens. *J Biol Chem* **276**, 6468-72.

Wilson JW, Schurr MJ, Leblanc CL, Ramamurthy R, Buchanan KL, Nickerson CA, 2002. Mechanisms of bacterial pathogenicity. *Postgrad Med J* **78**, 216-24.

Yuan X, Morano L, Bromley R, Spring-Pearson S, Stouthamer R, Nunney L, 2010. Multilocus sequence typing of *Xylella fastidiosa* causing Pierce's disease and oleander leaf scorch in the United States. *Phytopathology* **100**, 601-11.

Zaini PA, Fogaca AC, Lupo FG, Nakaya HI, Vencio RZ, Da Silva AM, 2008. The iron stimulon of *Xylella fastidiosa* includes genes for type IV pilus and colicin V-like bacteriocins. *J Bacteriol* **190**, 2368-78.

Zhou Y, Yang W, Kirberger M, Lee HW, Ayalasomayajula G, Yang JJ, 2006. Prediction of EF-hand calcium-binding proteins and analysis of bacterial EF-hand proteins. *Proteins* **65**, 643-55.

Chapter 2

The phage moron *PD0913,* transcriptionally regulated by calcium, is a negative regulator of twitching motility, cell adhesion and virulence in *Xylella fastidiosa.*

ABSTRACT

Xylella fastidiosa (Xf) is a plant pathogenic bacterium that lives in the xylem vessels of plants and the foregut of sharpshooter vectors, causing diseases worldwide. Virulence mechanisms of Xf involve systemic colonization of host plants through twitching movement, and development of biofilm leading to xylem vessel occlusion and water stress. Previous studies showed that Xf infection triggers a host response that leads to accumulation of calcium (Ca), and Ca is used by Xf to enhance its virulence traits. *PD0913*, which is annotated as phage-related gene, is transcriptionally regulated by Ca and was selected for functional analysis. PD0913 protein sequence has Ca-binding motifs and is part of a putative genomic island absent in a non-virulent strain, as revealed by comparative genomics. A *PD0913* mutant was generated by site-directed mutagenesis and characterized *in vitro* and *in planta* to determine the role of this gene in bacterial virulence under different Ca concentrations. Results showed that the absence of *PD0913* increased twitching motility, surface attachment at 2 mM Ca concentration, and virulence at 8 mM Ca concentration, compared to the WT. This suggests that PD0913 negatively regulates twitching motility, attachment, and virulence of *X. fastidiosa* under different levels of Ca concentrations.

INTRODUCTION

Xylella fastidiosa is a xylem-limited bacterium that is transmitted by sharpshooter insect vectors and has been associated with a large number of diseases in many economically important crops worldwide [1,2]. This bacterium causes Pierce's disease of grapevine (PD), citrus variegated chlorosis (CVC), and most recently olive quick decline syndrome (OQDS) that is affecting olive crops in Europe [3]. The virulence of *X. fastidiosa* involves colonization of host plants through twitching movement and development of biofilm leading to vessel occlusion and water stress [1,4].

Understanding the dynamics during the interaction between plant and pathogen is key to develop strategies to control disease. Mineral elements are required for various processes in the host plant and the pathogen, therefore ionome studies (i.e., quantification of mineral nutrient and trace elements composition) [5,6] have been useful to understand plant-pathogen interactions [6-9]. Essential micro- and macronutrients such as calcium (Ca) are required for a myriad of functions within cells and are under tight homeostatic control [10]. Ionomic studies identified that Ca concentration significantly increased in tobacco plants infected with *X. fastidiosa* [8]. Supplementation of Ca to cultures of *X. fastidiosa* increase biofilm formation, surface attachment, cell-to-cell aggregation, and twitching motility [11]. When ionome of *X. fastidiosa* was compared between biofilm and planktonic cells, Ca was significantly accumulated in biofilm cells together with other elements including copper (Cu), potassium (K), manganese (Mn), and zinc (Zn) [6] . The effect of Ca on twitching motility in *X. fastidiosa* was associated with a specific homologue of *pilY1*, a gene that is part of the type IV pilus and contains a Ca-binding motif [12]. Other *X. fastidiosa* genes regulating the effect of Ca on twitching motility or biofilm have not yet been identified.

Previous studies by our group using whole transcriptome characterization by RNA-Seq identified genes differentially expressed at higher concentrations of Ca [13]. Among these genes was *PD0913* that is annotated as a "phage-related protein" and has a Ca-binding motif [13]. The strong differential expression of this uncharacterized, phage-related gene in the putative genomic island comprising the open reading frames PD0906-PD0943 suggests that it may have a role in *X. fastidiosa* responses to changes of Ca concentration in the medium [13]. In addition, the absence of *PD0913* in the avirulent strain EB92-1 [13] and its presence in the other virulent strains suggest that this gene might be related to virulence traits in *X. fastidiosa*. The characteristic of being a phage related gene that has been retained prompted us to investigate if the gene could be classified as a phage moron defined as a former phage gene that adds more to the genome of the host. Therefore, the objective of this study was to perform the functional characterization of the uncharacterized *PD0913* gene under different concentrations of Ca *in vitro* and *in planta* to understand its role in the virulence of this pathogen. Our results indicate that this gene may be a negative regulator of twitching movement, surface attachment and plant virulence, and its effects are regulated by Ca concentration in the medium.

MATERIALS AND METHODS

Bacterial strains and culture conditions

X. fastidiosa strain TemeculaL [14] was used in this study as wild type (WT). Both WT and Δ*PD0913* were grown in Periwinkle Wilt (PW) [15] and PW with kanamycin (Km; 50 μg mL^{-1}) agar plates, respectively, and incubated at 28 ºC. All cell suspensions of *X. fastidiosa* were prepared as follows. After being recovered from -80 ºC glycerol stocks, cells were re-streaked and 7-days-

old bacteria were harvested using sterile loops and suspended in Pierce's Disease 2 (PD2) [15] broth to an optical density ($OD_{(600nm)}$) of 0.8. For plant inoculation experiments, bacterial suspensions were prepared using Phosphate-Buffered Saline (PBS) instead of PD2 [8].

Selection of *PD0913* gene and construction of the Δ*PD0913* mutant

PD0913 was identified using the BlastX program from the National Center for Biotechnology Information (NCBI) database. Conserved domains were identified in the protein sequence of the gene using MEME (Multiple Em for Motif Elicitation) [16] and Motif-based sequence analysis tools (FIMO) [17]. The cellular localization of PD0913 was obtained using Cell-Ploc 2.0 tool [18].

Natural competence and homologous recombination were used to generate *X. fastidiosa* Δ*PD0913* null mutant through site-directed mutagenesis, according to a protocol described elsewhere [19]. Briefly, genomic DNA of *X. fastidiosa* WT was extracted using a modified protocol of cetyltrimethylammonium bromide (CTAB) [20], and flanking upstream and downstream regions of the open reading frame (ORF) were amplified by PCR using two primer pairs (Table 1) that contain overlapping sequences to the Km resistance cassette from pUC4k. PCR products of the three fragments (upstream region, downstream region and Km) were purified using the Gel/PCR DNA Fragments Extraction kit (IBI Scientific, Chavenelle, IA). To obtain the fused PCR construct to mutate *PD0913*, an overlap-extension PCR was performed using as templates the three PCR products previously obtained. Purification of the fused PCR product was performed, and 10μL of it were mixed with WT cells (suspension at OD_{600nm} =0.25) on PD3 agar plates for transformation through natural competence. After DNA and cells settled for an hour, plates were incubated for 3 days at 28 ºC. Then, cells were harvested and suspended in 200 μL of PD3 [21] broth. Serial

dilutions were made and bacterial suspensions of 100 µL and 20 µL were plated onto PW with Km for selection until transformants were confirmed by PCR and whole genome sequencing using an Illumina Miseq sequencing platform (data not shown).

Table 1. Primers used in this study

Primer name	Function/Target	Sequence	Source
F1	Upstream *PD0913*	5'ATTGTTCTGTGGGCGTGTGT3'	This study
R1-KAN	Upstream *PD0913*	5'GGTATGAGTCAGCAACACCTTCGCGGCTAGTCCCAAAAA3'	This study
F3-KAN	Downstream *PD0913*	5'GTAACATCAGAGATTTTGAGGGAGTAGCGGTAATGCCTACTTT3'	This study
R3	Downstream *PD0913*	5'GCACACAAAGGAATGAGAAGAA3'	This study
KAN-F	Kanamycin cassette	5'AAGGTGTTGCTGACTCATACC3'	This study
KAN-R	Kanamycin cassette	5' CTCAAAATCTCTGATGTTAC3'	This study

Mutation was confirmed by whole genome sequence. For Illumina Miseq sequencing, cells cultured on PW agar plates were suspended in 400 µl of sterile MilliQ water and DNA was extracted using a modified CTAB protocol [20]. Extracted DNA was run through gel electrophoresis (1% agarose gel in TAE buffer) to detect RNA contamination followed by treatment with RNase A (ThermoFisher Scientific). Both DNA and RNA concentrations were verified with a Qubit® 2.0 Fluorimeter (Life Technologies, CA, USA) using the Qubit dsDNA and Qubit RNA HS Assay Kit (Thermo Fisher Scientific), respectively. DNA samples of 20 ng were then adjusted to 50 µl (2.5 ng/µl) volume by diluting in sterile MilliQ water. Samples were submitted to the Novogene Corporation Inc. for library preparation and sequencing. Paired-end reads were generated by multiplexing 12 libraries in a single lane on an Illumina MiSeq Micro (PE150) platform. Sequence adapter filtering, quality trimming and contaminant removal was

performed using BBDuk (https://jgi.doe.gov/data-and-tools/bbtools/bb-tools-user-guide/bbduk-guide/). De novo assemblies were constructed with SPAdes version 3.5.0 [22] with kmers of 127, 117, 107, 97, 87, 77, 67 using the 'careful' flag. Genome statistics including GC content, contig number, N50 and genome length were calculated with QUAST web interface [23].

Growth curves, planktonic and biofilm quantification at different Ca concentrations

Growth characteristics were quantified according to previously described methods [11]. Briefly, seven days-old cultures of TemeculaL WT and Δ*PD0913* grown in PW plates and PW+Km, respectively, were harvested and suspended in PD2 broth and PD2 broth supplemented with 2 mM and 4 mM Ca. Optical density was adjusted to OD_{600nm}= 0.8. Sterile polystyrene 96-well plates containing 190 µL PD2 broth per well were inoculated with 10 µL of the cell suspension. After 7 days of incubation in shaking conditions at 150 rpm and 28 °C, the total, planktonic (cells in suspension), and biofilm (cells adhered to the substrate) growth of cells were estimated by measuring OD_{600nm}. OD_{600nm} values were measured using Cytation 3 multimode imaging reader (BioTek Instruments Inc, Winooski, VT) and were adjusted by subtracting values from control wells. Growth rates were calculated as the slope of the line obtained by natural log-transformed growth values at the exponential growth phase (approximately 2 to 5 days) using the formula {rate = [ln (OD day 5) – ln (OD day2)]/time}. Planktonic growth was quantified by transferring the medium containing cells in suspension onto a new plate. The original 96-well plate was then rinsed 3 times with sterile Milli-Q water, biofilm was stained with 230 µL of 0.1% crystal violet for 20 min and the plate was rinsed once again three times with sterile Milli-Q water. At last, 230 µL of 95% ethanol was added and plates were agitated for 5 min at 150 rpm. The OD_{600nm} of plates was measured to quantify biofilm growth [24].

Quantification of twitching motility on agar plates and microfluidic chambers

Twitching motility was evaluated on PW without BSA agar plates, as previously described [11] with some modifications. Plates were supplemented with 2 mM, 4 mM Ca or 1.5 mM Egtazic acid (EGTA, a Ca chelator), while non-supplemented PW was used as control. Spots of TemeculaL WT and Δ*PD0913* cells were made in quadruplicate onto PW without BSA agar plates. After 4 and 7 days of incubation at 28 °C, the colony peripheral fringe morphology was examined under a Nikon Eclipse Ti inverted microscope (Nikon, Melville, NY), and the fringe width was measured (n=5) for each of the 4 colonies on each plate by using NIS- Elements software (Nikon, Melville, NY). Each treatment was replicated on 3 plates, for a total of 60 measurements per treatment.

Additionally, the twitching speed of WT and Δ*PD0913* cells was assessed using microfluidic chambers mounted onto an inverted microscope as previously described [11,25]. Briefly, the microfluidic chamber consists of a molded body of polydimethylsiloxane (PDMS) between a cover slide and a glass microscope slide. The design consists of two parallel microchannels (80 µm wide by 3.7 cm long and 50 µm deep). Two inlets and two outlets allow the flow media with the suspended bacteria to enter the chamber separately. Both channels can be simultaneously monitored under the microscope (Supplementary figure S1). Cell suspensions of each strain were introduced into the chambers together with PD2 broth as control and PD2 broth supplemented with 2 mM Ca independently and incubated for 2 h at a controlled flow rate of 0.25 µL min^{-1} to allow cells to attach to the glass slide surface. After that, time-lapse images were recorded every 30s for 1 h. The movement of *X. fastidiosa* cells was quantified by tracking their positions frame by frame, and the cell speed was calculated by measuring the up-stream

displacement over time. Three independent experiments were performed for each concentration of Ca.

Transmission electron microscopy

TEM imaging was used to observe the presence of type IV pili (structure involved in twitching motility). Strains were cultured as mentioned above and then transferred into PD3 agar plates for 3 days. Cells from the edges of the colony were suspended in 100 µL sterile water. 10 µL of this suspension was transferred to a formvar-carbon coated TEM grid, and cells were allowed to settle for 10 min. The leftover liquid was blotted out with a filter paper. The grid was then negatively stained with 6 µL of phosphotungstic acid (PTA) for 10 seconds, and, after removing the excess PTA, grids were air dried and observed under a Zeiss EM10 transmission electron microscope (Carl Zeiss, Oberkochen, Germany). Images were acquired with MaxIm DL software (Diffraction LTD, Ottawa, Canada).

Evaluation of adhesion force in microfluidic chambers

The strength of cell attachment to surfaces was evaluated using microfluidic chambers, as previously described [11,25]. Both strains were suspended in PD2 broth or PD2 broth supplemented with 2 mM Ca. The bacterial suspensions were introduced into the microfluidic channels (22 °C) through 1-mL plastic syringe connected to the chamber. Medium flow was introduced by a 5-mL plastic syringe controlled by an automated syringe pump (Pico Plus; Harvard Apparatus, Holliston, MA). The microfluidic chambers were mounted onto a Nikon Eclipse Ti inverted microscope (Nikon, Melville, NY) and observed at 40 X phase-contrast optics to monitor cell attachment. Medium speed flow was maintained at 0.25 µl min^{-1}, allowing cells to be attached (~2h). Then, the flow speed was adjusted to 1.0 µl min^{-1} for 1 h to remove non-attached cells. The medium flow

was then sequentially increased every 1 min by 10 µl min^{-1} from 1 to 120 µl min^{-1} to gradually remove the attached cells. Time-lapse microscopy images were acquired every 5 s during this time with a Nikon DS-Q1 digital camera (Nikon, Melville, NY) controlled by NIS-Elements software (Nikon, Melville, NY) to record the detachment of *X. fastidiosa* cells. The number of attached cells remaining in each frame was scored by using NIS-Elements software. The cell adhesion force and the percentage of attached cells were calculated as previously described [11,25]. Each treatment was evaluated four times in independent microfluidic chamber experiments.

Greenhouse Experiments

Seeds of *Nicotiana tabacum* 'Petite Havana SR1' (Plant Introduction (PI) number 552516) were germinated in Sunshine Mix #8 (Sun Gro Horticulture Canada Ltd., Vancouver, Canada). These plants were used to study host interactions with *X. fastidiosa* as previously described [8]. Greenhouse temperature was maintained between 20–25 °C and natural sunlight was used. After one month, 100 seedlings were transplanted into 4.5-inch pots. Plants were fertilized three times using Osmocote 19-6-12 (The Scotts Company, Marysville, OH). 30 to 40 days post-transplant, tobacco plants were inoculated with *X. fastidiosa* following a method previously described [8,26]. Briefly, a cut on the top of the stem leaving three healthy adult leaves in the lower portion of the plant was made. These plants were ready for inoculation and this point was determined as time zero. Cells of *X. fastidiosa* strain TemeculaL WT [14] and Δ*PD0913* were cultured on PW and PW+Km agar plates, respectively, at 28 ºC for 7 days. Bacteria were harvested from the plates and suspended in PBS to an optical density of OD_{600nm}= 0.8. Inoculation was performed on the base of the petiole through pinprick using a 23-gauge needle. A volume of 20 µL of inoculum was applied per leaf. Ten plants were used for each treatment infected with either WT, Δ*PD0913*, or PBS

(control plants), and 3 independent experiments were conducted (total of 30 plants were assessed per treatment). A second inoculation was performed one week after the first inoculation, following the same procedure described above. Once a week, Ca-amended treatment was applied on the base of plants with a solution of 100 mL of water (non-treated control), or water amended with 4 mM Ca or 8 mM Ca for each treatment. After 10 to 12 weeks of inoculation, symptoms were apparent and from that time point a weekly evaluation of plants was performed to determine measurements of incidence and severity. Incidence was determined by the proportion of plants showing leaf scorch per treatment, while severity was determined by the percentage of leaves showing symptoms of leaf scorch per plant. At the last time point of evaluation (5-6 weeks), samples were collected for further analysis by inductively coupled plasma with optical emission spectroscopy (ICP-OES) and qPCR, as described below.

Quantitative polymerase chain reaction (qPCR) was used to quantify the total population of *X. fastidiosa in planta*, as previously described [8,27]. Briefly, at the final time point of symptom evaluation, leaf petioles of plants from each treatment were collected. Fresh petioles were cut into small pieces and ~100 mg was selected for later analysis. Petiole samples were ground by using a mini Beadbeater 96 (Biospec Products, Bartlesville, OK) with 2.0 mm zirconia beads (Biospec Products, Bartlesville, OK) for 2-3 min at the highest speed. 1.5 mL PD2 broth was added to samples and mixed thoroughly. 500 µL-samples were stored at -20 ℃ and used for total *X. fastidiosa* population quantification by qPCR [8,28] after DNA extraction was performed as previously described.

Ionome Characterization

For leaf ionome analysis, five leaves from 5 different plants treated with 0 mM, 4 mM and 8 mM Ca were selected, following a previous protocol described with some modifications [8]. Briefly, leaves were dried at 65 ºC for 1 hour and then crushed to a fine powder using mortar and pestle. 10 mg of dry weight were sampled for each leaf and digested with 200 mL of mineral-free concentrated nitric acid (OPTIMA, Fisher Scientific, Waltham, MA) for 1 hour at 100 °C. 800 mL of ultra-pure, mineral-free water were added, and the samples were centrifuged at 13,000x g for 5 minutes to remove any remaining particles. Samples were analyzed by ICP-OES (Perkin Elmer 7100 DV, Waltham, MA) with simultaneous measurement of Ca, Cu, iron (Fe), K, magnesium (Mg), Mn, sodium (Na), phosphorus (P), and Zn. Mineral concentrations were determined by comparing emission intensities to a standard curve obtained from certified mineral standards (SPEX CertiPrep, Metuchen, NJ). Standard curves were confirmed by a re-analysis of standard solutions diluted in a matrix equivalent to the sample. Individual readings were the average of two intensity measurements and varied by less than 5%. Repeated analysis of different amounts (5 and 10 mg) of individual samples showed less than 5% variation.

For sap ionome analysis, five different plants from each treatment were selected. Sap samples were collected using a Scholander pump model 600 (PMS Instruments Company, Corvalis, OR) as previously described [9]. Approximately 100 µL of sap from each plant were sampled and stored overnight at -20° C. Then, samples were diluted using mineral-free water (1:8) for a total volume of 400 µL and analyzed by ICP-OES, as described above for leaf samples.

Statistical analyses

Data from planktonic growth, biofilm formation, twitching motility, adhesion force, disease severity analysis and Ca ionome of sap and leaves were analyzed according to the Holm-Sidak test using SigmaPlot software (Systat Software Inc., San Jose, CA). Total growth curve, total ionome characterization and percentage of attachment assays were analyzed by two-tailed Student's *t*-test.

RESULTS

In silico analysis of the *PD0913* gene of *X. fastidiosa*

In silico analysis was performed with *PD0913* since this gene is annotated as a "phage-related protein" with unknown function. The 1,527 bp (475 amino acids) open reading frame was aligned to all *X. fastidiosa* genomes available at NCBI using BlastN. Only one copy of the gene was found in the genomes of wild-type (WT) *X. fastidiosa* strains TemeculaL and Ann-1 while two homologous sequences (*PD0913* and *PD0926*) were found in *X. fastidiosa* strain Temecula1. Noteworthy, no copy of this gene was found in the avirulent strain EB92-1, confirming previous results [11,13]. Consistent with previous bioinformatic analysis [13], FIMO motif search tool identified a Ca-binding-related (Dx[DN]xDGxxD) motif located in the C-terminal region of PD0913. Moreover, 28 additional motifs were found in the protein sequence using the MEME tool analysis (Supplementary Table S1). Three main motifs were found in the scan: glycosylation, phosphorylation and myristoylation. Localization of the protein was determined by Cell-Ploc 2.0 to be on the periplasm, in accordance with the presence of a signal peptide sequence found at the 18^{th} position of the protein sequence flanked by the N-terminal. For functional analysis, site-directed mutagenesis was performed in *X. fastidiosa* strain TemeculaL and deletion was confirmed

by the absence of the *PD0913* gene and insertion of a Km-resistance cassette by PCR and whole genome sequencing analysis (data not shown). The generated mutant will be referred to as Δ*PD0913* from hereafter.

PD0913 affects planktonic growth and biofilm formation of *X. fastidiosa*

To characterize the effect of *PD0913* mutation in *X. fastidiosa*, growth curves, planktonic growth and biofilm formation were evaluated at different concentrations of Ca: 0 mM, 2 mM and 4 mM. Growth curves indicated reduced growth of Δ*PD0913*, showing significantly lower OD_{600} measurements than the WT in all Ca concentrations (Figure 1A). Since total growth measurements are affected by cells attaching to the side of the wells and/or precipitating, we calculated growth rates. No significant differences in growth rates were observed between the WT and mutant at any Ca concentration (Figure 1B). Planktonic growth was analyzed by measuring the supernatant of cultures at the final time point of evaluation, while biofilm formation was measured by staining cells attached to the 96-well plates with crystal violet. Similar planktonic growth tendencies were observed for both strains at different concentrations of Ca (0 mM, 2 mM and 4 mM), with planktonic cells being significantly higher in WT. Reduced planktonic growth was observed in both strains at 4 mM Ca, which was still significantly lower for Δ*PD0913* when compared to WT (Figure 1C). After 7 days post-inoculation (dpi), biofilm formation in PD2 medium and PD2 supplemented with 2 mM and 4 mM Ca was quantified for each strain. Biofilm formation of TemeculaL WT and Δ*PD0913* was significantly higher at 2 mM and 4 mM Ca compared to unamended PD2 media. No significant difference was observed between strains at 0 mM concentration (Figure 1D), however, biofilm formation was significantly different between Δ*PD0913* and WT at higher Ca concentrations (Figure 1D). To verify the higher biofilm formation

by the mutant at 4 mM Ca, this trait was also analyzed using Erlenmeyer flasks with continuous agitation. In this experimental set-up, Δ*PD0913* formed a thicker biofilm at 2 mM and 4 mM Ca concentration and remained attached throughout the assay, while the biofilm of WT cells was easily detached from the flask surface (Supplementary figure S2).

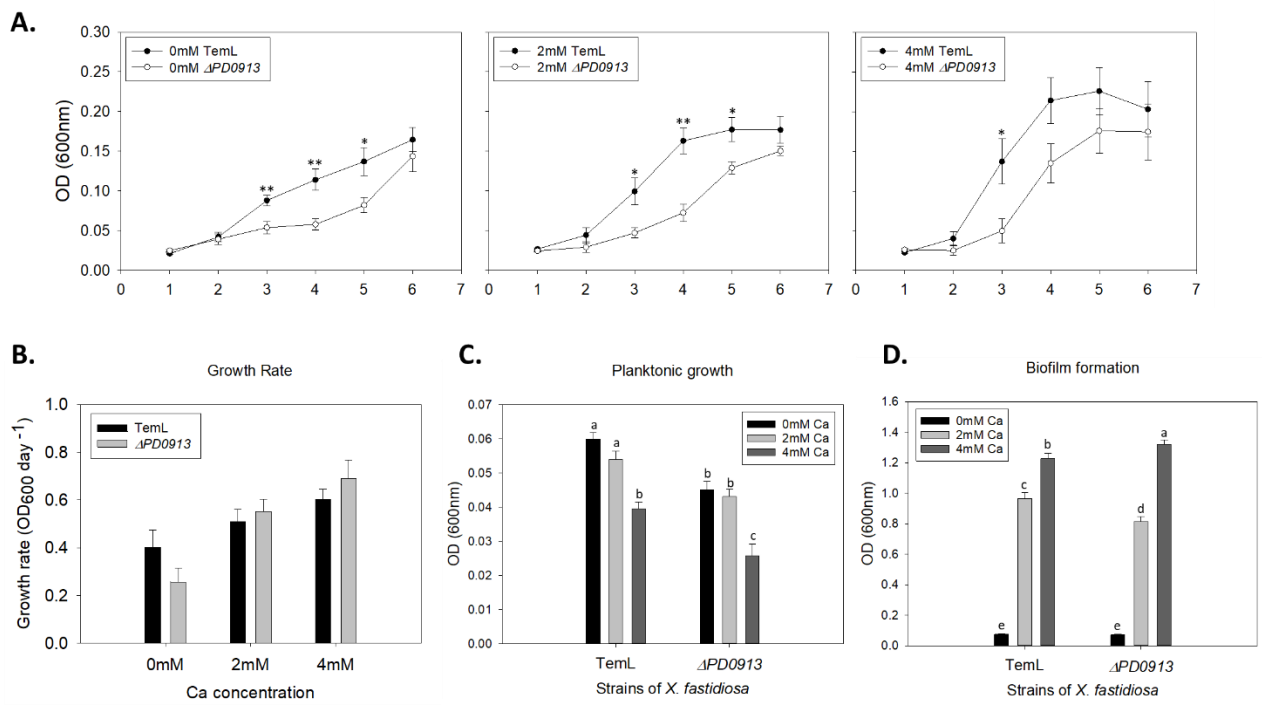

Figure 1. Growth curve, planktonic growth and biofilm formation quantification of *X. fastidiosa* WT and Δ*PD0913*. Both strains were grown in 96-well plates for 7 days in PD2 medium supplemented with 0 mM, 2 mM and 4 mM concentrations of $CaCl_2$. **A.** Growth curves of WT and Δ*PD0913* was measured daily by OD_{600nm} and plotted according to the Ca concentration in the media. **B.** Growth rate was calculated from the growth curve at the exponential growth phase (2 to 5 days). No significant statistical differences were observed among samples. **C.** Planktonic cells were collected from the supernatant and assessed by measuring OD_{600nm}. **D.** Biofilm formation was quantified by measuring the OD_{600nm} after crystal violet staining of attached cells.

Experiments were repeated independently six times. Mean values are shown in charts, and error bars represent standard error of the means. * and ** indicate significant differences ($p < 0.05$ and $p < 0.01$, respectively) of means between WT and Δ*PD0913*, as analyzed by the two-tailed Student's *t*-test. Letters above bars indicate significant differences ($p < 0.05$) according to one-way ANOVA - Holm-Sidak test (all pairwise multiple comparison procedures).

Deletion of *PD0913* results in higher twitching motility of *X. fastidiosa*

Twitching motility of WT and Δ*PD0913* was quantified by measuring colony fringe width of cells grown in PW without BSA agar plates supplemented with 0 mM, 2 mM and 4 mM Ca and 1.5 mM EGTA (Ca-chelator, negative control). Results revealed a wider peripheral fringe for Δ*PD0913* in comparison to WT at 0 mM, 2 mM and 4 mM Ca at four days evaluation (Figure 2A). The analysis of measurements of fringe width in Δ*PD0913* at both concentrations of 0 mM (mean = 65.11 µm ± 3.71) and 2 mM Ca (mean = 72.13 µm ± 2.43) showed that the mutant had significantly higher movement than WT at these two treatments (0 mM mean = 36.66 ± 4.47; and 2 mM mean = 53.30 ± 3.93). This suggests that the mutant had a greater rate of motility at 0 mM and 2 mM Ca (Figure 2B).

Since twitching motility increased on plates supplemented with Ca, we used microfluidic chambers to quantify the speed of movement of both strains growing under flow conditions at 0 mM and 2 mM Ca. Results showed a correlation with the observations obtained from colony fringe measurements. Ca significantly increased the movement of Δ*PD0913* cells (mean = 0.94 µm min^{-1}) compared to TemeculaL WT (mean = 0.52 µm min^{-1}) at 2 mM Ca. In addition, even when no Ca was supplemented to the medium, significant differences were observed between Δ*PD0913* (mean = 0.40 µm min^{-1}) and WT (mean = 0.33 µm min^{-1}) (Figure 2C).

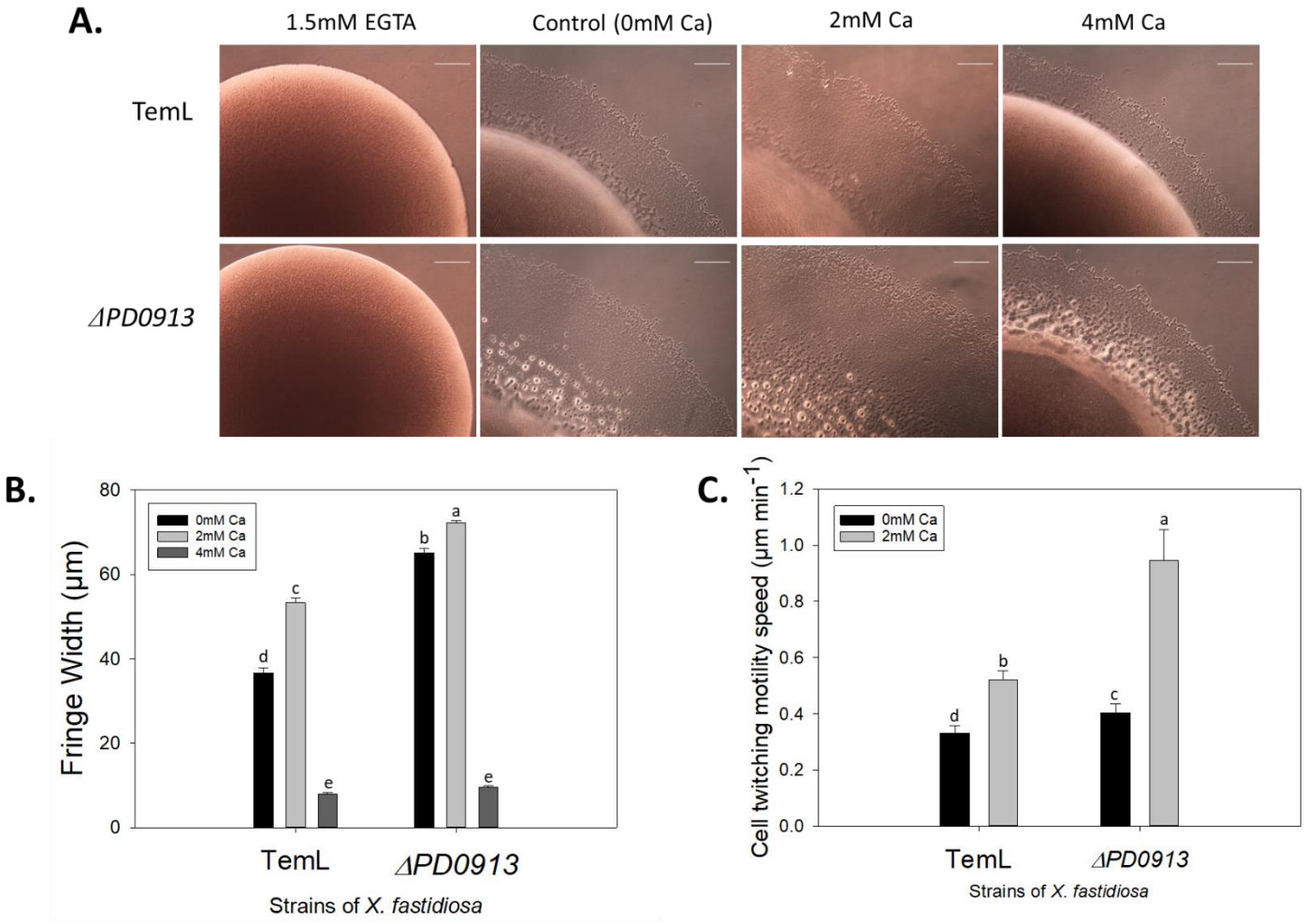

Figure 2. Twitching motility analysis of WT and Δ*PD0913* in different concentrations of Ca. A. Representative micrographs of colony fringe width of WT and Δ*PD0913* on PW without BSA plates supplemented with 0 mM, 2 mM and 4 mM Ca and 1.5 mM EGTA were analyzed after 4 days using an inverted microscope. Scale bar = 10 µm. **B.** Measurements of colony fringe width of WT and Δ*PD0913* on PW without BSA medium supplemented with 0 mM, 2 mM and 4 mM Ca. Means of measures of colony fringe width (n=15) for each treatment were plotted. **C.** Assessment of twitching motility speed of cells incubated in PD2 broth and PD2 broth

supplemented with 2 mM Ca in microfluidic chambers. Mean values are shown in charts. Three independent experiments were performed under the same conditions for all assays. Error bars represent standard error of the means. Letters above bars indicate significant differences ($p < 0.05$) according to the one-way ANOVA - Holm-Sidak test (all pairwise multiple comparison procedures).

Lastly, morphology of Δ*PD0913* and WT cells was visualized by TEM, since twitching assays showed a significant difference between their movement and speed. Micrographs revealed that both strains showed presence of Type I and Type IV pili, with no clear phenotypic differences among their pili (Figure 3).

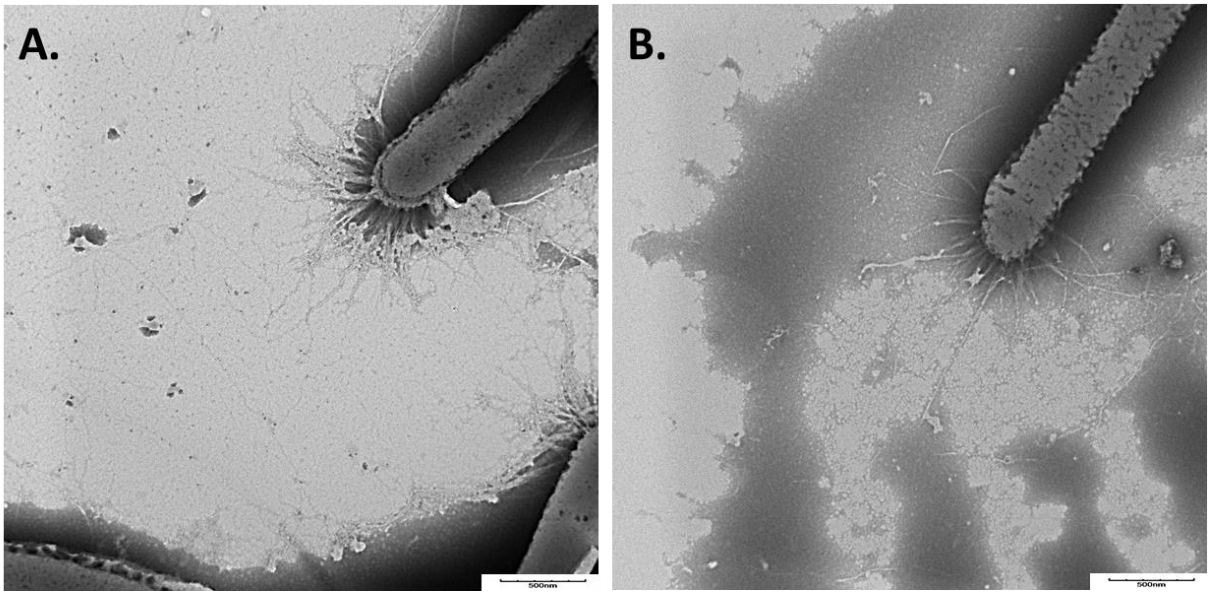

Figure 3. Transmission electron micrograph of negatively stained *X. fastidiosa strains*. **A.** TemeculaL (WT) **B.** Δ*PD0913* cells.

Ca increased substrate adhesion force in Δ*PD0913*

To assess bacterial attachment to surfaces under different medium conditions (PD2 broth and PD2 broth supplemented with 2 mM Ca), microfluidic chambers were used to measure adhesion force (AF) and quantify percentage of attached cells. Results showed that the addition of 2 mM Ca significantly (p = 0.022) increased AF of Δ*PD0913* cells (AF = 252 pN) compared to WT (AF = 215 pN). Although not significant (p = 0.053), the same tendency was observed with unamended medium, in which AF values were 235 pN for Δ*PD0913* and 205 pN for WT cells (Figure 4A). Percentage of cells attached to the microfluidic chamber at 0 mM was similar for both strains. Significant differences were found at 50 and 90 µm min^{-1}, while no significant difference was observed in any of the other evaluated flow rates (Figure 4B). Interestingly, at 2 mM Ca, a significant increase in the percentage of attached cells is observed from 60 through 120 µm min^{-1} in Δ*PD0913*, in comparison to WT (Figure 4C).

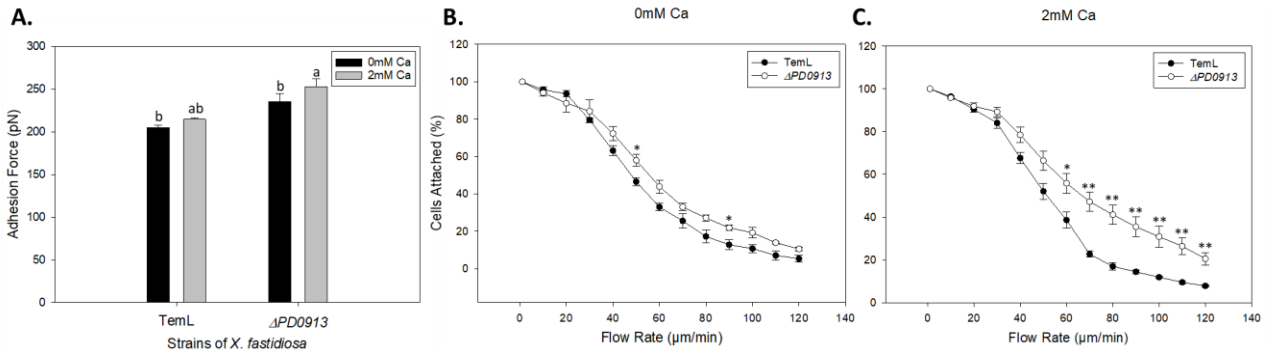

Figure 4. Adhesion force of *X. fastidiosa strains*. A. Measurement of adhesion force. WT and Δ*PD0913* cells were inoculated into PD2 broth and PD2 broth supplemented with 2 mM Ca in microfluidic chambers. Adhesion force was calculated as the ability of cells to remain attached to microfluidic chambers with increasing flow rates of medium broth. **B.** Number of *X. fastidiosa* cells attached to the microfluidic chamber surface with increasing flow rates. Data represent results

observed for WT and Δ*PD0913* cells inoculated into PD2 broth (0 mM Ca) **C.** Same analysis as in **B** for PD2 broth supplemented with 2 mM Ca. Four independent experiments were performed under the same conditions for all assays. Mean values are shown in charts, and error bars represent standard error of the means. Letters above bars indicate significant differences ($p < 0.05$) according to the one-way ANOVA - Holm-Sidak test (all pairwise multiple comparison procedures). * and ** indicate significant differences ($p < 0.05$ and $p < 0.01$, respectively) of means between WT and Δ*PD0913*, as analyzed by the two-tailed Student's *t*-test.

Ca supplementation in drench water increased *X. fastidiosa* virulence on tobacco plants infected with Δ*PD0913* compared to WT

Tobacco ('Petite Havana SR1') plants were inoculated with WT and Δ*PD0913* strains and virulence was assessed. Disease severity measurements expressed by leaf scorch percentage showed no significant difference between both strains when plants were watered with 0 mM and 4 mM added Ca concentration (Figure 5). Nevertheless, when watering was amended with 8 mM Ca concentration, plants infected with Δ*PD0913* showed higher values of disease severity than the WT from week 4 until week 6 of evaluation. In these time points of evaluation (weeks 4, 5 and 6), the percentage of leaf scorch in plants infected with Δ*PD0913* was, respectively, 55% ($p = 0.047$), 63% ($p = 0.046$) and 83% ($p = 0.044$); while plants infected with WT only reached 38%, 48% and 69% of disease severity (Figure 5).

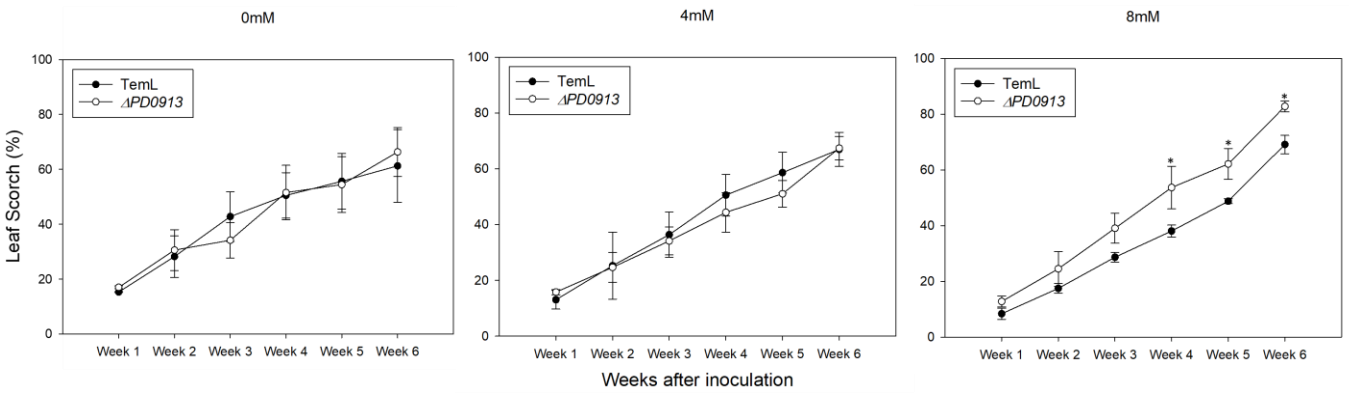

Figure 5. Disease severity analysis of WT and Δ*PD0913* in tobacco plants. Data on charts represent mean values of the percentage of leaves showing leaf scorch symptoms in tobacco plants (n=9) grown under greenhouse conditions and watered with either 0 mM, 4 mM and 8 mM of added Ca concentration. Plants were inoculated with either WT, Δ*PD0913* or PBS (control). Error bars represent standard error of the means. Three independent experiments were performed under the same conditions. Data shown in charts correspond to one representative experiment. * and ** indicate significant differences ($p < 0.05$ and $p < 0.01$, respectively) of means between WT and Δ*PD0913*, as analyzed by the two-tailed Student's *t*-test.

This difference in disease severity between strains at 8 mM Ca concentration was more evident when the position of the symptomatic leaves along the plant was considered, showing different spatial distribution of symptomatology between WT and mutant. Disease development was assessed considering relative position of leaves (leaves were numbered # 1-10 starting from the bottom of each plant). Leaves in the 1-4 position were the first to show symptoms (Figure 6). Once symptoms were detected above these leaves, they rapidly spread acropetally to the rest of the plant. The distribution of symptoms along each plant was similar between Δ*PD0913* and WT at 0 mM and 4 mM Ca amendments. However, at 8 mM Ca it was observed that leaves at higher

positions (# >4) showed consistently more symptoms in Δ*PD0913* than in WT after week 2 (Figure 6, charts in the right column).

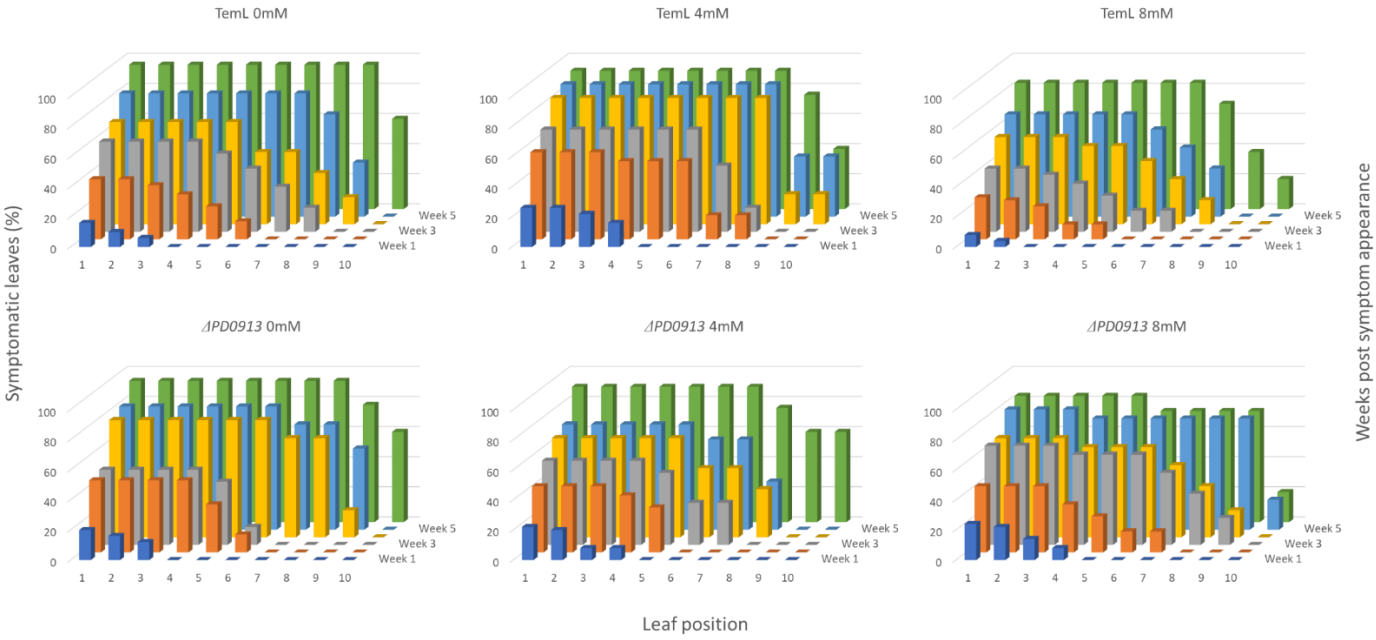

Figure 6. Progression of symptoms development in tobacco plants infected with the two strains of *X. fastidiosa* at different concentrations of Ca. Percentage of symptomatic leaves showing leaf scorch during six weeks of evaluation were numbered from bottom (#1) to top (#10) and are represented in the charts. Each chart represents values from five tobacco plants grown in greenhouse conditions in soil amended with water supplemented with 0 mM, 4 mM and 8 mM Ca concentration. Plants were inoculated with either WT, Δ*PD0913* or PBS (control, without symptoms development). Three independent experiments were performed under the same conditions. Data shown in charts correspond to one representative experiment.

Ca content in sap and leaves of plants infected with Δ*PD0913* was similar to WT

Ca concentration in sap (Figure 7A) and tobacco leaves (Figure 7B) of infected plants was determined by ICP-OES. A clear trend of increasing Ca concentration was observed in plant sap

of different treatments, indicating a correlation between Ca applied to the soil and the content of Ca in the sap. However, despite this trend, no significant differences were found among different levels of Ca added. Intriguingly, plants inoculated with Δ*PD0913* showed decreased levels of Ca at 4 mM Ca when compared to WT-inoculated plants (Figure 7A).

In leaves, significant increases of Ca were observed in plants inoculated with WT and Δ*PD0913* when compared to PBS-inoculated plants. Interestingly, Δ*PD0913* accumulated less Ca than WT when 8 mM Ca was supplemented to the soil (Figure 7B). Bacterial populations were assessed in these plants and no significant differences were found between WT and Δ*PD0913* (Supplementary figure S5).

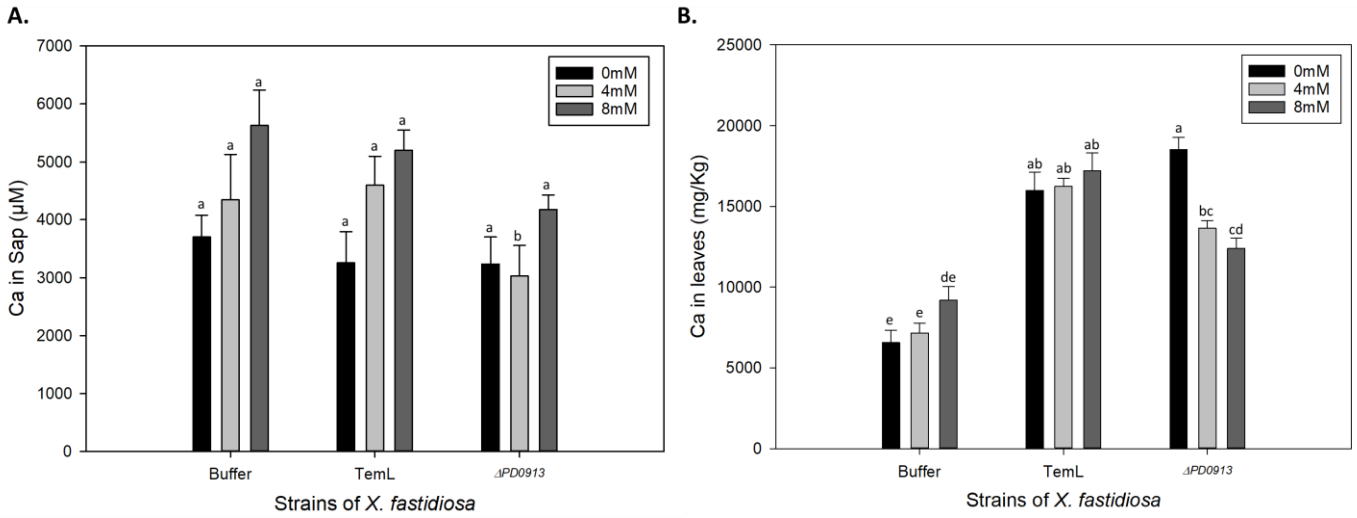

Figure 7. Concentration of calcium in sap and leaves of tobacco plants infected with WT and Δ*PD0913*. Mean Ca concentration in sap **(A)** and leaves (**B)** of five tobacco plants grown in greenhouse conditions in soil supplemented with 0 mM, 4 mM and 8 mM Ca. Plants were inoculated either with PBS (Control), WT or Δ*PD0913*, and Ca concentration was measured by ICP-OES. Three independent experiments were performed under the same conditions. Data shown in charts correspond to one representative experiment. Mean values are shown in charts, and error

bars represent standard error of the mean. Letters above bars indicate significant differences ($p < 0.05$) according to the one-way ANOVA - Holm-Sidak test (all pairwise multiple comparison procedures).

DISCUSSION

In this study, we performed the *in vitro* and *in planta* functional analysis of *PD0913*, a gene of unknown function (annotated as "phage-related protein") found in the plant pathogen *X. fastidiosa*. The *in silico* analysis of the 475 amino acids protein sequence showed some interesting motif results. Myristoylation, originally believed to be unique from eukaryotes and viruses have been identified in plant pathogenic bacteria. Bacterial proteins can undergo lipid modification after injection into the host [29]. Type III secretion system (TTSS) is responsible for the secretion of bacterial proteins into eukaryotic host cells [30]. Since *X. fastidiosa* lacks genes encoding TTSS [31] the transport inside the host plant is likely dependent on other mechanisms. Further research will be necessary to determine the secretion of these proteins inside the host and to further characterize the bacterial proteins in this pathosystem. Glycosylation, a common post-translational modification, is now well established in bacteria [32]. Accumulating evidence indicates a tight association of glycoproteins generated through N- and O- linked glycosylation with bacterial virulence [33]. Bacterial attachment to the host cell and modification of host proteins are some of the processes that bacterial glycosyltransferases participate [32]. Interestingly, both motifs (myristoylation and glycosylation) are involved in signaling process [29]. This is a very important mechanism in bacteria to control their growth and cell-to-cell communication, which can be required for virulence in *X. fastidiosa* [34]. *In vitro* results showed that the absence of *PD0913* affected the growth of mutant cells and increased twitching motility and surface attachment at 2

mM Ca concentration, but had no significant differences in biofilm formation when compared to the WT. *In planta* assays revealed that infection with Δ*PD0913* increased disease severity and symptoms distribution only at 8 mM Ca concentration. Our results thus suggest that *PD0913* is a negative regulator of twitching motility, adhesion to substrates and virulence, and this regulation is influenced by Ca concentration.

Analysis of growth curves suggested impaired growth of the mutant when compared to WT. But growth rates calculated at the log phase were similar for WT and Δ*PD0913* at different Ca concentrations. The apparent impairment in growth can be attributed to different factors such as cell attachment to well walls or interference of precipitating cells. The Δ*PD0913* cells had the highest adhesion force to substrates including the well of the microtiter plate, which may explain the reduction of OD_{600nm}. Overall, Δ*PD0913* performed at similar levels or higher than the WT in most of the parameters evaluated, including planktonic growth, biofilm formation, twitching motility, and cell surface attachment.

The regulation of gene expression is a key mechanism for bacterial survival in a variety of environments. To survive hostile environments, one particularly efficient and complex mechanism is the switch between free-living suspensions of single cells (or planktonic lifestyle) to a sessile lifestyle as surface-associated community enclosed in a self-produced polymeric matrix and attached to a surface, called biofilm. Ca plays both a structural and a regulatory role in the transition from free-living to surface-associated biofilm lifestyle [35]. Ca was previously suggested to play a role in the regulation of bacterial gene expression related to virulence factors and biofilm formation in *Pseudoalteromonas* sp. [36], *Pseudomonas putida* [37] and *Erwinia carotovora* [38]. Studies conducted by our group with *X. fastidiosa* showed increased attachment to surfaces, biofilm formation and twitching motility when Ca was supplemented in the medium [11]. Bacterial

attachment to surfaces and cell aggregation are important in early stages of biofilm development [11,39], while formation of exopolysaccharides (EPS) and cell-to-cell attachment seems more important at later stages. Ca has been observed to impact these later traits since genes related to production of EPS fastidian gum were upregulated at higher concentration of Ca [13]. Results from this study showed that Ca increased biofilm formation for both strains under 2 mM and 4 mM Ca, suggesting that *PD0913* is probably not the key gene responsible for Ca-induced increase in biofilm formation by *X. fastidiosa.* Nevertheless, *PD0913* seems to regulate adhesion to substrates (early stages of biofilm formation) since its deletion increased adhesion force, but only at the highest Ca concentrations tested here.

Contact with and adhesion of *X. fastidiosa* to substrates via pili are crucial for establishing spread and colonization [40]. Twitching motility is an important factor for the virulence of *X. fastidiosa* [2,41]. The colony fringe width and the cell twitching motility speed in microfluidic chambers obtained in this study demonstrated that both strains had an increase of movement at higher Ca concentrations. Curiously, movement was significantly higher for Δ*PD0913* at 2 mM Ca concentration compared to WT. Although it seems that cell adhesion and cell movement are functionally opposite, it has been demonstrated that adhesion helps bacteria to colonize in the early stages of biofilm formation, whereas in later stages, twitching can help bacteria to decolonize and recolonize another area [11]. Moreover, type IV pili can contribute to cell adhesion besides being mainly responsible for cell motility [11]. Our results demonstrated that Ca significantly enhanced the twitching movement of cells for both strains, but especially for Δ*PD0913* at 2 mM Ca. In *X. fastidiosa* the Ca regulation of twitching was demonstrated to be dependent on one of the homologs of PilY1 (PD1611), a structural protein of the type IV pili that contains a Ca-binding motif [12]. The same Ca-binding motif Dx[DN]xDGxxD [13,42] was found in our "phage-related protein"

PD0913. Considering that the deletion mutant still responded to Ca concentrations indicated that Δ*PD0913* is not critical to Ca mediated movement. However, it does act as a modulator for movement in *X. fastidiosa*.

Cell adhesion was determined by the measurements of adhesion force. WT cells showed AF = 205 pN, similar to values reported before of Δ = 203pN [25]. In a number of pathogens, cell adhesion as well as cell-to-cell aggregation relies on the presence of type I and type IV pili [35]. Previous results have shown that type I and type IV pili are not the only factors associated with attachment. Nonfimbrial adhesins present on the cell surface have been shown to possess a role in this function as well [43-46]. Further investigation would be needed to determine the number and type of fimbrial or afimbrial structures attached to the medium. Since leaf scorch symptom is associated with reduced water conductance caused by the blockage of xylem vessels by the presence of biofilm [47], our results indicate that symptoms were expected to be more severe at higher Ca concentrations. *N. tabacum* has been established as a useful model system to evaluate *X. fastidiosa* virulence [26,48]. Some advantages of using this host are the development of symptoms similar to that of the Pierce's disease of grapevines (leaf scorch) and the fact that it reduces the experimental time compared to other natural hosts, such as grapevine [9,26]. Virulence assessments showed an increase in disease development and virulence in plants infected with Δ*PD0913* at 8 mM Ca for the last three weeks of evaluation. This can be explained by the ability of the mutant to attach more strongly to surfaces, form more biofilm and move longer distances at increasing concentrations of Ca *in vitro*. Bacterial population assessment in infected petioles, show no difference between number of cells of WT and Δ*PD0913* (Supplementary figure S3). This is consistent with previous analyses of PD-affected grapevines showing no correlation between leaf-scorch symptoms and bacterial populations in host leaves and petioles [49]. The lack of differences

of bacterial populations *in planta* supports that the observed differences in symptomatology are not explained by number of cells that are present, but by other characteristics such as movement and biofilm.

An increase in Ca during *X. fastidiosa* infection was shown in multiple plant hosts in our previous studies [8,50]. Ca is an essential nutrient and has been described to play different roles and functions in the plant, such as component of cell walls and membranes, cell division and expansion, and secondary messenger in plant defense response [51,52]. In citrus plants infected with *X. fastidiosa*, genes involved in Ca-signaling were upregulated [53]. Ca-signaling is based on tightly regulated transient increases in the levels of the ion in different cellular compartments that are essential for the conversion of signals, which trigger multiple molecular pathways. In general, once plants are infected, Ca accumulation occurs in the site of infection triggering a signal that is translocated to distal parts of the plant, which activates the Systemic acquired resistance (SAR) [54,55]. Recently, differences in the content of Ca between two olive cultivars suggested that this host could be more sensitive to the changes of Ca in the interaction with *X. fastidiosa*, resulting in the development of disease symptoms [56]. In *X. fastidiosa*, Ca regulates virulence by increasing surface attachment, biofilm formation and twitching motility. Our results showed increased Ca concentrations in sap and leaves when Ca was supplemented to the soil. These results have important implications for disease progression *in planta*, where xylem sap is the source of Ca and other nutrients for *X. fastidiosa*. Xylem fluid chemistry is dynamic and can be affected by plant genotype, time of year, time of day, soil fertilization status, and temperature [57].

We hypothesize that Δ*PD0913* may be related to allowing detachment of *X. fastidiosa* cells in xylem vessels under condition of high Ca in the sap, such as observed when plants are infected with *X. fastidiosa* [50]. Detachment can be a strategy to allow more twitching movement (also

positively regulated by Ca) [11] needed to further colonize the plant host. Since twitching was found here to be negatively regulated by *PD0913*, this gene may be important to finely tune movement during infection by this pathogen.

Acknowledgements

This work was funded by California Department of Food and Agriculture (CDFA), Pierce's disease, glassy winged sharpshooter (PD/GWSS) program, the Auburn University Internal Grant Program (P.C. and L.D.), HATCH AAES (Alabama Agricultural Experiment Station) program provided to N.P, P.C. and L.D, and the Department of Entomology and Plant Pathology (Auburn University) GRA program (L.G.).

SUPPLEMENTARY DATA

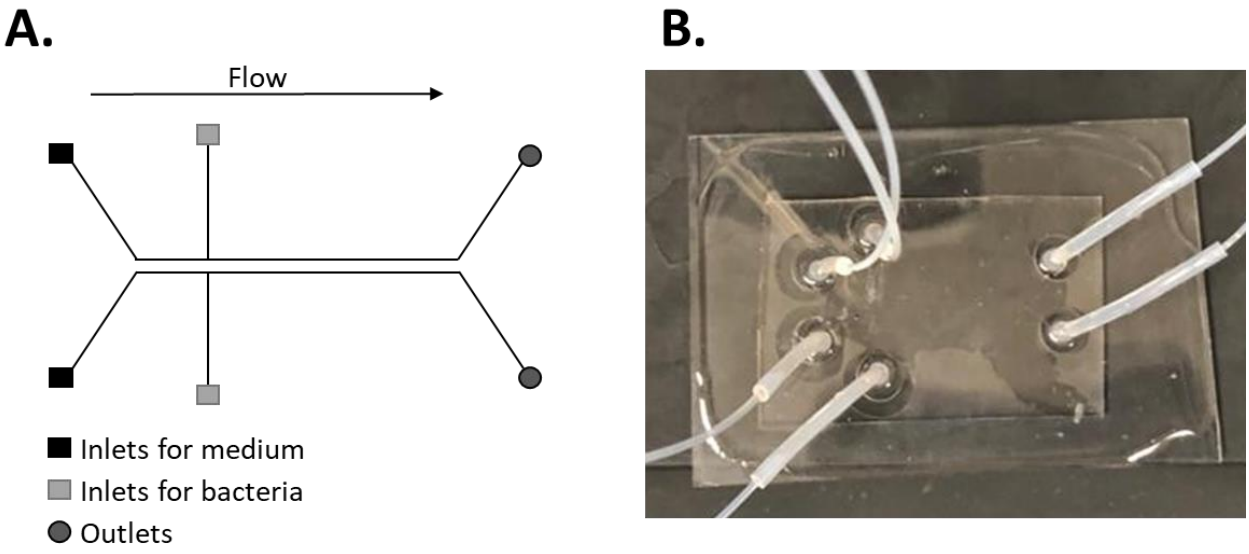

Figure S1: Microfluidic chamber (MC) representation. A. Diagram shows top view of MC and description of the inlets and outlets. **B.** Picture shows top view of an assembled MC.

Table S1. Motif search in PD0913.

Motif	Start	*p*-values		Sites	
	308	1.02E-09	DPVLCGQVRI	**QWRIEC**	NLRPDVKVSG
	348	3.37E-08	DAMEYSSLVL	**QWRTAC**	AVERATGVAS
	214	1.00E-06	DKCPDGMLED	**PVRHEC**	EFDRKECPLG
	139	4.84E-11	EVVMHADAAT	**HRIIAVH**	TGTVCDALNY
	466	3.79E-09	LVLLFSALSS	**FRIISGI**	SKE
	115	3.24E-08	YSNFNNGTRS	**CFVGWK**	PSANSSSCEV
	128	5.32E-08	GWKPSANSSS	**CEVVMH**	ADAATHRIIA
	104	3.81E-09	QNDVYTFSDN	**YYSNFN**	NGTRSCFVGW
	83	9.09E-08	VLDSPSAVVD	**YYSYYT**	SCSEKQNDVY

	226	8.57E-10	RHECEFDRKE	**CPLGQMR**	APDGTCVKTS
	245	4.12E-08	DGTCVKTSDS	**CPSGQAR**	GADGACKRDK
	206	1.94E-07	KNVGGVCVDK	**CPDGMLE**	DPVRHECEFD
	333	7.32E-14	GGGCDSVPVC	**TGKKCDAMEY**	SSLVLQWRTA
	146	1.01E-11	AATHRIIAVH	**TGTVCDALNY**	KDDCLSHPGY
	160	2.21E-08	CDALNYKDDC	**LSHPGY**	VYKSGGSGAV
	52	7.88E-08	GAAQSNLQYQ	**LCMSGY**	TNTGRVKTGD
	414	6.18E-11	SAGGDDKDAS	**KFDDQGRGY**	SRSCFEPLTV
	33	1.77E-10	SAPIATPASG	**IFSDQAEAY**	GAAQSNLQYQ
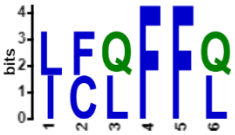	446	2.82E-08	GSELTIDLSP	**LCQFFQ**	VGGRLVLLFS
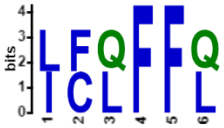	5	3.20E-08	MRRV	**IFLFFL**	VFCSSVFAAP

	45	1.15E-07	SDQAEAYGAA	**QSNLQY**	QLCMSGYTNT
	195	1.63E-07	VPAKPQCSLD	**QKNVGG**	VCVDKCPDGM
	371	6.36E-09	VASGGSGDRD	**PNVAAIK**	DALTGKDGVV
	58	2.16E-08	LQYQLCMSGY	**TNTGRVK**	TGDRQYVVVL
	428	6.17E-08	QGRGYSRSCF	**EPLTVD**	VFGSELTIDL
	437	8.76E-08	FEPLTVDVFG	**SELTID**	LSPLCQFFQV
	185	4.44E-09	VSAVEGYGDC	**VPAKPQC**	SLDQKNVGGV
	16	1.23E-08	FLFFLVFCSS	**VFAAPKC**	SAPIATPASG
	95	1.07E-07	SYYTSCSEKQ	**NDVYTF**	SDNYYSNFNN
	455	2.29E-07	PLCQFFQVGG	**RLVLLF**	SALSSFRIIS
	278	2.31E-09	DDEQSGKDGD	**EGRSSFSW**	SGGCDVAPSC

	392	1.21E-08	GKDGVVDTGD	**EGKPSSAF**	SDGSSAGGDD
	326	6.57E-08	RPDVKVSGGG	**CDSVPVC**	TGKKCDAMEY
	289	9.45E-08	GRSSFSWSGG	**CDVAPSC**	SGDPVLCGQV
	266	2.69E-08	ACKRDKDGDG	**KPDDEQ**	SGKDGDEGRS
	316	2.02E-06	RIQWRIECNL	**RPDVKV**	SGGGCDSVPV
	356	4.04E-07	VLQWRTACAV	**ERATGV**	ASGGSGDRDP
	67	4.04E-07	YTNTGRVKTG	**DRQYVV**	VLDSPSAVVD
	25	2.03E-08	SVFAAPKCSA	**PIATPA**	SGIFSDQAEA
	121	4.28E-06	GTRSCFVGWK	**PSANSS**	SCEVVMHADA
	258	2.48E-07	GQARGADGAC	**KRDKDG**	DGKPDDEQSG

	380	8.11E-07	DPNVAAIKDA	**LTGKDG**	VVDTGDEGKP
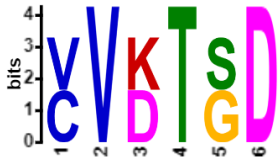	238	7.62E-07	LGQMRAPDGT	**CVKTSD**	SCPSGQARGA
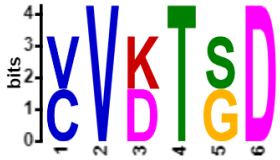	386	1.10E-06	IKDALTGKDG	**VVDTGD**	EGKPSSAFSD
	220	1.14E-08	MLEDPVRHEC	**EFDRKE**	CPLGQMRAPD
	406	4.24E-06	SSAFSDGSSA	**GGDDKD**	ASKFDDQGRG
	302	7.99E-07	APSCSGDPVL	**CGQVRI**	QWRIECNLRP
	179	1.62E-06	SGGSGAVSAV	**EGYGDC**	VPAKPQCSLD
	252	3.67E-07	SDSCPSGQAR	**GADGAC**	KRDKDGDGKP
	173	9.48E-06	PGYVYKSGGS	**GAVSAV**	EGYGDCVPAK
	166	8.33E-07	KDDCLSHPGY	**VYKSGG**	SGAVSAVEGY

	73	4.70E-06	VKTGDRQYVV	**VLDSPS**	AVVDYYSYYT
	272	6.24E-07	DGDGKPDDEQ	**SGKDGD**	EGRSSFSWSG
	363	6.41E-06	CAVERATGVA	**SGGSGD**	RDPNVAAIKD
	89	5.95E-07	AVVDYYSYYT	**SCSEKQ**	NDVYTFSDNY
	296	6.19E-06	SGGCDVAPSC	**SGDPVL**	CGQVRIQWRI
	466	1.50E-08	LVLLFSALSS	**FRIISG**	ISKE
	400	1.26E-04	GDEGKPSSAF	**SDGSSA**	GGDDKDASKF

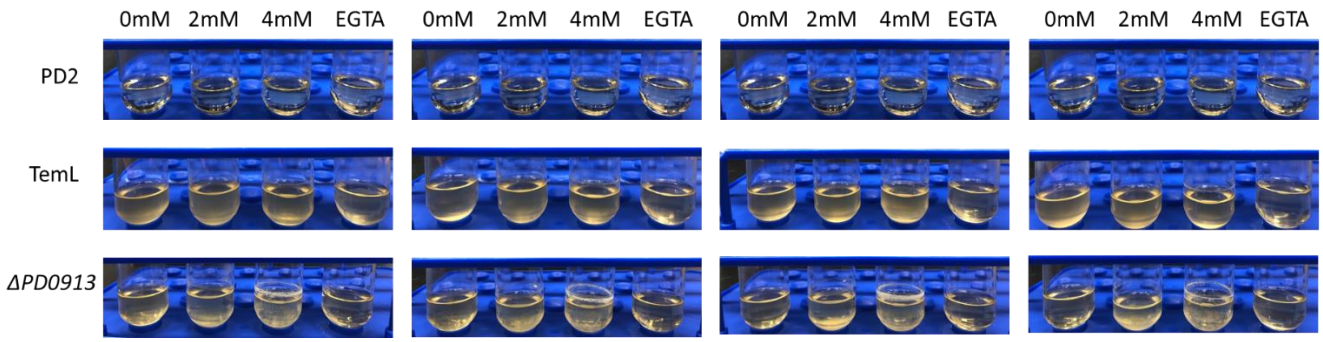

Figure S2: Images of biofilm growth of *X. fastidiosa* TemeculaL and Δ*PD0913* on glass flasks. *X. fastidiosa* strains growth in PD2 media (PD2) or PD2 media supplemented with 0 mM, 2 mM and 4 mM $CaCl_2$ and 1.5 mM EGTA. Biofilm growth is observed at the air-liquid interface on the wall of flasks, especially in flasks of Δ*PD0913* supplemented with 2 mM and 4 mM Ca.

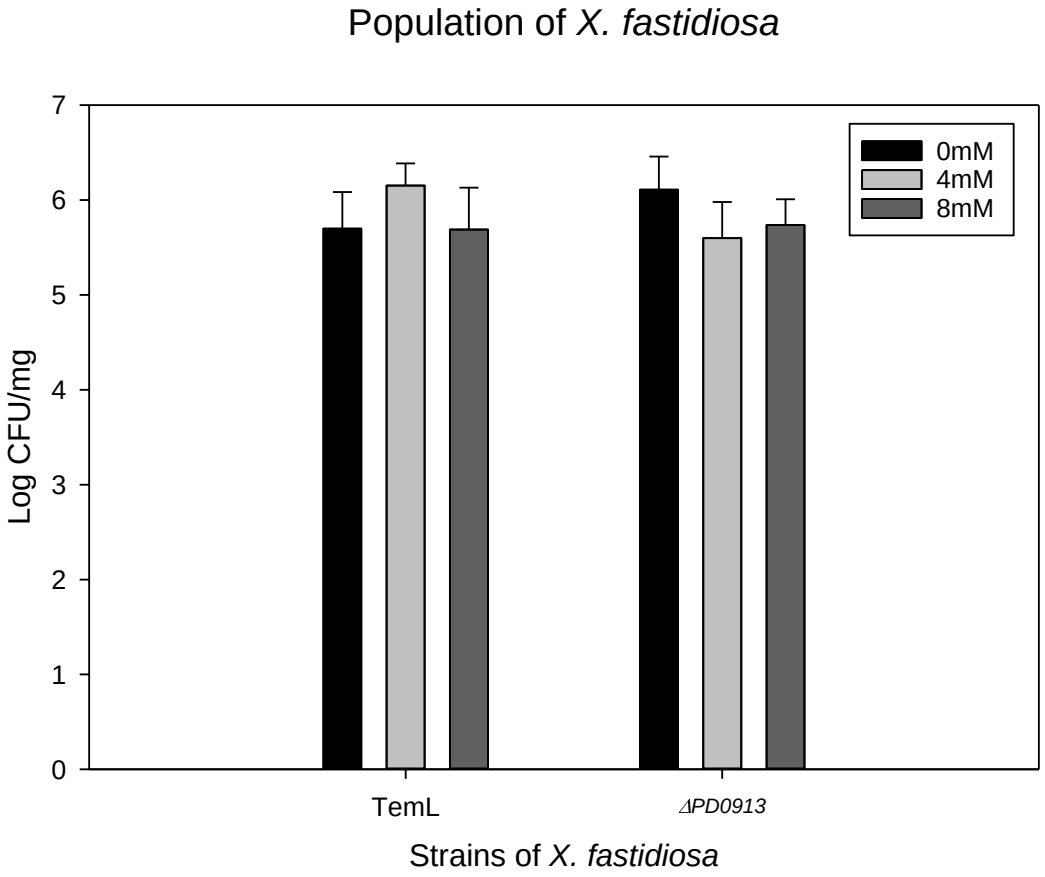

Figure S3: Quantification of the *X. fastidiosa* population in tobacco plants. Bacterial populations were assessed at the last time point of evaluation (6 weeks) using DNA extracted from petioles of tobacco plants infected with WT and Δ*PD0913.* Total population of *X. fastidiosa* was measured by qPCR. Three independent experiments were performed under the same conditions.

Data shown in charts correspond to one representative experiment. Data represent means and standard errors.

REFERENCES

1. Hopkins D. L. , P.A.H. Xylella fastidiosa Cause of Pierce's Disease of Grapevine and Other Emergent Diseases. **2002**.
2. Chatterjee, S.; Almeida, R.P.; Lindow, S. Living in two worlds: the plant and insect lifestyles of Xylella fastidiosa. *Annual review of phytopathology* **2008**, *46*, 243-271, doi:10.1146/annurev.phyto.45.062806.094342.
3. Saponari, M.; Boscia, D.; Nigro, F.; Martelli, G.P. Identification of DNA Sequences Related to Xylella Fastidiosa in Oleander, Almond and Olive Trees Exhibiting Leaf Scorch Symptoms in Apulia (Southern Italy). *J Plant Pathol* **2013**, *95*, 668-668.
4. Krivanek, A.F.; Stevenson, J.F.; Walker, M.A. Development and Comparison of Symptom Indices for Quantifying Grapevine Resistance to Pierce's Disease. *Phytopathology* **2005**, *95*, 36-43, doi:10.1094/PHYTO-95-0036.
5. Salt, D.E.; Baxter, I.; Lahner, B. Ionomics and the study of the plant ionome. *Annu Rev Plant Biol* **2008**, *59*, 709-733, doi:10.1146/annurev.arplant.59.032607.092942.
6. Cobine, P.A.; Cruz, L.F.; Navarrete, F.; Duncan, D.; Tygart, M.; De La Fuente, L. Xylella fastidiosa differentially accumulates mineral elements in biofilm and planktonic cells. *PLoS One* **2013**, *8*, e54936, doi:10.1371/journal.pone.0054936.
7. Williams, L.; Salt, D.E. The plant ionome coming into focus. *Curr Opin Plant Biol* **2009**, *12*, 247-249, doi:10.1016/j.pbi.2009.05.009.
8. De La Fuente, L.; Parker, J.K.; Oliver, J.E.; Granger, S.; Brannen, P.M.; van Santen, E.; Cobine, P.A. The bacterial pathogen Xylella fastidiosa affects the leaf ionome of plant hosts during infection. *PLoS One* **2013**, *8*, e62945, doi:10.1371/journal.pone.0062945.
9. Oliver, J.E.; Sefick, S.A.; Parker, J.K.; Arnold, T.; Cobine, P.A.; De La Fuente, L. Ionome changes in Xylella fastidiosa-infected Nicotiana tabacum correlate with virulence and discriminate between subspecies of bacterial isolates. *Mol Plant Microbe Interact* **2014**, *27*, 1048-1058, doi:10.1094/MPMI-05-14-0151-R.
10. Dominguez, D.C. Calcium signalling in bacteria. *Mol Microbiol* **2004**, *54*, 291-297, doi:10.1111/j.1365-2958.2004.04276.x.
11. Cruz, L.F.; Cobine, P.A.; De La Fuente, L. Calcium increases Xylella fastidiosa surface attachment, biofilm formation, and twitching motility. *Applied and environmental microbiology* **2012**, *78*, 1321-1331, doi:10.1128/AEM.06501-11.
12. Cruz, L.F.; Parker, J.K.; Cobine, P.A.; De La Fuente, L. Calcium-Enhanced Twitching Motility in Xylella fastidiosa Is Linked to a Single PilY1 Homolog. *Applied and environmental microbiology* **2014**, *80*, 7176-7185, doi:10.1128/AEM.02153-14.
13. Parker, J.K.; Chen, H.; McCarty, S.E.; Liu, L.Y.; De La Fuente, L. Calcium transcriptionally regulates the biofilm machinery of Xylella fastidiosa to promote continued biofilm development in batch cultures. *Environmental microbiology* **2016**, *18*, 1620-1634, doi:10.1111/1462-2920.13242.
14. Potnis, N.; Kandel, P.P.; Merfa, M.V.; Retchless, A.C.; Parker, J.K.; Stenger, D.C.; Almeida, R.P.P.; Bergsma-Vlami, M.; Westenberg, M.; Cobine, P.A., et al. Patterns of

inter- and intrasubspecific homologous recombination inform eco-evolutionary dynamics of Xylella fastidiosa. *ISME J* **2019**, *13*, 2319-2333, doi:10.1038/s41396-019-0423-y.
15. Davis, M.J.; Purcell, A.H.; Thomson, S.V. Pierce's disease of grapevines: isolation of the causal bacterium. *Science* **1978**, *199*, 75-77, doi:10.1126/science.199.4324.75.
16. Bailey, T.L.; Elkan, C. Fitting a mixture model by expectation maximization to discover motifs in biopolymers. *Proc Int Conf Intell Syst Mol Biol* **1994**, *2*, 28-36.
17. Grant, C.E.; Bailey, T.L.; Noble, W.S. FIMO: scanning for occurrences of a given motif. *Bioinformatics* **2011**, *27*, 1017-1018, doi:10.1093/bioinformatics/btr064.
18. Chou, K.-C.; Shen, H.-B. Cell-PLoc 2.0: an improved package of web-servers for predicting subcellular localization of proteins in various organisms. *Natural Science* **2010**, *02*, 1090-1103, doi:10.4236/ns.2010.210136.
19. Kandel, P.P.; Chen, H.; De La Fuente, L. A Short Protocol for Gene Knockout and Complementation in Xylella fastidiosa Shows that One of the Type IV Pilin Paralogs (PD1926) Is Needed for Twitching while Another (PD1924) Affects Pilus Number and Location. *Applied and environmental microbiology* **2018**, *84*.
20. Doyle, J.J.; Doyle, J.L. A rapid DNA isolation procedure for small quantities of fresh leaf tissue. *Phytochemical Bulletin* **1987**.
21. Davis, M.J.; French, W.J.; Schaad, N.W. Axenic Culture of the Bacteria Associated with Phony Disease of Peach and Plum Leaf Scald. *Curr Microbiol* **1981**, *6*, 309-314, doi:Doi 10.1007/Bf01566883.
22. Bankevich, A.; Nurk, S.; Antipov, D.; Gurevich, A.A.; Dvorkin, M.; Kulikov, A.S.; Lesin, V.M.; Nikolenko, S.I.; Pham, S.; Prjibelski, A.D., et al. SPAdes: a new genome assembly algorithm and its applications to single-cell sequencing. *J Comput Biol* **2012**, *19*, 455-477, doi:10.1089/cmb.2012.0021.
23. Gurevich, A.; Saveliev, V.; Vyahhi, N.; Tesler, G. QUAST: quality assessment tool for genome assemblies. *Bioinformatics* **2013**, *29*, 1072-1075, doi:10.1093/bioinformatics/btt086.
24. Zaini, P.A.; De La Fuente, L.; Hoch, H.C.; Burr, T.J. Grapevine xylem sap enhances biofilm development by Xylella fastidiosa. *FEMS Microbiol Lett* **2009**, *295*, 129-134, doi:10.1111/j.1574-6968.2009.01597.x.
25. De La Fuente, L.; Montanes, E.; Meng, Y.; Li, Y.; Burr, T.J.; Hoch, H.C.; Wu, M. Assessing adhesion forces of type I and type IV pili of Xylella fastidiosa bacteria by use of a microfluidic flow chamber. *Applied and environmental microbiology* **2007**, *73*, 2690-2696, doi:10.1128/AEM.02649-06.
26. Francis, M.; Civerolo, E.L.; Bruening, G. Improved Bioassay of Xylella fastidiosa using Nicotiana tabacum cultivar SR1. *Plant Dis* **2008**, *92*, 14-20, doi:10.1094/Pdis-92-1-0014.
27. Ge, Q.; Cobine, P.A.; De La Fuente, L. Copper Supplementation in Watering Solution Reaches the Xylem But Does Not Protect Tobacco Plants Against Xylella fastidiosa Infection. *Plant Dis* **2020**, *104*, 724-730, doi:10.1094/PDIS-08-19-1748-RE.
28. Francis, M.; Lin, H.; Cabrera-La Rosa, J.; Doddapaneni, H.; Civerolo, E.L. Genome-based PCR primers for specific and sensitive detection and quantification of *Xylella fastidiosa*. *Eur. J. Plant Pathol.* **2006**, *115*, 203-213, doi:10.1007/s10658-006-9009-4.
29. Maurer-Stroh, S.; Eisenhaber, F. Myristoylation of viral and bacterial proteins. *Trends Microbiol* **2004**, *12*, 178-185, doi:10.1016/j.tim.2004.02.006.

30. Thomas, N.A.; Brett Finlay, B. Establishing order for type III secretion substrates – a hierarchical process. *Trends in Microbiology* **2003**, *11*, 398-403, doi:10.1016/s0966-842x(03)00155-0.
31. Zhang, S.; Chakrabarty, P.K.; Fleites, L.A.; Rayside, P.A.; Hopkins, D.L.; Gabriel, D.W. Three New Pierce's Disease Pathogenicity Effectors Identified Using Xylella fastidiosa Biocontrol Strain EB92-1. *PLoS One* **2015**, *10*, e0133796, doi:10.1371/journal.pone.0133796.
32. Lu, Q.; Li, S.; Shao, F. Sweet Talk: Protein Glycosylation in Bacterial Interaction With the Host. *Trends Microbiol* **2015**, *23*, 630-641, doi:10.1016/j.tim.2015.07.003.
33. Ribet, D.; Cossart, P. Post-translational modifications in host cells during bacterial infection. *FEBS Lett* **2010**, *584*, 2748-2758, doi:10.1016/j.febslet.2010.05.012.
34. Chatterjee, S.; Newman, K.L.; Lindow, S.E. Cell-to-cell signaling in Xylella fastidiosa suppresses movement and xylem vessel colonization in grape. *Mol Plant Microbe Interact* **2008**, *21*, 1309-1315, doi:10.1094/MPMI-21-10-1309.
35. King, M.M.; Kayastha, B.B.; Franklin, M.J.; Patrauchan, M.A. Calcium Regulation of Bacterial Virulence. *Adv Exp Med Biol* **2020**, *1131*, 827-855, doi:10.1007/978-3-030-12457-1_33.
36. Sarkisova, S.; Patrauchan, M.A.; Berglund, D.; Nivens, D.E.; Franklin, M.J. Calcium-induced virulence factors associated with the extracellular matrix of mucoid Pseudomonas aeruginosa biofilms. *J Bacteriol* **2005**, *187*, 4327-4337, doi:10.1128/JB.187.13.4327-4337.2005.
37. Espinosa-Urgel, M.; Salido, A.; Ramos, J.L. Genetic analysis of functions involved in adhesion of Pseudomonas putida to seeds. *J Bacteriol* **2000**, *182*, 2363-2369, doi:10.1128/jb.182.9.2363-2369.2000.
38. Flego, D.; Pirhonen, M.; Saarilahti, H.; Palva, T.K.; Palva, E.T. Control of virulence gene expression by plant calcium in the phytopathogen Erwinia carotovora. *Mol Microbiol* **1997**, *25*, 831-838, doi:10.1111/j.1365-2958.1997.mmi501.x.
39. Guilhabert, M.R.; Kirkpatrick, B.C. Identification of Xylella fastidiosa antivirulence genes: hemagglutinin adhesins contribute a biofilm maturation to X. fastidios and colonization and attenuate virulence. *Mol Plant Microbe Interact* **2005**, *18*, 856-868, doi:10.1094/MPMI-18-0856.
40. De La Fuente, L.; Burr, T.J.; Hoch, H.C. Mutations in type I and type IV pilus biosynthetic genes affect twitching motility rates in Xylella fastidiosa. *J Bacteriol* **2007**, *189*, 7507-7510, doi:10.1128/JB.00934-07.
41. Burdman, S.; Bahar, O.; Parker, J.K.; De La Fuente, L. Involvement of Type IV Pili in Pathogenicity of Plant Pathogenic Bacteria. *Genes* **2011**, *2*, 706-735, doi:10.3390/genes2040706.
42. Parker, J.K.; Cruz, L.F.; Evans, M.R.; De La Fuente, L. Presence of calcium-binding motifs in PilY1 homologs correlates with Ca-mediated twitching motility and evolutionary history across diverse bacteria. *FEMS Microbiol Lett* **2015**, *362*, doi:10.1093/femsle/fnu063.
43. Guilhabert, M.R.; Hoffman, L.M.; Mills, D.A.; Kirkpatrick, B.C. Transposon mutagenesis of Xylella fastidiosa by electroporation of Tn5 synaptic complexes. *Mol Plant Microbe Interact* **2001**, *14*, 701-706, doi:10.1094/MPMI.2001.14.6.701.

44. Lindow, S.E.; Feil, H. Effects of fimbrial (FimA, FimF) and afimbrial (XadA, HxfB) adhesins on the adhesion of Xylella fastidiosa to surfaces. *Proceedings of the 2005 Pierce's Disease* **2005**.
45. Feil, H.; Feil, W.S.; Lindow, S.E. Contribution of Fimbrial and Afimbrial Adhesins of Xylella fastidiosa to Attachment to Surfaces and Virulence to Grape. *Phytopathology* **2007**, *97*, 318-324, doi:10.1094/PHYTO-97-3-0318.
46. Caserta, R.; Takita, M.A.; Targon, M.L.; Rosselli-Murai, L.K.; de Souza, A.P.; Peroni, L.; Stach-Machado, D.R.; Andrade, A.; Labate, C.A.; Kitajima, E.W., et al. Expression of Xylella fastidiosa fimbrial and afimbrial proteins during biofilm formation. *Applied and environmental microbiology* **2010**, *76*, 4250-4259, doi:10.1128/AEM.02114-09.
47. Choi, H.-K.; Iandolino, A.; Goes da Silva, F.; Cook, D. Water deficit modulates the response of *Vitis vinifera* to the Pierce's disease pathogen *Xylella fastidiosa*. *Molecular Plant-Microbe Interactions* **2013**, 10.1094/MPMI-09-12-0217-R, doi:10.1094/MPMI-09-12-0217-R.
48. Lopes, S.A.; Ribeiro, D.M.; Roberto, P.G.; Franca, S.C.; Santos, J.M. Nicotiana tabacum as an experimental host for the study of plant-Xylella fastidiosa interactions. *Plant Dis* **2000**, *84*, 827-830, doi:Doi 10.1094/Pdis.2000.84.8.827.
49. Gambetta, G.A.; Fei, J.; Rost, T.L.; Matthews, M.A. Leaf scorch symptoms are not correlated with bacterial populations during Pierce's disease. *Journal of experimental botany* **2007**, *58*, 4037-4046, doi:10.1093/jxb/erm260.
50. Oliver, J.E.; Cobine, P.A.; De La Fuente, L. Xylella fastidiosa Isolates from Both subsp. multiplex and fastidiosa Cause Disease on Southern Highbush Blueberry (Vaccinium sp.) Under Greenhouse Conditions. *Phytopathology* **2015**, *105*, 855-862, doi:10.1094/PHYTO-11-14-0322-FI.
51. Marschner, H. *Mineral Nutrition of Higher Plants*; Academic Press: San Diego, California, 1995.
52. Lecourieux, D.; Ranjeva, R.; Pugin, A. Calcium in plant defence-signalling pathways. *New Phytol* **2006**, *171*, 249-269, doi:10.1111/j.1469-8137.2006.01777.x.
53. Rodrigues, C.M.; de Souza, A.A.; Takita, M.A.; Kishi, L.T.; Machado, M.A. RNA-Seq analysis of Citrus reticulata in the early stages of Xylella fastidiosa infection reveals auxin-related genes as a defense response. *Bmc Genomics* **2013**, *14*, doi:Artn 676 10.1186/1471-2164-14-676.
54. Park, S.W.; Kaimoyo, E.; Kumar, D.; Mosher, S.; Klessig, D.F. Methyl salicylate is a critical mobile signal for plant systemic acquired resistance. *Science* **2007**, *318*, 113-116, doi:10.1126/science.1147113.
55. Durner, J.; Shah, J.; Klessig, D.F. Salicylic acid and disease resistance in plants. *Trends in Plant Science* **1997**, *2*, 266-274, doi:10.1016/s1360-1385(97)86349-2.
56. D'Attoma, G.; Morelli, M.; Saldarelli, P.; Saponari, M.; Giampetruzzi, A.; Boscia, D.; Savino, V.N.; De La Fuente, L.; Cobine, P.A. Ionomic Differences between Susceptible and Resistant Olive Cultivars Infected by Xylella fastidiosa in the Outbreak Area of Salento, Italy. *Pathogens* **2019**, *8*, doi:10.3390/pathogens8040272.
57. Andersen, P.C.; Brodbeck, B.V. Diurnal and Temporal Changes in the Chemical Profile of Xylem Exudate from Vitis-Rotundifolia. *Physiol Plantarum* **1989**, *75*, 63-70, doi:DOI 10.1111/j.1399-3054.1989.tb02064.x.

Chapter 3

Virulence assessment of *Xylella fastidiosa* susbp. *fastidiosa* strains from grapes using the model host *Nicotiana tabacum*

1. ABSTRACT

Xylella fastidiosa (Xf) subsp. *fastidiosa* causes Pierce's disease of grapevine (PD) that has a great economic impact on the California grape industry. Isolates of Xf are genetically very similar, but differences in infection symptomatology and virulence have been indicated by biological traits studies. 122 Xf subsp. *fastidiosa* genomes from symptomatic grapevines were obtained from symptomatic grapevines of five geographic locations across California. To characterize the phenotypic variability among this collection, *Nicotiana tabacum* (tobacco) SR1 was used since different subspecies of Xf are capable of colonize and cause leaf scorch symptoms in this model plant. Tobacco plant inoculation in greenhouse and virulence assessments over time were performed in 41 selected isolates. For virulence assessments area under disease progression curve (AUDPC), percentage of leaf scorch, and severity were determined. Isolates Je32, Je86, Je96 and Je121 showed the highest numbers in virulence assays when compared to TemeculaL and WM1-1 (reference controls). Contrastingly, Je98, Je111 and Je118 showed the lowest values on AUDPC, incidence and severity. No correlation was found between virulence and host cultivar or geographical location of the isolates. These results indicates that virulence differences between isolates were apparent, and have potential implications for understanding the context of genomic variability, host adaptation and geographic location on the identification and selection of resistant cultivars for the development and improvement of disease management on this bacterium.

2. INTRODUCTION

Xylella fastidiosa is a gram-negative, xylem-limited plant pathogenic bacterium that affects several economically important agricultural crops (Hopkins & Purcell, 2002). The pathogen spread via xylem after being transmitted by sap-feeding insect vectors as sharpshooters and leafhoppers from the Cicadellidae family (Sicard et al., 2018, Janse & Obradovic, 2010). Symptoms of leaf scorch are believed to be caused by the formation of bacterial biofilm in the xylem vessels, that block and disrupt the flow of water and nutrients within the host (Chatterjee et al., 2008a).

X. fastidiosa has been divided into five subspecies, namely, *fastidiosa, multiplex, pauca, sandyi* and *morus*. Four out of the five subspecies are found in the United States: *X. fastidiosa* subsp. *multiplex* causes leaf scorch disease on oak, elm, and peach, *X. fastidiosa* subsp. *sandyi* causes oleander leaf scorch, *X. fastidiosa* subsp. *morus* recently isolated from mulberry and most importantly, *X. fastidiosa* subsp. *fastidiosa* causes Pierce's disease of grape (Nunney et al., 2014b). *X. fastidiosa* subsp. *pauca* isolated from citrus and coffee located in Brazil and Costa Rica (Vanhove et al., 2019). Classification of *X. fastidiosa* in subspecies first used a multilocus sequence typing approach. This approach was also useful to determine the evolutionary history and diversity of this bacterium (Scally et al., 2005, Nunney et al., 2012). Subspecies demonstrate a certain level of host specificity (Almeida et al., 2008, Oliver et al., 2014, Oliver et al., 2015), but this is rapidly changing due to extensive homologous recombination present in *X. fastidiosa* (Almeida et al., 2008, Nunney et al., 2012, Nunney et al., 2014b, Coletta-Filho et al., 2016, Nunney et al., 2014a). Regardless of the wide host range, *X. fastidiosa* isolates from different host plants are genetically similar (Parker et al., 2012). For instance, subsp. *pauca* and *fastidiosa* have an identity amino acid average of 96% and shared 98% of their genes (Van Sluys et al., 2003). To explain relationships between *X. fastidiosa* subspecies, genetic analysis of

multiple environmentally mediated genes that plays a role in *X. fastidiosa* host interactions have been used (Parker et al., 2012). Despite this limited genetic variation, *X. fastidiosa* isolates differ in phenotypic characters associated with virulence such as plant host range, symptom type, and disease severity (Oliver et al., 2014, Oliver et al., 2015). But phenotypic characterization of *X. fastidiosa* isolates have been very limited, due to the difficulty and long times needed for in planta virulence assessments. It is important to further characterize the phenotypic diversity among isolates of *X. fastidiosa*.

Virulence variation among isolates have only been looked in a small number of studies (Cruz et al., 2012, Oliver et al., 2014, Oliver et al., 2015, Lopes et al., 2000, Francis et al., 2008), even though many *X. fastidiosa* isolates already have their full genome sequenced (Simpson et al., 2000, Vanhove et al., 2019, Vanhove et al., 2020). Severity of disease differs greatly among hosts and virulence comparisons among *X. fastidiosa* strains can be useful to understand the biology of this pathogen. Differences in the virulence of a pathogen among host species can occur because i) hosts differ in their resistance or tolerance to infection, or ii) due to underlying genetic variation in the pathogen. Understanding the complex interactions between plant, pathogen and vector can lead to effective disease control. The lack of a good experimental host created some difficulties to those studying potential pathogenicity genes in *X. fastidiosa* due to extended periods to express symptoms after inoculation. Model host *Nicotiana tabacum* is capable of showing differences in host colonization and symptomatology caused by the infection with *X. fastidiosa* (Lopes et al., 2000, Francis et al., 2008). Tobacco has been used as a model system to evaluate different aspects on the interaction with *X. fastidiosa*, for example ionomic changes (De La Fuente et al., 2013), gene bacterial function (Chen et al., 2017, Navarrete & De La Fuente, 2015), and natural competence and recombination (Kandel et al., 2016). Since studies to predict isolate virulence are

lacking, tobacco assays could be a useful tool to evaluate multiple strains in greenhouse conditions, saving considerable time and space.

The goal of this study was to evaluate the differences in virulence caused by *X. fastidiosa* isolates evidenced by symptom development or bacterial spatial movement in a common host. 122 subsp. fastidiosa isolates were obtained from symptomatic grapevines of five geographic locations across California (Vanhove et al., 2020). 42 strains were chosen from this collection and were inoculated into *Nicotiana tabacum* to study the effects on colonization and development of the symptoms. Considering the geographical origin of isolation in California, two groups of strains could be defined for each location, based on virulence. This work will contribute to determine phenotypic groups that will be used to select strains to be tested in grapevines.

3. RESULTS

3.1 *Symptoms in tobacco caused by X. fastidiosa vary by isolate.*

Symptoms of *X. fastidiosa* infection began to show in *N. tabacum* between 10-12 weeks postinoculation. Discoloration on the base of the leaves followed by leaf necrosis was observed as typical leaf scorch symptoms (Figure 1). As disease progressed, symptoms generally spread from the base of the leave toward the stem following the typical infection by *X. fastidiosa* that moves acropetally, spreading symptoms from the point of inoculation to the rest of the plant (Francis et al., 2006). No symptoms beyond the occasional yellow leaf were observed in control plants, while plants in each isolate group showed leaf scorch, bleaching of the veins and persistent cupping or curling.

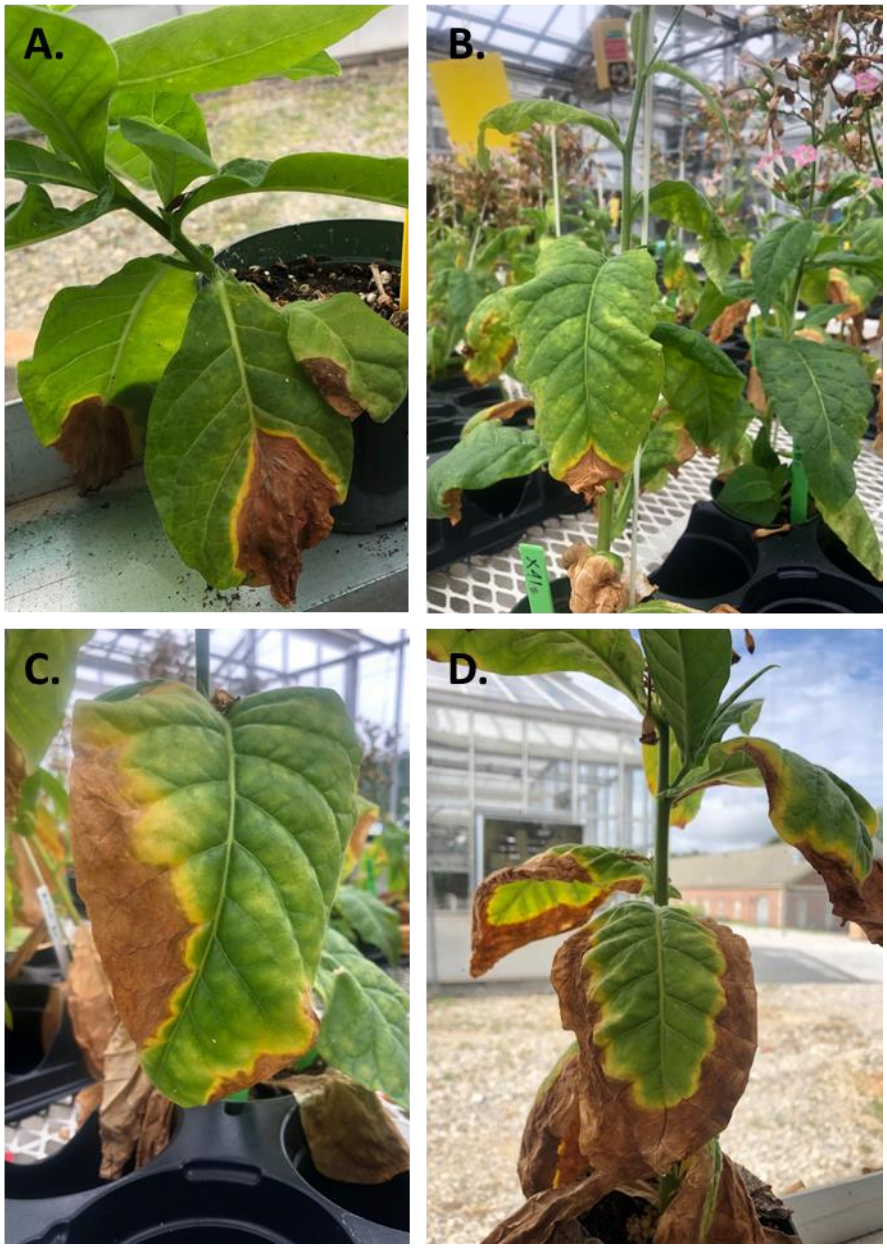

Figure 3-1. Symptoms observed in tobacco plants infected with different strains of *Xylella fastidiosa*. A. Typical leaf scorch symptom **B.** Discoloration **C.** Bleaching of the vein **D.** Cupping or curling at different stages of development in tobacco leaves infected with *X. fastidiosa* strains under greenhouse conditions.

To compare the virulence between isolates three parameters were consider: i) AUDPC based on leaf scorch, ii) leaf scorch percentage (number of leaves showing symptom by plant) and iii) severity (determined by a scale rating the leaf scorch percentage by symptomatic leaf in the plant) (Table 1). Differences between isolates were apparent on the three evaluated aspects over time.

Table 3-1. Scale for disease severity rating giving to each leaf on infected plants

Severity rating	Proportion of leave affected	Predominant symptoms	Leaf examples
0	None	None	
1	0-20% of the leaf	Leaf yellowing appears along leaf tip or margin	
2	20-40% of the leaf	Previously yellowing start to scorch	

3	40-60% of the leaf	Scorch on the tip of the leaf and yellow halo surrounding the scorch	
4	60-80% of the leaf	Scorch and yellowing take more than half leaves	
5	80-100% of the leaf	Severe leaf scorching / Necrosis	

At least 29 strains out of the 41 have higher AUDPC values when compared to both reference control strains TemeculaL and the more virulent WM1-1. Values above 50 were found for Je32, Je86, Je96 and Je121. Lower values of AUDPC were observed for Je22, Je28, Je 51, Je 111 and Je118 strains, those values were close to 20 and to TemeculaL (control) (Figure 2).

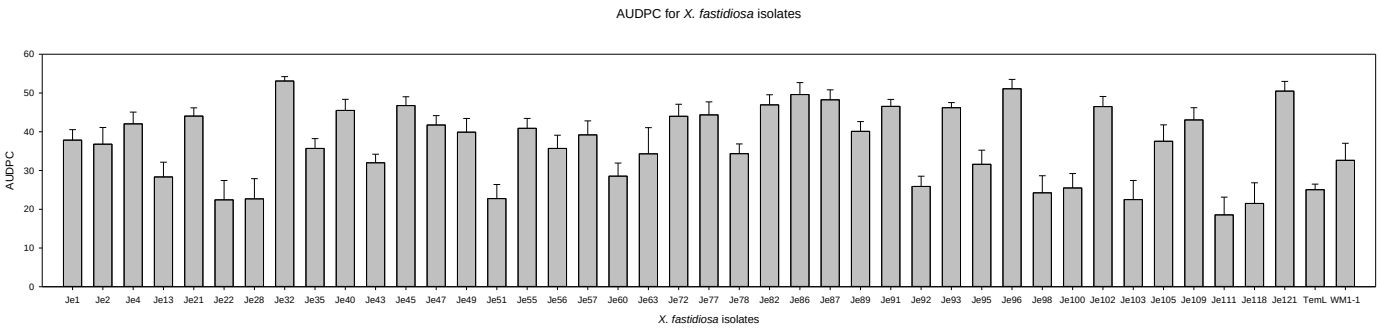

Figure 3-2. Area under disease progress curve (AUDPC) of *Xylella fastidiosa* isolates. Tobacco plants infected with the different isolates of *X. fastidiosa* were evaluated. Mean of AUDPC based on leaf scorch per isolate during seven weeks of evaluation was used for the graph.

AUDPC was also compared between the two first independent experiments. Interestingly, common isolates between experiment 1 and 2 showed similar values of AUDPC, which indicates the reproducibility of the experiments (Figure 3).

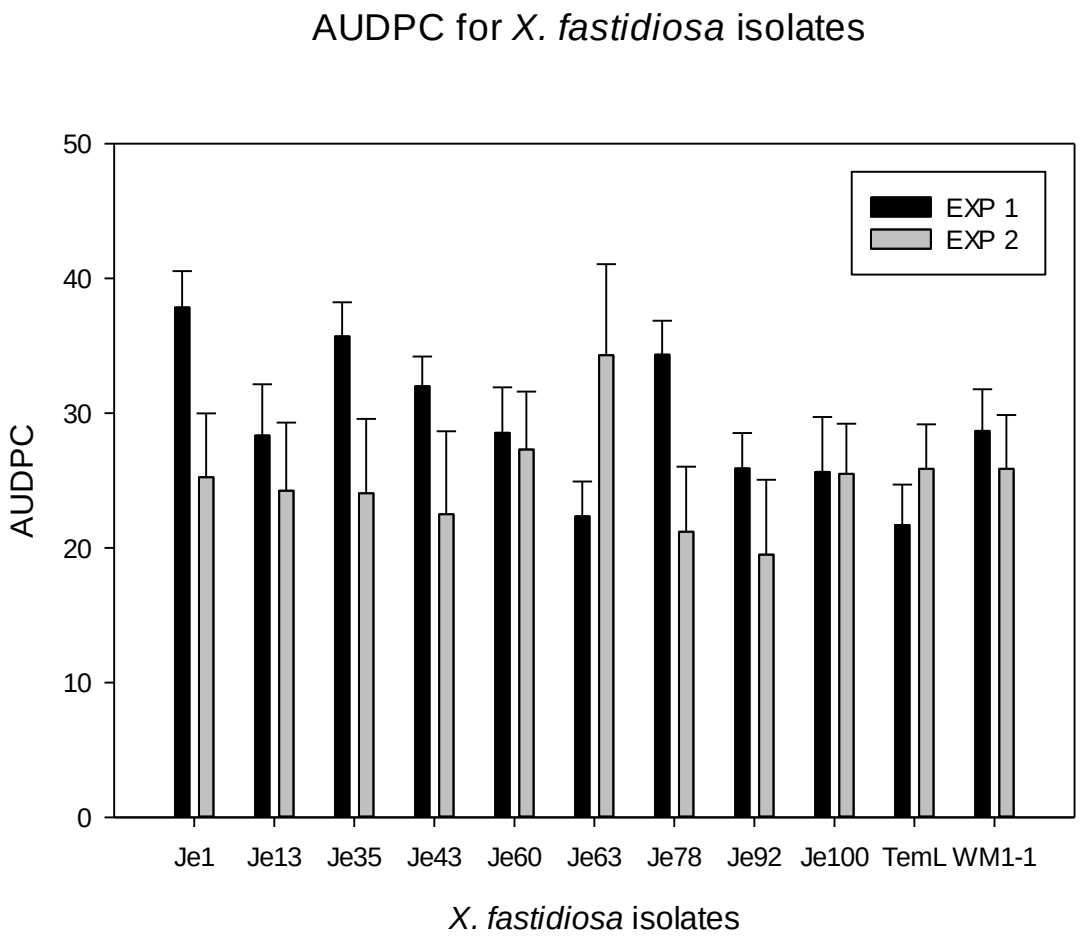

Figure 3-3. AUDPC of *Xylella fastidiosa* common isolates between experiment 1 and 2. Tobacco plants infected with the different isolates were evaluated. Mean of AUDPC based on leaf scorch per isolate during seven weeks of evaluation was used for the graph.

To facilitate the analysis, the progression of leaf scorch was divided by the five geographic areas where the samples were taken: Santa Barbara, Napa, Sonoma, Bakersfield and Temecula. Grouping of the isolates resulted in four isolates for Santa Barbara, seven for Bakersfield, eight for Napa, nine for Temecula and thirteen for Sonoma. For the first group (Santa Barbara), we observed that isolate Je98 sets apart from the other three isolates having the less percentage of leaf scorch inside the group. Je1 showed higher values of leaf scorch from week 1 to week 5. On the

last two weeks of evaluation Je4 takes the lead with values closer to 90% (Figure 4A). Bakersfield showed a clear separation in two groups for the percentage of leaf scorch. The first group formed by three isolates with values between 13.75% - 55%. The second group, most virulent one with values of leaf scorch between 32% - 100% (Figure 4B). Napa showed two isolates (Je13 and Je92) with the lowest values of leaf scorch percentage, while Je87 and Je 96 among others were the most virulent (Figure 4C). Temecula with nine isolates, showed a clear division into two groups in leaf scorch values from week 4. Four isolates showed values of leaf scorch 40% - 58.75% from week 4 to 7. The other five isolates showed 65% - 100% leaf scorch in the same evaluated period (Figure 4D). Sonoma, the group with more representative isolates showed more consistency in values of leaf scorch between strains in the three first weeks, except for Je32 isolate that has higher values than the rest of the group. Around week five three groups can be observed: i) four isolates in values around 45% ii) one isolate with a 64% value and iii) eight isolates with leaf scorch percentages between 77 to 100% (Figure 4E). Variation of leaf scorch progression over time was observed for all isolates evaluated on this study.

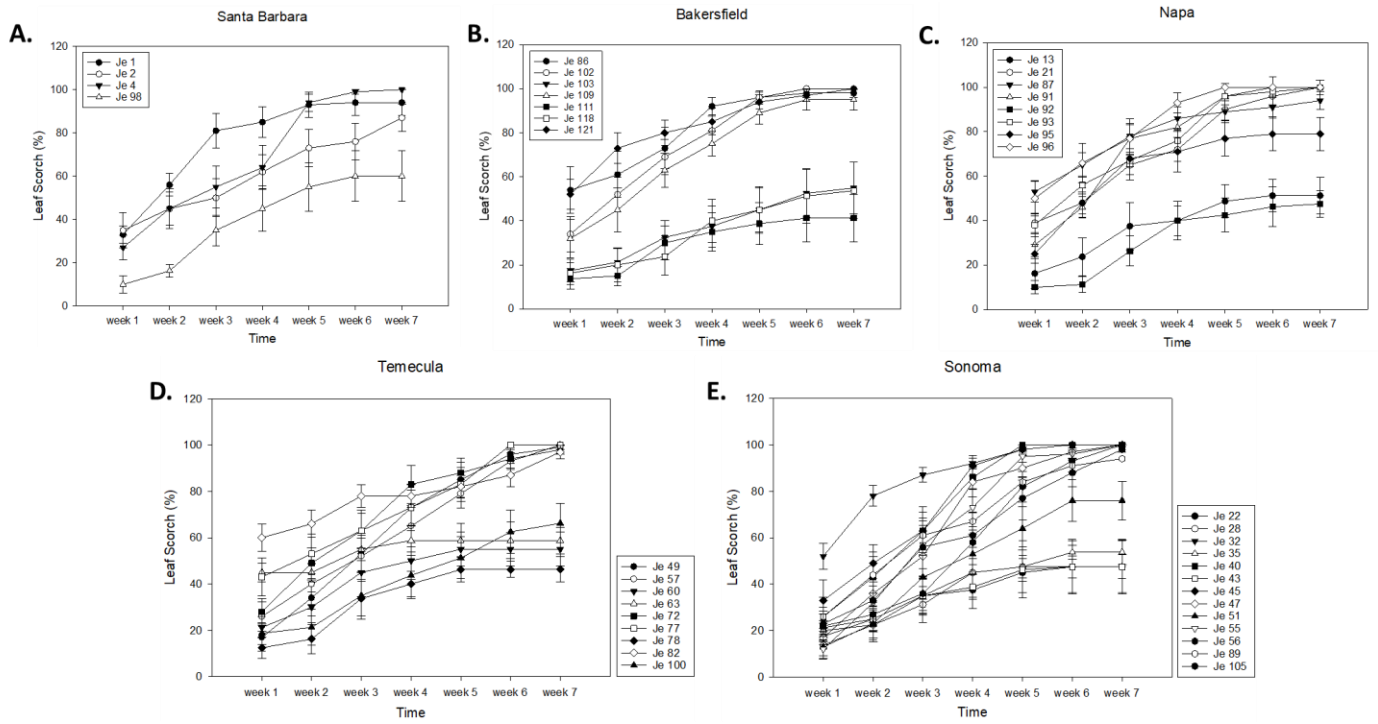

Figure 3-4. Percentage of leaf scorch for tobacco plants infected with *X. fastidiosa* isolates. Groups of strains were organized by geographic location and organized by increasing number of isolates tested per location. **A.** Santa Barbara. **B.** Bakersfield **C.** Napa **D.** Temecula and **E.** Sonoma. Mean of the percentage of leaves showing scorch symptoms per plant (n=10). Ten plants were considered for each isolate. Error bars correspond to standard error of the means. Data used for graph corresponds to one experiment.

As mentioned above, values of severity were also determined using a disease symptoms scale (Table 1). All geographic groups were compared to Temecula 1 and WM1-1 as reference controls. In Santa Barbara Je2 and Je 4 showed the higher grades of severity (Figure 5A). In Bakersfield, while four isolates reached grades of severity higher than WM1-1, three isolates showed to be less virulent than TemeculaL (Figure 5B). In the Napa group five isolates were the most severe, and between those isolates Je91 and Je 93 reached the higher grade of severity (5)

(Figure5C). For the Temecula group, at least three isolates were less virulent than TemeculaL, one has almost the same values of severity as TemeculaL and five isolates were more severe than WM1-1 (Figure5D). In Sonoma, eight isolates were more virulent that WM1-1. Je32, Je40, Je45 and Je55 reached grade 5 on the last week of evaluation (Figure 5E).

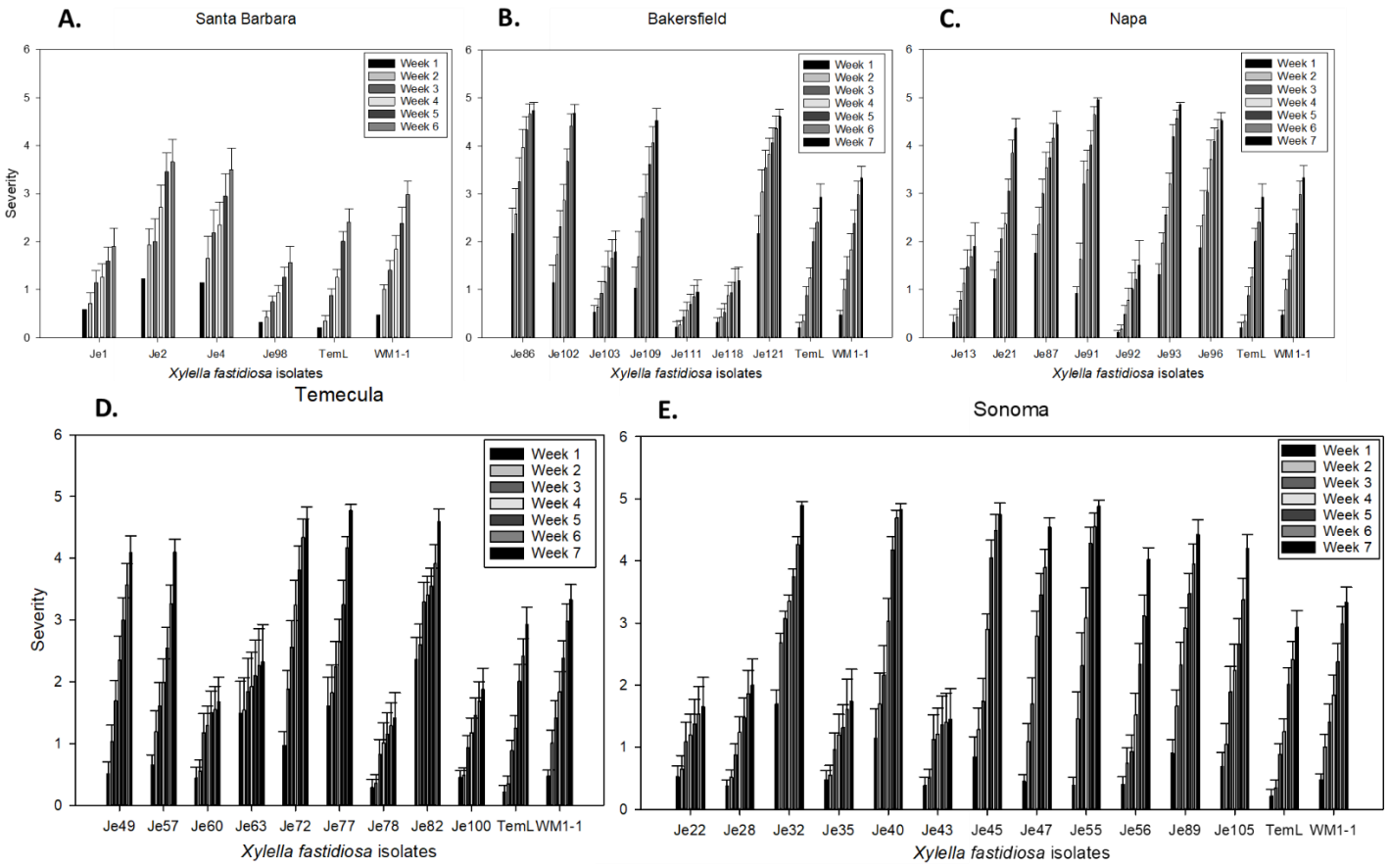

Figure 3-5. Severity of symptoms caused by infection of *X. fastidiosa* isolates in tobacco plants. Groups were established by geographic location and crescent order of isolates forming the group. **A.** Santa Barbara. **B.** Bakersfield **C.** Napa **D.** Temecula and **E.** Sonoma. Mean of the rating assigned by leaves showing scorch symptoms per plant (n=10). Ten plants were considered for each isolate. Error bars correspond to standard error of the means. Data used for graph corresponds to one experiment.

4. DISCUSSION

This study was based on 41 out of the 122 subsp. *fastidiosa* isolates obtained from symptomatic grapevines of five geographic locations across California (Vanhove et al., 2020).

Tobacco plants showed differences in AUDPC, leaf scorch and severity among isolates. Our findings provide valuable information for assessing the risk of each isolate, which could be useful to understand the biology of this pathogen. PD resistance has been identified in multiple *Vitis* species (Deyett et al., 2019, Kyrkou et al., 2018). A single source of resistance PDR1 from *Vitis arizonica*, a wild southwestern grape accession, has been used to develop high quality wine grapes with PD resistance (Krivanek et al., 2006). Other sources of resistance or tolerance have been identified, but their efficacy against multiple isolates of *X. fastidiosa* has not been evaluated. This is the first report on virulence variations between 41 isolates of *X. fastidiosa* subsp. *fastidiosa* on tobacco. Differences in virulence evidenced by symptom development will determine phenotypic groups that will be used to select strains to be tested in grapevines.

To mitigate the impacts and risks that plant pathogens cause is important to understand the pathogen evolution and the origin of pathogenicity and virulence. Until recently, populations of *X. fastidiosa* have been isolated due to geographical and host barriers (Sicard et al., 2018). A human-mediated invasion was associated with the recent emergence of this pathogen in Europe (Saponari et al., 2013). Interestingly, a study suggest that a single genotype from Central America was introduce to California causing PD across the major grape regions on the state (Nunney et al., 2010). There is limited genetic variability among the *X. fastidiosa* species (Van Sluys et al., 2003). Within the species, recombination have been recognized as a main driver of genetic diversity (Nunney et al., 2014b, Kandel et al., 2017). Previous work indicated that recombination within subsp. *fastidiosa* in California is more frequent than in other populations of *X. fastidiosa* studied (Vanhove et al., 2019). Research is needed to better understand the variability of *X. fastidiosa* in California and how this might impact PD resistant grape breeding. This pathogen represents an opportunity to study local adaptation. Biotic and abiotic factors can generate selective pressures

that lead to higher fitness in a specific population related/compared to other (local adaptation) (Giraud et al., 2017). Furthermore, grapevines in California had been affected by recombination of endemic subsp. *multiplex* with the singly-introduced genotype potentially facilitating adaptation to grapevines and environmental conditions for subsp. *fastidiosa* (Vanhove et al., 2019). Host specificity is not well understood, and the genetic determinants are almost entirely unknown. It has been suggested that host adaptation of this bacterium is mediated by gene regulation in response to environmental conditions (Killiny & Almeida, 2011). Recently, a study showed the influence of physical factors on the distribution of this plant-pathogen. Specifically, two lineages were formed due the physical barrier between two counties (Mayacamas mountains) (Vanhove et al., 2020). Another factor that can contribute to the establishment of the bacterium is the climate, temperature and precipitation has been previously shown to be a limiting factor for *X. fastidiosa* survivor in grapevines (Purcell & Hopkins, 1996, Vanhove et al., 2020). Future studies should consider the interactions of abiotic factors and pathogen adaptation to different agroecosystems.

Isolates could efficiently colonize their tobacco plants after pinprick inoculation. Je32, Je86, Je96 and Je121 caused more severe symptoms than the others isolates examined, and achieved the higher values for AUDPC, leaf scorch and severity. In a previous study from our group, WM1-1 was the isolate that caused the most symptoms on tobacco (Oliver et al., 2014). Our results showed that this strain showed fewer symptoms here that several other isolates described above. Intriguingly, Je98, Je111 and Je118 showed significantly less severe symptoms than any of the other *X. fastidiosa* subsp. *fastidiosa* isolates from grape. This information should be useful since due to low symptom severity on grape compared to another *X. fastidiosa* subsp. *fastidiosa* isolates, EB92-1 an isolate from elderberry has been used for cross-protection (biocontrol) in grape (Hopkins, 2005). Interestingly, in each location the analysis of leaf scorch

showed two groups of isolates with high and low virulence. This can be useful for future studies on comparative genomics to understand basis of virulence in *X. fastidiosa*. Concomitant with this study, virulence assays are been developed in grape plants by our collaborator (R. Naegele, data not shown). Preliminary results showed differences in virulence among strains for both the tobacco and grape experiments, but these differences were not consistent between grape and tobacco (Data not shown). Potential causes for the differences in virulence between the isolates and the two hosts are not known, but host adaptation factors may be involved. Formation of tyloses is well characterized in grape in response to *X. fastidiosa* that is known to play a role in the severity of symptoms (Baccari & Lindow, 2011, Sun et al., 2013), while tobacco is not known to form tyloses (Bonsen & Kucera, 1990). For this reason it will be interesting to compare our results with the ones in grape once they become available.

Here, our study demonstrated virulence differences between isolates. These isolates revealed the presence of traits associated with climatic variables and evidence of local adaptation (Vanhove et al., 2020). Taking together this information can be useful to understand the biology of this pathogen to develop control methods against *X. fastidiosa*.

5. EXPERIMENTAL PROCEDURES

5.1 Selection of strains

X. fastidiosa strain TemeculaL (Van Sluys et al., 2003) and WM1-1 (more aggressive strain) (Parker et al., 2012, Oliver et al., 2014) were used in this study as wild-type (WT). *X. fastidiosa* isolates consisted of 41 *X. fastidiosa* subsp. *fastidiosa* isolates originally obtained from grapevine plants showing Pierce's disease symptoms across California (Table 2) (Vanhove et al.,

2020). The isolates were randomly selected from the five different counties: Santa Barbara, Temecula, Bakersfield, Sonoma and Napa. After selection, all cell suspensions of *X. fastidiosa* were prepared as follows. After being recovered from -80 ºC glycerol stocks, bacteria were grown and re-streaked in Periwinkle Wilt (PW) (Davis et al., 1978). For plant inoculation experiments, 7-days-old bacteria were scraped with sterilized loop and suspended in Phosphate-Buffered Saline (PBS) to an optical density ($OD_{(600nm)}$) of 0.8.

Table 3-2. List of *X. fastidiosa* subsp. *fastidiosa* isolates

Isolate Code	Vineyard	County	Variety
Je1		Santa Barbara	Chardonnay
Je2		Santa Barbara	Pinot Noir
Je4		Santa Barbara	Pinot Noir
Je13	Newsome	Sonoma	Malbec
Je21	Newsome	Sonoma	Malbec
Je22	Spring Mountain	Napa	Merlot
Je28	Spring Mountain	Napa	Merlot
Je32	Corn Creek	Napa	Merlot
Je35	Corn Creek	Napa	Merlot
Je40	Black Stallion	Napa	Merlot
Je43	Yount Mill	Napa	Cabernet Sauvignon
Je45	Yount Mill	Napa	Cabernet Sauvignon
Je47	Big Ranch Road	Napa	Cabernet Sauvignon
Je49	Big Ranch Road	Napa	Cabernet Sauvignon
Je51	Silverado	Napa	Merlot
Je55	Oak Knoll road	Napa	Cabernet Sauvignon
Je56	Oak Knoll road	Napa	Cabernet Sauvignon

Je57	Stage Leap	Napa	?
Je60	Site 1, Scarlet Royal	Bakersfield	Scarlet Royal
Je63	Site 2, Flames	Bakersfield	Flames
Je72	Site 3, Red Globe	Bakersfield	Red Globe
Je77	Site 3, Red Globe	Bakersfield	Red Globe
Je78	Site 4, Holiday	Bakersfield	Holiday
Je82	Site 4, Holiday	Bakersfield	Holiday
Je86	FP	Temecula	
Je87	Saini	Sonoma	
Je89	Gallo Chiotti	Sonoma	
Je91	Vino Ranch 30	Sonoma	
Je92	MacMurray	Sonoma	Gruner Veltliner
Je93	MacMurray	Sonoma	Gruner Veltliner
Je95	Rudd	Sonoma	Chardonnay
Je96	Olson	Sonoma	Chardonnay
Je98	CC	Temecula	
Je100	CC	Temecula	
Je102	CC 2	Temecula	
Je103	CC 2	Temecula	
Je105	FP	Temecula	
Je109	LNA	Temecula	
Je111	LNA	Temecula	
Je118	BV	Temecula	
Je121	BV	Temecula	
TemeculaL		Temecula	Temecula
WM1-1	Georgia*	Lumpkin county	Mourvedre

5.2 Greenhouse experiments

Tobacco (*Nicotiana tabacum*) plants from cultivar SR1 “Petite Havana” were grown in greenhouse conditions: 20 - 25 ℃ temperature, in 4.5-inch rounded pots and natural light. Tobacco seeds were planted in sunshine mix (Sun Gro Horticulture Canada Ltd., Vancouver, Canada). Fertilization was scheduled for three times during the growing period and whenever the leaves

were turning yellow with a slow release fertilizer (Peter's Professional 20-10-20 PeatLite Special; The Scotts Company, Marysville, OH, U.S.A.). Inoculation was made in cut plants with three mature leaves following a previously described protocol (Francis et al., 2008, De La Fuente et al., 2013). Briefly, 20µL of each *X. fastidiosa* isolate suspension in PBS were applied on the petiole base of the three leaves through needle pin-prick method. The inoculum consisted of each of the 43 strains suspended in PBS at OD_{600}=0.8. Ten plants were inoculated per isolate treatment, and inoculation with only PBS was used as a control treatment. Each isolate was tested in one experiment, except for a subset of 9 isolates that were tested in two independent experiments.

5.3 Disease progression and virulence assays

Plants were maintained in the greenhouse for 3-4 months. 12 -14 weeks after inoculation, symptoms became evident and a weekly evaluation of leaf scorch, AUDPC and severity was performed. AUDPC was calculated based on the midpoint rule method (Campbell & Madden, 1990) as follows: $AUDPC= \Sigma [(yi + yi+1)/2](ti+1 – ti)$, where i = the number of assessment times, y = disease severity score for each plant at each assessment, and t = time at each assessment. Leaf scorch was determined by the number of leaves showing scorch symptoms per plants / total leaves multiply by 100. Severity was assessed by giving a score for each leaf as described in Table 1.

6. ACKNOWLEDGMENTS

This research was funded by a grant from the California Department of Food and Agriculture (CDFA) (Project #16006/17005), Pierce's disease, glassy winged sharpshooter (PD/GWSS) program; and the Department of Entomology and Plant Pathology at Auburn

University. We also thank Marcus Vinicius Merfa, Deepak Shantharaj and Ranlin Liu for assistance in the inoculation of the isolates on the greenhouse.

7. REFERENCES

Almeida, R.P., Nascimento, F.E., Chau, J., Prado, S.S., Tsai, C.W., Lopes, S.A., and Lopes, J.R. (2008) Genetic structure and biology of *Xylella fastidiosa* strains causing disease in citrus and coffee in Brazil. *Appl Environ Microbiol* **74**: 3690-3701.

Baccari, C., and Lindow, S.E. (2011) Assessment of the Process of Movement of *Xylella fastidiosa* Within Susceptible and Resistant Grape Cultivars. *Phytopathology* **101**: 77-84.

Bonsen, K.J.M., and Kucera, L.J. (1990) Vessel Occlusions in Plants - Morphological, Functional and Evolutionary Aspects. *Iawa Bulletin* **11**: 393-399.

Campbell, C.L., and Madden, L.V. (1990) *Introduction to Plant Disease Epidemiology*. New York: Wiley.

Chatterjee, S., Almeida, R.P., and Lindow, S. (2008) Living in two worlds: the plant and insect lifestyles of *Xylella fastidiosa*. *Annu Rev Phytopathol* **46**: 243-271.

Chen, H., Kandel, P.P., Cruz, L.F., Cobine, P.A., and De La Fuente, L. (2017) The Major Outer Membrane Protein MopB Is Required for Twitching Movement and Affects Biofilm Formation and Virulence in Two *Xylella fastidiosa* strains. *Mol Plant Microbe Interact* **30**: 896-905.

Coletta-Filho, H.D., Francisco, C.S., Lopes, J.R., De Oliveira, A.F., and Da Silva, L.F. (2016) First report of olive leaf scorch in Brazil, associated with *Xylella fastidiosa* subsp. pauca.

Cruz, L.F., Cobine, P.A., and De La Fuente, L. (2012) Calcium increases *Xylella fastidiosa* surface attachment, biofilm formation, and twitching motility. *Appl Environ Microbiol* **78**: 1321-1331.

Davis, M.J., Purcell, A.H., and Thomson, S.V. (1978) Pierce's disease of grapevines: isolation of the causal bacterium. *Science* **199**: 75-77.

De La Fuente, L., Parker, J.K., Oliver, J.E., Granger, S., Brannen, P.M., van Santen, E., and Cobine, P.A. (2013) The bacterial pathogen *Xylella fastidiosa* affects the leaf ionome of plant hosts during infection. *PLoS One* **8**: e62945.

Deyett, E., Pouzoulet, J., Yang, J.I., Ashworth, V.E., Castro, C., Roper, M.C., and Rolshausen, P.E. (2019) Assessment of Pierce's disease susceptibility in *Vitis vinifera* cultivars with different pedigrees. *Plant Pathology* **68**: 1079-1087.

Francis, M., Civerolo, E.L., and Bruening, G. (2008) Improved Bioassay of *Xylella fastidiosa* using Nicotiana tabacum cultivar SR1. *Plant Disease* **92**: 14-20.

Francis, M., Lin, H., Rosa, J.C.-L., Doddapaneni, H., and Civerolo, E.L. (2006) Genome-based PCR Primers for Specific and Sensitive Detection and Quantification of *Xylella fastidiosa*. *European Journal of Plant Pathology* **115**: 203-213.

Giraud, T., Koskella, B., and Laine, A.L. (2017) Introduction: microbial local adaptation: insights from natural populations, genomics and experimental evolution. *Mol Ecol* **26**: 1703-1710.

Hopkins, D.L. (2005) Biological Control of Pierce's Disease in the Vineyard with Strains of *Xylella fastidiosa* Benign to Grapevine. *Plant Dis* **89**: 1348-1352.

Hopkins, D.L., and Purcell, A.H. (2002) *Xylella fastidiosa*: Cause of Pierce's Disease of Grapevine and Other Emergent Diseases. *Plant Dis* **86**: 1056-1066.

Janse, J.D., and Obradovic, A. (2010) *Xylella fastidiosa*: Its Biology, Diagnosis, Control and Risks. *Journal of Plant Pathology* **92**: S35-S48.

Kandel, P.P., Lopez, S.M., Almeida, R.P., and De La Fuente, L. (2016) Natural Competence of *Xylella fastidiosa* Occurs at a High Frequency Inside Microfluidic Chambers Mimicking the Bacterium's Natural Habitats. *Appl Environ Microbiol* **82**: 5269-5277.

Kandel, P.P., Almeida, R.P.P., Cobine, P.A., and De La Fuente, L. (2017) Natural Competence Rates Are Variable Among *Xylella fastidiosa* Strains and Homologous Recombination Occurs In Vitro Between Subspecies fastidiosa and multiplex. *Mol Plant Microbe Interact* **30**: 589-600.

Killiny, N., and Almeida, R.P. (2011) Gene regulation mediates host specificity of a bacterial pathogen. *Environ Microbiol Rep* **3**: 791-797.

Krivanek, A.F., Riaz, S., and Walker, M.A. (2006) Identification and molecular mapping of PdR1, a primary resistance gene to Pierce's disease in Vitis. *Theor Appl Genet* **112**: 1125-1131.

Kyrkou, I., Pusa, T., Ellegaard-Jensen, L., Sagot, M.F., and Hansen, L.H. (2018) Pierce's Disease of Grapevines: A Review of Control Strategies and an Outline of an Epidemiological Model. *Front Microbiol* **9**: 2141.

Lopes, S.A., Ribeiro, D.M., Roberto, P.G., Franca, S.C., and Santos, J.M. (2000) Nicotiana tabacum as an experimental host for the study of plant-*Xylella fastidiosa* interactions. *Plant Disease* **84**: 827-830.

Navarrete, F., and De La Fuente, L. (2015) Zinc Detoxification Is Required for Full Virulence and Modification of the Host Leaf Ionome by *Xylella fastidiosa*. *Mol Plant Microbe Interact* **28**: 497-507.

Nunney, L., Yuan, X., Bromley, R.E., and Stouthamer, R. (2012) Detecting genetic introgression: high levels of intersubspecific recombination found in *Xylella fastidiosa* in Brazil. *Appl Environ Microbiol* **78**: 4702-4714.

Nunney, L., Schuenzel, E.L., Scally, M., Bromley, R.E., and Stouthamer, R. (2014a) Large-scale intersubspecific recombination in the plant-pathogenic bacterium *Xylella fastidiosa* is associated with the host shift to mulberry. *Appl Environ Microbiol* **80**: 3025-3033.

Nunney, L., Hopkins, D.L., Morano, L.D., Russell, S.E., and Stouthamer, R. (2014b) Intersubspecific recombination in *Xylella fastidiosa* Strains native to the United States: infection of novel hosts associated with an unsuccessful invasion. *Appl Environ Microbiol* **80**: 1159-1169.

Nunney, L., yuan, X., Bromley, R., Hartung, J.S., Montero-Astua, M., Moreira, L. et al. (2010) Population Genomic Analysis of a Bacterial Plant Pathogen: Novel Insight into the Origin of Pierce's Disease of Grapevine in the U.S.

Oliver, J.E., Cobine, P.A., and De La Fuente, L. (2015) *Xylella fastidiosa* Isolates from Both subsp. multiplex and fastidiosa Cause Disease on Southern Highbush Blueberry (Vaccinium sp.) Under Greenhouse Conditions. *Phytopathology* **105**: 855-862.

Oliver, J.E., Sefick, S.A., Parker, J.K., Arnold, T., Cobine, P.A., and De La Fuente, L. (2014) Ionome changes in *Xylella fastidiosa*-infected Nicotiana tabacum correlate with virulence and discriminate between subspecies of bacterial isolates. *Mol Plant Microbe Interact* **27**: 1048-1058.

Parker, J.K., Havird, J.C., and De La Fuente, L. (2012) Differentiation of *Xylella fastidiosa* strains via multilocus sequence analysis of environmentally mediated genes (MLSA-E). *Appl Environ Microbiol* **78**: 1385-1396.

Purcell, A.H., and Hopkins, D.L. (1996) Fastidious xylem-limited bacterial plant pathogens. *Annu Rev Phytopathol* **34**: 131-151.

Saponari, M., Boscia, D., Nigro, F., and Martelli, G.P. (2013) Identification of DNA Sequences Related to *Xylella fastidiosa* in Oleander, Almond and Olive Trees Exhibiting Leaf Scorch Symptoms in Apulia (Southern Italy). *Journal of Plant Pathology* **95**: 668-668.

Scally, M., Schuenzel, E.L., Stouthamer, R., and Nunney, L. (2005) Multilocus sequence type system for the plant pathogen *Xylella fastidiosa* and relative contributions of recombination and point mutation to clonal diversity. *Appl Environ Microbiol* **71**: 8491-8499.

Sicard, A., Zeilinger, A.R., Vanhove, M., Schartel, T.E., Beal, D.J., Daugherty, M.P., and Almeida, R.P.P. (2018) *Xylella fastidiosa*: Insights into an Emerging Plant Pathogen. *Annu Rev Phytopathol* **56**: 181-202.

Simpson, A.J., Reinach, F.C., Arruda, P., Abreu, F.A., Acencio, M., Alvarenga, R. et al. (2000) The genome sequence of the plant pathogen *Xylella fastidiosa*. The *Xylella fastidiosa* Consortium of the Organization for Nucleotide Sequencing and Analysis. *Nature* **406**: 151-159.

Sun, Q., Sun, Y., Walker, M.A., and Labavitch, J.M. (2013) Vascular occlusions in grapevines with Pierce's disease make disease symptom development worse. *Plant Physiol* **161**: 1529-1541.

Van Sluys, M.A., de Oliveira, M.C., Monteiro-Vitorello, C.B., Miyaki, C.Y., Furlan, L.R., Camargo, L.E. et al. (2003) Comparative analyses of the complete genome sequences of Pierce's disease and citrus variegated chlorosis strains of *Xylella fastidiosa*. *J Bacteriol* **185**: 1018-1026.

Vanhove, M., Sicard, A., Ezennia, J., Leviten, N., and Almeida, R.P.P. (2020) Population structure and adaptation of a bacterial pathogen in California grapevines. *Environ Microbiol* **22**: 2625-2638.

Vanhove, M., Retchless, A.C., Sicard, A., Rieux, A., Coletta, H.D., De La Fuente, L. et al. (2019) Genomic Diversity and Recombination among *Xylella fastidiosa* Subspecies. *Applied and Environmental Microbiology* **85**.

Chapter 4

Design and construction of an in-plant super expression cassette for transgene expression of *CAX3*

1. ABSTRACT

Xylella fastidiosa (Xf) is a Gram-negative, insect-transmitted, xylem-limited bacterium that causes disease in many economic and ecological important host plants. Preliminary results indicate that Ca supplementation in tobacco caused more severe symptoms and increased populations of Xf, and that infection of tobacco with Xf results in significant changes in the leaf ionome. To predict initial candidate genes for Ca regulation, we combined data from four different sources 1) the ionomics database, iHub a publicly accessible database created and hosted by Purdue University; 2) the common data from two published gene expression studies on Xf-host interactions; and 3) the most recent comprehensive analysis in grapes. Gene comparison between sources resulted in *CAX3* gene as a candidate. *CAX3* belongs to a family of endomembrane cation exchangers (CAXs) transports Ca^{2+} and other cations. Previous results showed that increase expression of *CAX3* could affect the cytosolic Ca concentrations and in turn initiate a cascade of responses leading to leaf scorch. To define the role of *CAX3* in the interaction with Xf and prove that more Ca flowing through the xylem will cause higher disease severity, an overexpression of CAX3 was made using the Gateway system. Two different markers were used: GUS and GFP, and tobacco plants were transformed by *Agrobacterium*. Plants could not develop from the calli generated by *Agrobacterium*- mediated transformation. We hypothesized that CAX3 can alter the phenotype and development of the plants and that is why no plant was grown, and we propose that Ca application in the medium can restore the phenotype.

2. INTRODUCTION

Xylella fastidiosa is a xylem-limited bacterial pathogen that causes devastating plant diseases, including Pierce's disease on grape, citrus variegated chlorosis, olive quick decline syndrome, and many others (Almeida & Nunney, 2015, Sicard et al., 2018). Leaf scorch is one of the most characteristic symptoms of the diseases caused by *X. fastidiosa* and has been related to biofilm formation inside xylem vessels blocking water and nutrients passage (Chatterjee et al., 2008a). Ionome (mineral nutrient and trace elements found in an organism) characterization during infection showed spatial and temporal changes in tobacco plants (De La Fuente et al., 2013). Bacterial infection was found to cause significant increases in concentrations of Ca prior to the appearance of symptoms (De La Fuente et al., 2013, Oliver et al., 2014).

Calcium (Ca^{2+}) acts as an important secondary messenger in plant cells. Ca^{2+} also stabilizes cell membranes by connecting adjacent polar head groups of membrane lipids (Legge et al., 1982, Hirschi, 2004). It also protects membranes from adverse effects of stress such as salinity (Cramer et al., 1985), freezing injury (Arora & Palta, 1988), and heat stress (Tawfik et al., 1996, Kleinhenz & Palta, 2002, Saidi et al., 2009). Ca homeostasis maintains the concentration of extracellular Ca^{2+} in the millimolar range, whereas the cytoplasmic concentration of Ca^{2+} is in the nanomolar to micromolar range (Kauss, 1987, Gilroy et al., 1993). In unstimulated cells, cytosolic Ca^{2+} concentrations are usually maintained at lower levels, around 100 nM (Sanders et al., 1999). Cytosolic concentrations are essential for the conversion of signals. Transient elevations of cytosolic Ca are observed in response to red light, touch, cold shock, and pathogen infection/challenge (Hirschi et al., 1996, Hirschi, 1999, Ma et al., 2009). Ca^{2+} transient elevations have been observed in both compatible and incompatible plant-pathogen interactions. Ca

antiporters and efflux pumps are important to maintain the cytoplasmic calcium at low levels and restoring the normal Ca^{2+} levels after perturbation (Tuteja & Mahajan, 2007).

The plant vacuolar membrane is known to possess high capacity H^+/Ca^{2+} exchange activity. One class of transporter protein that mediates the transport of both Ca^{2+} and other metal ions is the Cation/H^+ Exchanger (CAX), a secondary energized transporter that is dependent on a proton (H^+) gradient across a membrane, and usually localized at an acidic compartment such as the vacuole (Schumaker & Sze, 1985, Blumwald & Poole, 1986). As H^+-coupled antiporters, CAXs can mediate the movement of a cation against its concentration gradient and out of the cytosol. Thus it has been proposed that a primary cellular function of the CAX proteins is to restrict cytosolic accumulation of certain free metal ions, such as manganese (Mn^{2+}) or cadmium (Cd^{2+}) to provide tolerance against metal toxicity, and to maintain a low cytosolic resting concentration of Ca^{2+}, to prevent Ca^{2+} toxicity and prime the generation of cytosolic Ca^{2+} signals (Hirschi et al., 2000, Pittman et al., 2009). Although CAXs are just one class of ion transporter able to mediate such housekeeping functions, a wealth of evidence now indicates their importance to plants, especially during abiotic stress.

CAX genes encoding cation/proton exchangers play a crucial role in the sequestration of cations such as Mn^{2+}, sodium (Na), lithium (Li), and Cd^{2+}, as well as Ca^{2+}, into the vacuole using proton gradients provided by H^+ pumps such as H^+-pyrophosphatase or H^+-ATPase (Korenkov et al., 2007, Pittman, 2011, Shigaki & Hirschi, 2006, Shigaki et al., 2010, Zhao et al., 2009). Six *CAX* genes have been identified so far in the Arabidopsis genome (Shigaki & Hirschi, 2006). *CAX3,* a tonoplast-localized transporter, has been shown to participate in plant responses to excess levels of Na and Li and pH fluctuation (Zhao et al., 2009). Interestingly, *CAX3* (and s*CAX3*), which is most similar to CAX1 (77% identical at the amino acid level), is at best a weak

vacuolar Ca transporter when expressed in yeast cells (Shigaki & Hirschi, 2000, Cheng et al., 2005). Interplay between *CAX1* and *CAX3* has been suggested through genetic studies and yeast expression assays (Cheng et al., 2005). Understanding of the biological roles these *CAX* transporters play in cell growth and in response to environmental stresses, is only beginning to emerge.

Four different databases were used to predict candidate genes for Ca-regulation in the Xf-infected tobacco plants. *CAX3* was one of the genes identified as in common from the four different sources. Increased expression of *CAX3* was found in response to infection with *X. fastidiosa*. This study had the objective of performing functional analysis in plants overexpressing *CAX3*, since this gene have been suggested to show regulation of Ca in response to infection in other systems.

3. RESULTS

3.1 Use of the 2X 35S enhancer–promoter to obtain high-level, *CAX3*-specific transgene expression

CAX3 was selected from different databases (ionome and transcriptome analyses) that evaluated the interaction between different plants and *X. fastidiosa*. The sequence was blasted in the tobacco genome and then confirmed by PCR. To obtain modified Gateway Entry cassettes for overexpression, we first generated a pCR8/GW/TOPO vector by introducing a *CAX3* fragment. GUS and GFP were chosen for localization analyses. This vector has then been used as mother plasmid for subsequent cloning. The modified Entry vectors containing the tagged ORFs of interest were then recombined by site-specific recombination (SSR) into binary Gateway overexpression vectors pMDC84 and pMDC140 from the Laboratory of Plant Systems Biology (PSB; Ghent

University, Belgium) (Figure 1). These vectors have a 35S Cauliflower Mosaic Virus (CaMV) promoter/terminator and a hygromycin-B resistance cassette.

We chose to use these binary Destination vectors over others due to the flexibility they offer with respect to selectable markers and promoters. A further advantage is that they have a kanamycin bacterial selectable marker, whereas the entry vectors contain a spectinomycin resistance cassette, thus allowing easy selection of the correct recombined product after the Gateway recombination reaction. After characterization and verification of the construction, *E. coli* colonies with the T-DNA binary vector were mobilized (by bacterial conjugation or transformation) into an appropriate *Agrobacterium* strain LBA4404.

Figure 4-1. Modified Overexpression vectors. *CAX3* sequence was introduced in the vector between the *attR1* and *attR2* recombination sites to generate modified vectors. A. pMDC84 vector with GFP marker and B. pMDC140 with GUS marker.

3.2 Tobacco plants transformed by *Agrobacterium*

Suspension-cultured tobacco leaf disks were transformed by co-cultivating with *A. tumefaciens* containing the binary vector pMDC84 and pMDC140. The Hygromycin-resistant transformants formed calli of about 1 to 2 mm diameter within 20 days on agar medium containing 30mg/mL of hygromycin, whereas untreated tobacco cells did not grow on the antibiotic plates.

Transformation frequency was dependent on the physiological state of the tobacco cells and overgrowth was observed in these experiments.

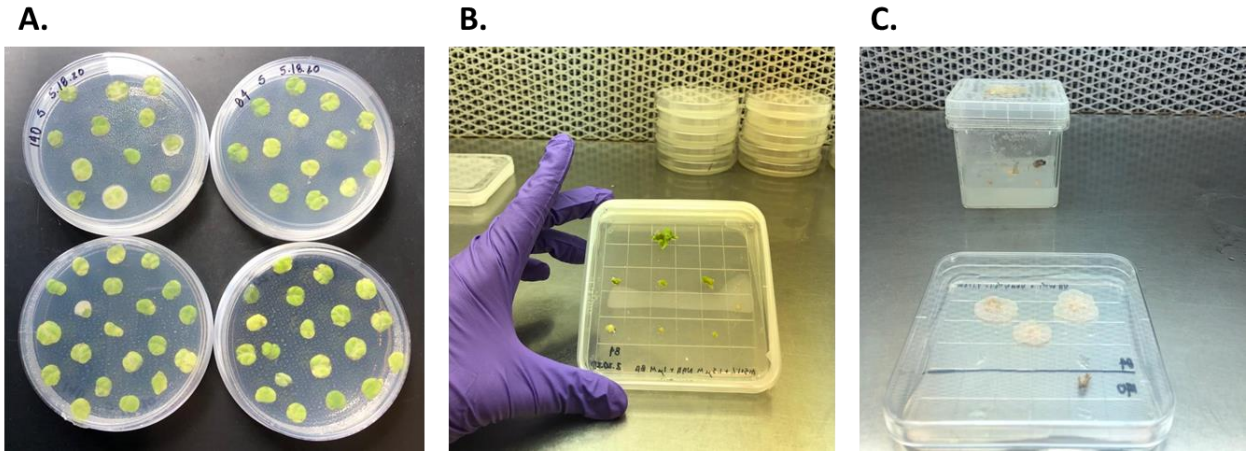

Figure 4-2. Transformation of tobacco-cultured cells with *A. tumefaciens* containing pMDC84 and pMDC140 binary vectors. A. Two-week-old tobacco cells were co-cultivated with *A. tumefaciens* containing pMDC84 and pMDC140. **B.** Transformed calli selected on the Murashige and Skoog agar medium containing 30mg/mL of hygromycin. **C.** *Agrobacterium* overgrowth surrounding the calli in the selection medium.

4. DISCUSSION

Plant xylem, the system that conveys water and dissolved minerals from the roots to the photosynthetic organs, can serve as a growth niche for microbes including bacterial pathogens. *X. fastidiosa* is only found in the water-conducting xylem vessels of plants and in the foregut of different types of xylem-sap feeding leafhopper insect vectors (Chatterjee et al., 2008a). It is believed that *X. fastidiosa* biofilm formation is responsible for disrupting the passage of water and nutrients (Goodwin et al., 1988, Chatterjee et al., 2008a, Dandekar et al., 2012). Mineral nutrient and trace elements (ionome) studies (Salt et al., 2008) have been shown as an appropriate indicator of the physiological status of the whole plant, and therefore have been used to elucidate the effects

of bacterial infection on the host (Cobine et al., 2013, De La Fuente et al., 2013, Oliver et al., 2014). Ionome changes has been described in the interaction of tobacco plants with *X. fastidiosa*. Ca is one of the elements that showed to be upregulated in that interaction (De La Fuente et al., 2013). Changes in Ca^{2+}concentration had also been detected during effector-triggered immunity (ETI), specifically in the incompatible interactions between *Pseudomonas syringae pv. tomato* (containing *avrRpm1*) and *RPM1* in *Arabidopsis (Grant et al., 2000).* Interestingly, the pattern and dynamics of changes in Ca^{2+} concentrations were quite different in compatible and incompatible plant-pathogen interactions (Lecourieux et al., 2006), which may be related to the distinct defense responses in pathogen-associated molecular pattern (PAMP)-triggered immunity (PTI) and ETI. These changes in intracellular Ca^{2+}concentration were shown to correlate with the subsequent defense related physiological responses in host cells such as production of reactive oxygen species (ROS) and nitric oxide (NO), as well as induced expression of pathogenicity-related (PR) genes (Zhang et al., 2014).

CAX are exchangers that control the homeostasis of several elements including Ca (Hirschi et al., 1996, Cheng et al., 2005, Punshon et al., 2012, Modareszadeh et al., 2020). The first plant H^+/Ca^{2+} exchangers to be functionally expressed, AthCAX1 and AthCAX2 (Currently known as CAX1 and CAX2), were cloned from *A. thaliana* by suppression of yeast mutants defective in vacuolar Ca^{2+} transport (Hirschi et al. 1996). Since then, more antiporters have been named with a CAX prefix but have no solid criteria for the classification. Plant CAXs are classified into three major types of CAXs: type I (CAXs similar to Arabidopsis thaliana CAX1, found in plants, fungi, and bacteria), type II (CAXs with a long N-terminus hydrophilic region, found in fungi, Dictyostelium, and lower vertebrates), and type III (CAXs similar to Escherichia coli ChaA, found in bacteria) (Shigaki et al 2006). In Arabidopsis, CAX1, CAX3, and CAX4 form Type IA CAXs,

and CAX2, CAX5, and CAX6 are grouped into Type I B CAXs (Shigaki1 and K. D. Hirschi, 2005). Some determinants of cation specificity in CAXs have been characterized. For example, the nine-amino-acid-long region of CAX1 has been shown to confer calcium transport ability to its close non-calcium-transporting homologue CAX3 (Shigaki et al. 2001). Recent genetic studies in planta suggested a functional association between the CAX transporters (Cheng et al., 2005). *CAX3* was found to be upregulated in the interaction of tobacco plants and *X. fastidiosa*. *CAX1* and *CAX3* appears to form a heteromers which confer different biological properties and causes significant alterations in plant growth including stunting and tip necrosis. In total, these perturbations cause dramatic alterations in the ionome (Cheng et al., 2005). Altered phenotypes as necrosis of young leaves, often followed by necrosis of the apical meristem and brownish and short roots were described in other studies (Hirschi, 1999). Interestingly, the symptoms described before were related to the expression of *CAX1* and *CAX3* in different tissues in *Arabidopsis*. For instance, preferential GUS expression for *CAX1* was seedlings, young leaves and lateral buds, while *CAX3* had strong GUS staining in primary and lateral root tips and the root elongation region of the plant (Cheng et al., 2005). This alterations in morphology emphasize the fact that modulated expression of a H^+/Ca^{2+} antiporter is important for normal growth and several biological responses. We can infer based in this information that perturbing multiple CAX transporters causes significant alterations in plant growth. Agreeing with those studies our experiments showed modified phenotype, since the calli developed after the agrobacterium mediated transformation but could not grow into a plant. This effect might be related with the overexpression of the gene. And perhaps it might be reverted when adding Ca to the medium to abrogate these sensitivities, as showed by other studies that obtained some altered phenotype affecting growth parameters that were reversible when Ca was added to the plant growth media (Hirschi, 1999).

In our experiments mediated *Agrobacterium* transformation overexpressing *CAX3* resulted in *Agrobacterium* overgrowth in most of the experiments. Overgrowth is one of the major problems of plant genetic transformation, and *Agrobacterium* can be seen to grow out of control on explants and eventually destroy the explants (Liu et al. 2016). In most cases, once overgrowth occurs, it is impossible to reverse. The best-known solution is to begin again with another transformation experiment. Is possible that growth of the calli was affected by the *CAX3* Agrobacterium-mediated transformation.

5. MATERIAL AND METHODS

5.1 Plant Material - Tissue Culture

Seeds of *Nicotiana tabacum* 'Petite Havana SR1' (Plant Introduction (PI) number 552516) were grown for 4 weeks at ~25°C on a 14h light/10h dark cycle in magenta boxes containing one-half strength Murashige and Skoog (MS) medium (Murashige and Skoog, 1962), 2% (w/v) sucrose and 1% (w/v) agar, pH 5.7 (standard media) (Murashige & Skoog, 1962). Inside the hood and using sterile material, tobacco seeds were put inside an Eppendorf (1.5 or 2.0 mL). 1mL of 70% ethanol was added and stirred for 2min. After washing the ethanol out, 1.5mL of 5% hypochlorite was added and vortexed for 2min. The hypochlorite was discarded, and the seeds were rinsed four times with sterile water. 500µL of water was added to the seeds and they were spread in magenta boxes containing germination medium. Yellowish leaves were avoided to improve the transformation rate.

5.2 Plasmid DNA Constructs and Plant Transformation

To make translational fusions to GUS and GFP reporter genes, *CAX3* region was amplified from tobacco genomic DNA by PCR using the primers described in Table 1. Resulting PCR products were digested with the restriction enzyme EcoRI. The 2-kb PCR products of *CAX3* sequences were cloned into the pENTR/D-TOPO vector (Promega, Madison, WI). The *CAX3*-TOPO gene was subcloned into the plant expression vector pMDC84 and pMDC140, which is driven by a cauliflower mosaic virus 35S promoter. All the recombinant plasmids and empty vector controls were introduced into *Agrobacterium tumefaciens* LB4404 (Life Technologies, Grand Island, NY) (Sambrook et al., 1989) (Figure 3).

Table 4-1. Primers used in this study

Primer name	Function/Target	Sequence	Source
***CAX3* - F**	*CAX3* forward	5'TCATCATCAGCACCAGCAG3'	This study
***CAX3* - R**	*CAX3* reverse	5'TAGGCTCAGCAACTCAAATTGC3'	This study
***CAX3*GUS-F**	Upstream *CAX3*	5'GTGCGCCAGGAGAGTTGTTG3'	This study
***CAX3*GUS-R**	Middle of *GUS*	5'GACCTCGACTCTAGAACTAG3'	This study
***CAX3*GFP-F**	Upstream *CAX3*	5'CATCGCAAGACCGGCAACAG3'	This study
***CAX3*GFP-R**	Middle of *GFP*	5'GGAGAGGACCTCGACTCTAG3'	This study

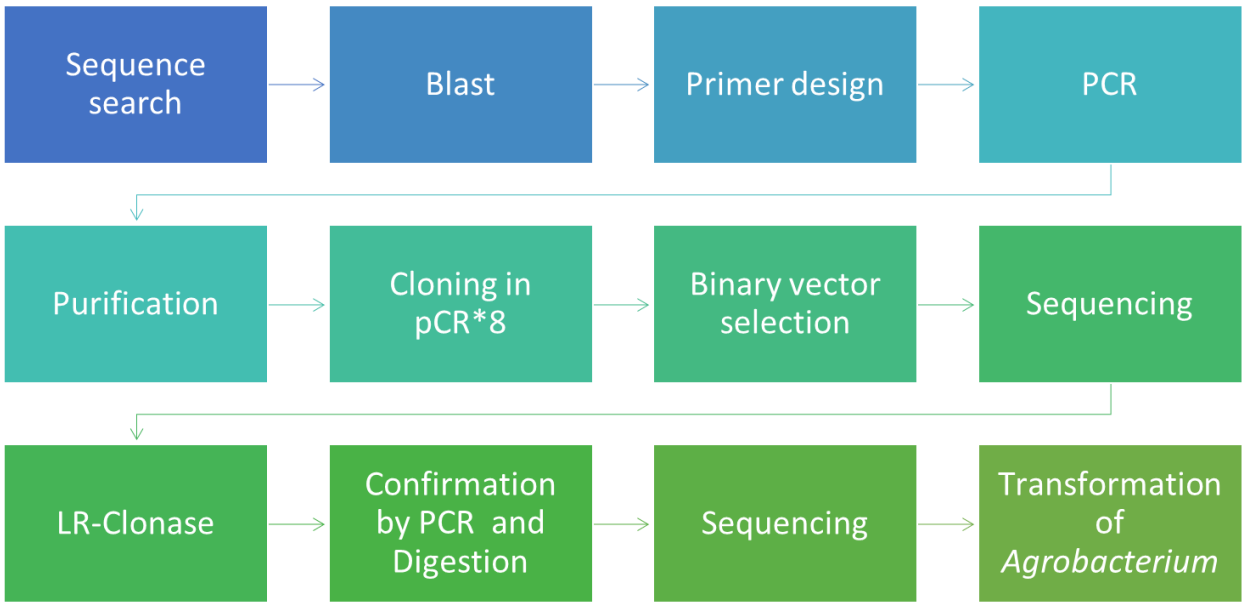

Figure 4-3. Scheme of the pipeline for the construction of *CAX3* overexpression cassette.

These strains were used to transform *Nicotiana tabacum* 'Petite Havana SR1' (Plant Introduction (PI) number 552516) according to published methods (Hirschi, 1999). Briefly, tobacco leaf disc were cut from leaves growth in the magenta boxes. The discs were placed inside petri dishes, always maintaining them in liquid MS medium. Disks were placed with the abaxial face turned up in MS co-cultivation medium. 15µL of the *Agrobacterium* resuspended culture were added in each leaf disk placed onto MS co-cultivation medium. The infected leaf disks were kept for 3 days in the dark at 24°C. Then, the disks were transferred to MS selective medium containing 30mg/mL and the plates were placed under the light until the shoots appear. Once the calli were formed, the shoots were excised and placed in magenta boxes containing rooting medium until the roots develop. The inoculum of *Agrobacterium* was prepared as follows. *Agrobacterium* containing each vector (pMDC84 and pMDC140) were grown in appropriate solid YEP broth (5 g NaCl, 10 g peptone and 5g yeast extract per liter distilled water) for three days. Pre culture was

prepared in 10mL YEP liquid medium containing the appropriate antibiotics and grow overnight at 28°C and 220 rpm. On the transformation day 5mL of pre culture grown overnight was transfer to fresh 50mL YEP with the same antibiotics and grow at 28°C and 220 rpm, until the OD_{600} was between 0.6 and 0.8. Cells were centrifuge for 15 – 20 min at 3500rpm and suspended in MS liquid medium, according to: $C_1 \times V_1 = C_2 \times V_2$, where C_1 is the OD reached in the 50mL YEP, V_1 is the volume of what was centrifuged, C_2 is 1 (OD corresponding to 10^8 cells) and V_2 is the volume will be used to suspend the cells after centrifugation.

6. REFERENCES

Almeida RPP, Nunney L, 2015. How Do Plant Diseases Caused by *Xylella fastidiosa* Emerge? *Plant Dis* **99**, 1457-67.

Arora R, Palta JP, 1988. In Vivo Perturbation of Membrane-Associated Calcium by Freeze-Thaw Stress in Onion Bulb Cells : Simulation of This Perturbation in Extracellular KCl and Alleviation by Calcium. *Plant Physiol* **87**, 622-8.

Blumwald E, Poole RJ, 1986. Kinetics of Ca2+/H+ Antiport in Isolated Tonoplast Vesicles from Storage Tissue of Beta-Vulgaris L. *Plant Physiol* **80**, 727-31.

Chatterjee S, Almeida RP, Lindow S, 2008. Living in two worlds: the plant and insect lifestyles of *Xylella fastidiosa*. *Annu Rev Phytopathol* **46**, 243-71.

Cheng NH, Pittman JK, Shigaki T, *et al.*, 2005. Functional association of Arabidopsis CAX1 and *CAX3* is required for normal growth and ion homeostasis. *Plant Physiol* **138**, 2048-60.

Cobine PA, Cruz LF, Navarrete F, Duncan D, Tygart M, De La Fuente L, 2013. *Xylella fastidiosa* differentially accumulates mineral elements in biofilm and planktonic cells. *PLoS One* **8**, e54936.

Cramer GR, Lauchli A, Polito VS, 1985. Displacement of Ca by Na from the plasmalemma of root cells : a primary response to salt stress? *Plant Physiol* **79**, 207-11.

Dandekar AM, Gouran H, Ibanez AM, *et al.*, 2012. An engineered innate immune defense protects grapevines from Pierce disease. *Proc Natl Acad Sci U S A* **109**, 3721-5.

De La Fuente L, Parker JK, Oliver JE, *et al.*, 2013. The bacterial pathogen *Xylella fastidiosa* affects the leaf ionome of plant hosts during infection. *PLoS One* **8**, e62945.

Gilroy S, Bethke PC, Jones RL, 1993. Calcium homeostasis in plants. *J Cell Sci* **106 (Pt 2)**, 453-61.
Goodwin PH, Devay JE, Meredith CP, 1988. Roles of water stress and phytotoxins in the development of Pierce's disease of the grapevine. *Physiological and Molecular Plant Pathology* **32**, 1-15.

Grant M, Brown I, Adams S, Knight M, Ainslie A, Mansfield J, 2000. The RPM1 plant disease resistance gene facilitates a rapid and sustained increase in cytosolic calcium that is necessary for the oxidative burst and hypersensitive cell death. *Plant Journal* **23**, 441-50.

Hirschi KD, 1999. Expression of Arabidopsis CAX1 in tobacco: altered calcium homeostasis and increased stress sensitivity. *Plant Cell* **11**, 2113-22.

Hirschi KD, 2004. The calcium conundrum. Both versatile nutrient and specific signal. *Plant Physiol* **136**, 2438-42.

Hirschi KD, Korenkov VD, Wilganowski NL, Wagner GJ, 2000. Expression of arabidopsis CAX2 in tobacco. Altered metal accumulation and increased manganese tolerance. *Plant Physiol* **124**, 125-33.

Hirschi KD, Zhen RG, Cunningham KW, Rea PA, Fink GR, 1996. CAX1, an H+/Ca2+ antiporter from Arabidopsis. *Proc Natl Acad Sci U S A* **93**, 8782-6.

Kauss H, 1987. Some Aspects of Calcium-Dependent Regulation in Plant-Metabolism. *Annual Review of Plant Physiology and Plant Molecular Biology* **38**, 47-72.

Kleinhenz MD, Palta JP, 2002. Root zone calcium modulates the response of potato plants to heat stress. *Physiol Plant* **115**, 111-8.

Korenkov V, Hirschi K, Crutchfield JD, Wagner GJ, 2007. Enhancing tonoplast Cd/H antiport activity increases Cd, Zn, and Mn tolerance, and impacts root/shoot Cd partitioning in Nicotiana tabacum L. *Planta* **226**, 1379-87.

Lecourieux D, Ranjeva R, Pugin A, 2006. Calcium in plant defence-signalling pathways. *New Phytol* **171**, 249-69.

Legge RL, Thompson JE, Baker JE, Lieberman M, 1982. The Effect of Calcium on the Fluidity and Phase Properties of Microsomal Membranes Isolated from Postclimacteric Golden Delicious Apples. *Plant and Cell Physiology*.

Ma W, Qi Z, Smigel A, Walker RK, Verma R, Berkowitz GA, 2009. Ca2+, cAMP, and transduction of non-self perception during plant immune responses. *Proc Natl Acad Sci U S A* **106**, 20995-1000.

Modareszadeh M, Bahmani R, Kim D, Hwang S, 2020. *CAX3* (cation/proton exchanger) mediates a Cd tolerance by decreasing ROS through Ca elevation in Arabidopsis. *Plant Mol Biol*.

Murashige T, Skoog F, 1962. A Revised Medium for Rapid Growth and Bio Assays with Tobacco Tissue Cultures. *Physiologia Plantarum* **15**, 473-97.

Oliver JE, Sefick SA, Parker JK, Arnold T, Cobine PA, De La Fuente L, 2014. Ionome changes in *Xylella fastidiosa*-infected Nicotiana tabacum correlate with virulence and discriminate between subspecies of bacterial isolates. *Mol Plant Microbe Interact* **27**, 1048-58.

Pittman JK, 2011. Vacuolar Ca(2+) uptake. *Cell Calcium* **50**, 139-46.

Pittman JK, Edmond C, Sunderland PA, Bray CM, 2009. A cation-regulated and proton gradient-dependent cation transporter from Chlamydomonas reinhardtii has a role in calcium and sodium homeostasis. *J Biol Chem* **284**, 525-33.

Punshon T, Hirschi K, Yang J, Lanzirotti A, Lai B, Guerinot ML, 2012. The role of CAX1 and *CAX3* in elemental distribution and abundance in Arabidopsis seed. *Plant Physiol* **158**, 352-62.

Saidi Y, Finka A, Muriset M, *et al.*, 2009. The heat shock response in moss plants is regulated by specific calcium-permeable channels in the plasma membrane. *Plant Cell* **21**, 2829-43.

Salt DE, Baxter I, Lahner B, 2008. Ionomics and the study of the plant ionome. *Annu Rev Plant Biol* **59**, 709-33.

Sanders D, Brownlee C, Harper JF, 1999. Communicating with calcium. *Plant Cell* **11**, 691-706.

Schumaker KS, Sze H, 1985. A Ca2+/H+ Antiport System Driven by the Proton Electrochemical Gradient of a Tonoplast H+-Atpase from Oat Roots. *Plant Physiol* **79**, 1111-7.

Shigaki T, Hirschi K, 2000. Characterization of CAX-like genes in plants: implications for functional diversity. *Gene* **257**, 291-8.

Shigaki T, Hirschi KD, 2006. Diverse functions and molecular properties emerging for CAX cation/H+ exchangers in plants. *Plant Biol (Stuttg)* **8**, 419-29.

Shigaki T, Mei H, Marshall J, Li X, Manohar M, Hirschi KD, 2010. The expression of the open reading frame of Arabidopsis CAX1, but not its cDNA, confers metal tolerance in yeast. *Plant Biol (Stuttg)* **12**, 935-9.

Sicard A, Zeilinger AR, Vanhove M, *et al.*, 2018. *Xylella fastidiosa*: Insights into an Emerging Plant Pathogen. *Annu Rev Phytopathol* **56**, 181-202.
Tawfik AA, Kleinhenz MD, Palta JP, 1996. Application of calcium and nitrogen for mitigating heat stress effects on potatoes. *American Potato Journal* **73**, 261-73.

Tuteja N, Mahajan S, 2007. Calcium signaling network in plants: an overview. *Plant Signal Behav* **2**, 79-85.

Zhang L, Du L, Poovaiah BW, 2014. Calcium signaling and biotic defense responses in plants. *Plant Signal Behav* **9**, e973818.

Zhao J, Shigaki T, Mei H, Guo YQ, Cheng NH, Hirschi KD, 2009. Interaction between Arabidopsis Ca2+/H+ exchangers CAX1 and *CAX3*. *J Biol Chem* **284**, 4605-15.